UNITED NATIONS EDUCATIONAL, SCIENTIFIC AND CULTURAL ORGANIZATION
INTERNATIONAL ATOMIC ENERGY AGENCY
INTERNATIONAL CENTRE FOR THEORETICAL PHYSICS
I.C.T.P., P.O. BOX 586, 34100 TRIESTE, ITALY, CABLE: CENTRATOM TRIESTE

H4.SMR/1011 - 5

Fourth Workshop on Non-Linear Dynamics and Earthquake Prediction

6 - 24 October 1997

Structures Formed During Landers-Big Bear, California Earthquake Sequence

A.M. JOHNSON

Purdue University
Depts. of Mathematics and
Earth & Atmospheric Sciences
West Lafayette, Indiana, U.S.A.

STRUCTURES FORMED DURING LANDERS-BIG BEAR, CALIFORNIA EARTHQUAKE SEQUENCE

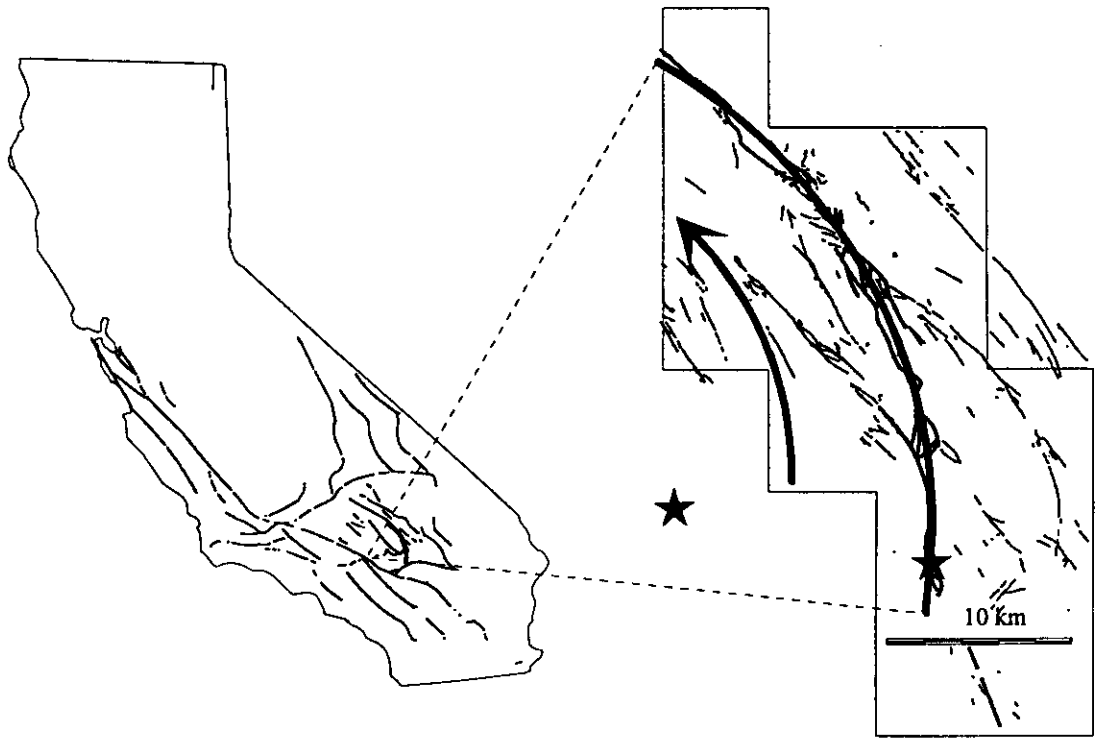

by

Arvid M. Johnson
and
Robert W. Fleming

GEOCAT Program
International Program of Geologic Catastrophes
Purdue University

1997

TABLE OF CONTENTS

TEXT FIGURES

ABSTRACT

Ground rupture that occurred during the 28 June 1992 Landers-Big Bear, California, earthquake sequence has provided an unusual opportunity to map structures that form near the ground surface during strike-slip faulting. The largest structure, which is illustrated in an index-scale map, is the *Landers-Big Bear rotating block*. This block is defined on the east by an arcuate rupture 80-90 km long consisting of *en echelon*, right-stepping right-lateral fault zones that change orientation from north to south. The entire 1992 fault rupture defines an arc of about 60° with a radius of 70-80 km centered near the San Andreas fault zone to the west. In 1992 the Landers-Big Bear block rotated counterclockwise relative to surrounding ground, and deformed internally. Deformation within the rotating block may have caused the left-lateral earthquake sequence near Big Bear Lake.

The arcuate Landers rupture is not a single fault, but rather is a composite of parts of no fewer than four named fault zones, from the Camp Rock in the north to the Johnson Valley in the south. The parts of fault zone in the Landers rupture step right to form large releasing stepovers several kilometers long and wide, connected by right-lateral fault zones and tension cracks. Within the Homestead-Emerson and Kickapoo stepovers are duplex structures, consisting of multiple right-lateral rupture zones. Measurements of shift across elements of the duplex structures by other investigators indicate that there was primarily right-lateral shift, but also growth of pull-apart basins. A zone of tension cracks trending at a high angle to the right-stepping Emerson and Camp Rock faults reflects growth of another pull-apart basin there.

Our mapping is intended to contribute to the understanding of structures within these larger rupture zones. One such structure at Landers is the *belt of shear zones*, which seems to characterize a large part of the Landers rupture, at least wherever we have examined it. The belts are only mentioned here because we have described them previously. Our more recent research shows, mainly, that belts of shear zones range from about 50 m to 500 m wide, and that they pass through bedrock as well as consolidated and unconsolidated alluvium.

One of the most spectacular structures we mapped is *Tortoise Hill tectonic ridge* which incrementally grew in height during the 1992-Landers, California, earthquake. The ridge is in strike-slip terrain, within the right-lateral, Emerson fault zone. Tortoise Hill was elevated up to 1 m vertically along bounding shear zones on the northeast and southwest as about 3 m of right-lateral shift was accommodated across the fault zone. Fortuitously, we located a group of survey points in the Tortoise Hill area that had been placed by a public utility company. Data for the measured deformation comes from a resurvey of those points and from analytical photogrammetric measurements on pre- and post-earthquake aerial photography.

Global Position System (GPS) and triangulation studies for length of base-line changes on the scale of kilometers by others indicate that the regional deformation east and west of the Emerson fault zone in the Tortoise Hill area is *left-lateral* shearing on the order of 10^{-5}. This deformation reflects the elastic rebound. Our studies indicate that deformations in the form of normalized length changes are smaller than our limit of accuracy (about $3x10^{-4}$) to within about 100 m of the belt of shear zones. Within the shear zones and ridge, though, we measure right-lateral deformations up to 10^{-2}. At the center of the ridge, the deformation is smaller than $3x10^{-4}$. There is also dilation normal to the long axis of the ridge suggesting that the rock within the ridge may have increased in volume.

Leveling measurements of differential vertical displacement indicate that ground more than 3 to 4 kilometers southwest away from the ridge was not uplifted. Where uplift began, it gradually increased from about 5 cm/km to perhaps 10 cm/km at the southwest side of the ridge. Total uplift to the southwest side of the ridge was about 0.2 m. From there, the uplift became localized and quickly reached a peak value of about 1 m within the ridge. The pattern is gentle tilting of a broad area to the southwest and an abrupt uplift of the ridge within the bounds of the surrounding belts of shear zones. The greatest growth of the ridge is at the crest of an elliptically-shaped area centered on the high ground of the ridge. Toward the northwest from the ridge, uplift ended within about 1 km of the ridge; the area on the northeast side of the Emerson fault zone in this area was down-dropped at least 0.3 m as part of the releasing stepover to the Camp Rock fault zone.

The *Headquarters duplex structure*, along the Homestead Valley fault zone, is on the order of hundreds of meters long and tens of meters wide. It formed at a *releasing stepover* between fault elements, about one kilometer long, that defines the northeast side of the Homestead Valley fault zone. The individual faults connecting the bounding faults of the duplex structure are tens of meters long and accommodated mainly right-lateral shift. The individual connecting faults, themselves, are made up of even shorter fault elements, a few meters long, that accommodated right-lateral shift and have *restraining steps*. At the Pipes Wash releasing stepover, along the Homestead Valley fault zone, a different kind of structure formed. Instead of a duplex structure, a left-lateral shear zone formed, bounding a rotating block within the stepover. The left-lateral rupture shows classic examples of *ramps* that formed along oblique, strike-slip/normal faults.

Two areas of the Kickapoo fault zone, which connects the Johnson Valley and Homestead Valley fault zones, contain classic *en echelon ruptures* at several scales. At the Charles Road area, the fault zone itself is composed of restraining, stepping fault elements 800 m long that accommodate both

normal shift and right-lateral, strike shift. Some of these ruptures consist of shorter fault elements, about 250 m long, arranged with restraining steps. Parts of these shorter fault elements consist of even–shorter fault elements, about 25 m long, also arranged with restraining steps. The directions of the en echelon elements of progressively–shorter lengths become progressively oriented about 40° farther to the east. The walls of the Kickapoo fault zone are oriented N7°E. The 800-m fault elements that compose the fault zone are oriented about N17°E. The 250-m fault elements are oriented about N24°E. The 25-m fault elements are oriented about N45°E.

INTRODUCTION

The June 28, 1992, M_s 7.5 earthquake at Landers, California, which occurred about 10 km south of the community of Yucca Valley, California (Figure 1), produced spectacular ground rupturing more than 80 km in length (Hough and others, 1993). The ground rupturing, which was dominated by right-lateral shearing, extended along at least four distinct faults arranged broadly *en echelon*. The faults were connected through wide transfer zones by stepovers, consisting of right-lateral fault zones and tension cracks.

Figure 1. Location map, showing *en echelon* fault zones that activated during the 1992 Landers, California earthquake. Epicenter of main shock (M 7.6) was near Landers at the south end of the ruptures. Inset figure shows some of the major faults in southern California.

The Landers earthquakes occurred in the desert of southeastern California, where details of ruptures were well preserved, and patterns of rupturing were generally unaffected by urbanization. The structures were varied and well-displayed and, because the differential displacements were so large, spectacular. The scarcity of vegetation, the aridity of the area, the compactness of the alluvium and bedrock, and the relative isotropy and brittleness of surficial materials collaborated to provide a marvelous visual record of the character of the deformation zones. In following pages we present a series of analecta—that is, verbal clips or snippets—dealing with a variety of structures, including belts of shear zones, segmentation of ruptures, rotating fault block, *en echelon* fault zones, releasing duplex structures, spines, and ramps. All of these structures are documented with detailed maps in text figures or in plates. Our purpose is to describe the structures and to present our understanding of the mechanics of their formation. Hence, most descriptions focus on structures where we have information on differential displacements as well as spatial data on the position and orientation of fractures.

Our understanding of these structures is based on mapping, and we have mapped in two, quite different ways. We have mapped fractures at a scale of 1:200 (or rarely, 1:500) using a total-station theodolite to establish a local array of control points. After the points were plotted, we reoccupied the points in the field to make controlled drawings of the surrounding fractures and disrupted ground. We also used photogeologic methods in the laboratory to map ruptures from post-earthquake aerial photographs at a scale of 1:6000. Those areas mapped in detail in the field and those mapped from photographs are clear on the plates and figures because the maps made in the field have appended kinematic information, whereas those made in the laboratory show only traces of fractures of some type.

For some areas we have compared the maps made by the two methods and conclude that the photogeologic maps show traces of fractures that are subsets of the traces visible in the field and shown in our detailed maps. The post-earthquake aerial photography was taken in the morning at a low sun angle. Fractures that contain westerly facing scarps are particularly distinct (in shadow), but those without a vertical offset or facing easterly are poorly expressed or invisible. Thus, in general, one needs to realize that features that could not be definitely identified as fractures, or fractures that were invisible in the photographs, will be missing in the photogeologic parts of maps. The traces shown in areas mapped photogrammetrically, though, almost always represent fractures.

Ultimately we redrafted, compiled and reduced several map sheets to produce the maps presented here. The maps were scanned and saved as a TIFF computer file, converted to lines with Adobe STREAMLINE, and imported into a drafting program Micrografx DESIGNER where they were finished as drawings.

There are several purposes in presenting detailed descriptions of ground ruptures of the Landers earthquake sequence: The main shock of the Landers earthquake was the largest to occur in the United States since the Great Alaskan, Good Friday Earthquake of 1964, and it produced even more clearly surface-rupture patterns than the 1906 San Francisco earthquake. The maximum credible, differential, lateral displacements at Landers—as much as 400 cm[1]—are comparable to the maximum credible values for the 1906 San Francisco earthquake[2]. They are much larger than those in the 1971 San Fernando and 1989 Loma Prieta earthquakes, [100 to 200 cm]; the 1964 Borrego Peak and Managua Nicaragua earthquakes, [20 to 30 cm]; or the

---

[1] There is a strange tendency for earthquakes to be characterized by exaggerated estimates of "maximum displacement." For example, at Landers, maximum displacement has been reported to be 6 to 7 m based on one spot measurement along Galway Lake Road (Engineering and Science, 1992; Sieh and others, 1993) within an area of complex deformation where the structural context for the exaggerated displacement is lacking. This value belies measurements half as large both north and south of Galway Lake Road. See, also, the following note.

[2] Values of up to 6.4 m for the 1906 San Francisco earthquake were reported by G. K. Gilbert, but he warned (to deaf ears) that these values almost certainly are exaggerations resulting from special conditions in soft ground, such as lurching or other superficial adjustments. Yet, 6.4 m is the number typically reported for the San Francisco earthquake and used in all kinds of calculations!

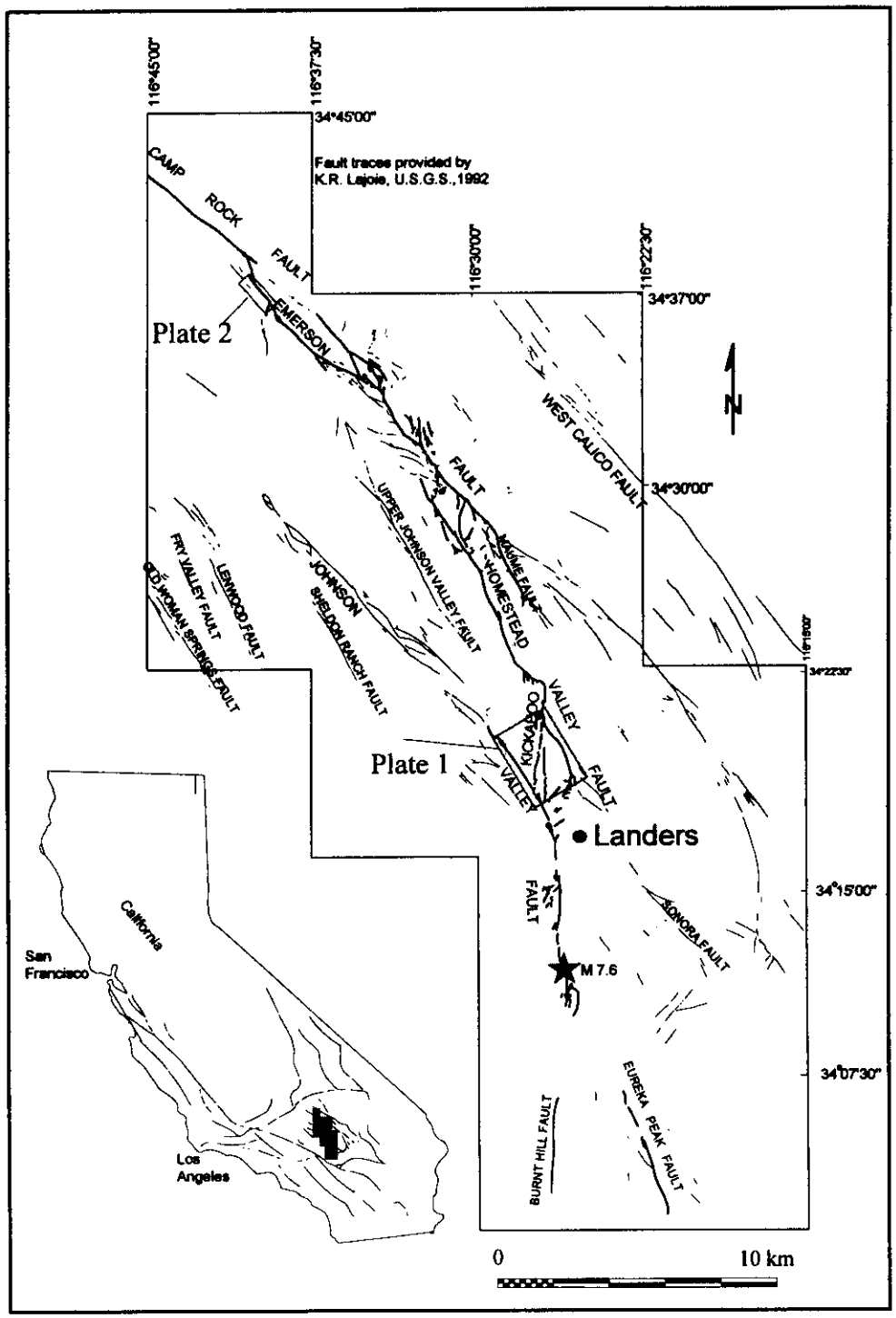

Figure 1. Location map, showing en echelon fault zones that activated during the 1992 Landers, California earthquake. Epicenter of main shock (M 7.6) was near Landers at the south end of the ruptures. Inset figure shows some of the major faults in southern California.

1966 Parkfield earthquakes, [5 to 8 cm], (Gilbert, 1907; Lawson, 1908; Bonilla and others, 1971; Brown and others, 1967, 1973; Clark, 1972; Kamb and others, 1971; Sharp, 1975). The Landers earthquake is also the largest since the revolution of plate tectonics theory (ca. 1965) and the inception of the National Earthquake Hazards Reduction Program (ca. 1970). The earthquake produced the most spectacular surface rupture since adoption of many types of hazards criteria for the siting of major engineering structures such as nuclear power plants and dams, and critical facilities such as schools, hospitals, and fire departments, and thus will become a benchmark for revisions of hazards criteria. It is the largest and most disruptive earthquake since development of ideas about "capable" faults and fault segmentation, and since enactment of California's landmark Alquist-Priolo Act, which is concerned with "setbacks" of houses, vital utilities, and other structures from active faults. The extensive surface rupture at Landers will have major implications for future regulations concerning earthquake hazards, including the potential hazards of ruptured containment structures for nuclear waste and other extremely toxic waste. For all these reasons, the Landers earthquake, and the associated ground rupture, is scientifically important. But the descriptions are also important as the observational basis for modeling and testing of theories of faulting that must follow if we are to understand processes of faulting. Incomplete and inaccurate descriptions made during previous earthquakes have limited the validity of follow-up investigations, especially those conducted after the surface evidence of ground rupture has been weathered or otherwise modified.

PART I. BASIC CONSIDERATIONS

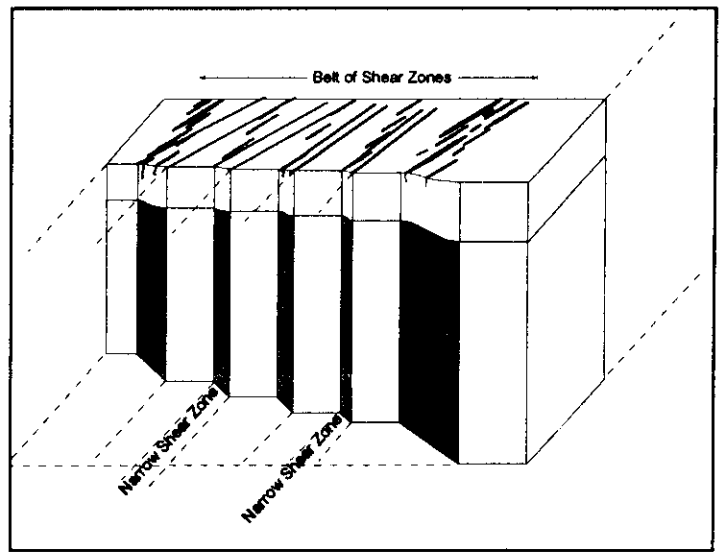

BELTS OF SHEAR ZONES (SPLINTERING) AT LANDERS

The idea that broad belts of shear zones, rather than narrow shear zones or slip surfaces, form during a faulting-earthquake episode has been revived as a result of observations made of ground ruptures at Landers. Almost 80 years ago, following the 1906 San Francisco earthquake, shear zones and belts of shear zones were recognized along the San Andreas fault (Gilbert, 1907; Lawson, 1908), but the idea has since been largely ignored. It has been ignored because faults have become idealized as slip surfaces, characterized by length of rupture and distribution of slip. Thus, rather than describing the nature of actual surface rupturing, earthquake investigators have idealized surface rupturing. Our approach has been to describe actual surface rupturing.

Early Recognition of Shear Zones

Lawson's Description of Typical Rupture Zone Formed During the 1906 San Francisco Earthquake

During the 1906 San Francisco earthquake, a part of the San Andreas fault zone at least 300 km long (almost four times the length of rupture at Landers) ruptured with large differential right-lateral displacements (Gilbert, 1907, p. 5; Lawson, 1908, p. 2). The rupture was along what was called the *fault-trace*, defined as the manifestation of the "intersection of the fault plane or narrow zone with the surface of the ground" (Lawson, 1908, p. 3). In the following quote, Andrew Lawson describes a broad shear zone, as wide as 100 m, as well as a narrow shear zone with long, *en echelon* fractures at an acute clockwise angle to the walls of the shear zone. The zone of most intense rupture, "the fault-trace or rupture plane," was on one side or the other of a shear zone:

> ....the surface of the ground was torn and heaved in furrow-like ridges. Where the surface consisted of grass sward, this was usually found to be traversed by a network of rupture lines diagonal in their orientation to the general trend of the fault...The width of the zone of surface rupturing varied usually from 3 ft up to 50 ft or more. Not uncommonly there were auxiliary cracks either branching from the main fault-trace obliquely for 100 to 300 ft, or lying subparallel to it and not...directly connected to it. Where these auxiliary cracks were features of the fault-trace, the zone of surface disturbance which included them frequently had a width of 300 ft. *The displacement appears thus not always to have been confined to a single line of rupture, but to have been distributed over a zone of varying width.* Generally, however, the greater part of the dislocation within this zone was confined to the main line of rupture, usually marked by a narrow ridge of heaved and torn sod ...Nearly all attempts at the measurement of the [differential] displacement were concerned with horizontal offsets on fences, roads and other surface structures at the point of their intersection by the principal rupture plane, and ignore for the most part any [differential] displacement that may be distributed on either side of this in the *zone of movement*." (Lawson, 1908, p. 53; italics ours).

Figure 2. Types of surface ruptures recognized by G.K. Gilbert along 1906 break of San Andreas fault zone north of San Francisco (from Gilbert, 1928, p. 13). Arrows show directions of shift of underlying crustal blocks.

Figure 3. Ideal vertical sections of normal A and reverse B faults and subsidiary slickened partings, illustrating the relations of the attitude of the partings (from Gilbert, 1928, p. 13).

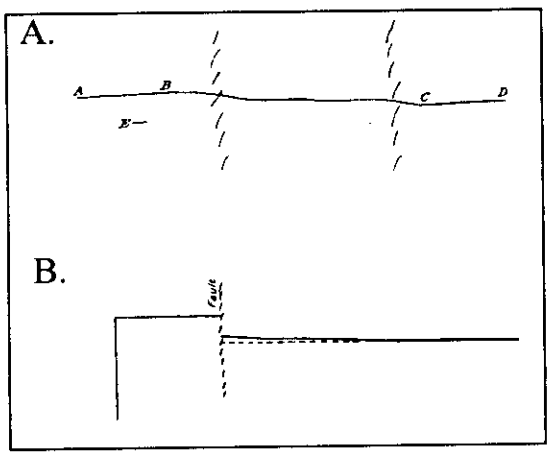

Figure 4. Deformed fences on farm of E.R. Strain, near Woodville, California. 1906 earthquake ruptures (from G.K. Gilbert, in Lawson, 1908, p. 71) . The upper diagram shows two zones of concentrated shearing and an intervening zone of more diffuse shearing. The lower diagram, somewhat north of the one described above, shows the continuation of the shear zone shown near B. The fence is broken and offset 8.5 feet. On one side of the fault the fence is straight. The other the fence is deformed as it approaches the trace.

Gilbert's description of zones of rupture

In a report on normal faults near Salt Lake City, G.K. Gilbert (1928, p. 13) described zones along the 1906 rupture of the San Andreas fault zone north of San Francisco (Figure 2 and Figure 3) as follows:

> Slipping surfaces of another class are not parallel but oblique to the main fault surface. Their obliquity follows a law, and the law is illustrated by analogous phenomena connected with the California earthquake of 1906. The fault movement which caused that earthquake was horizontal, on a plane trending northwest. ...The visible expression of the faulting was mainly in a surface mantle of earth and included a system of oblique cracks, such as are shown diagrammatically in [Figure 2]. In places (a, [Figure 2]) the fault trace included two walls, with relative displacement as indicated by arrows, and between them a belt of broken earth. The principal cracks within the belt were oblique, as indicated. In other places (b, [Figure 2]) the walls were not developed and

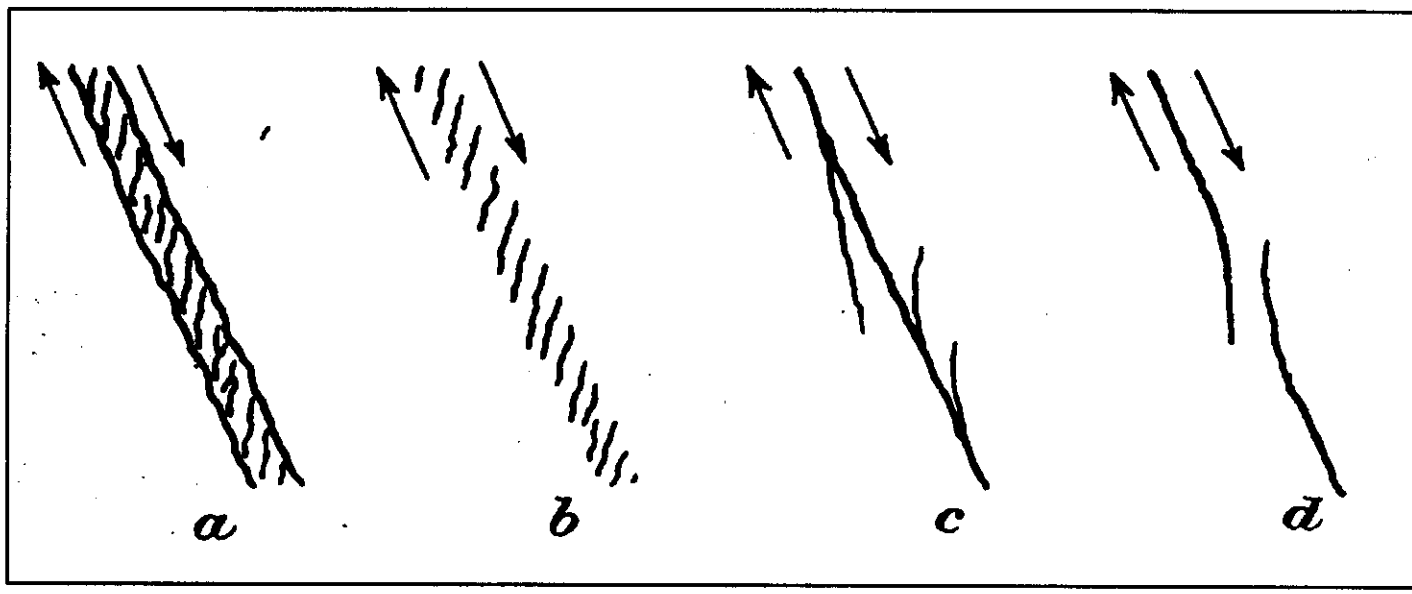

Figure 2. Types of surface ruptures recognized by G.K. Gilbert along 1906 break of San Andreas fault zone north of San Francisco (from Gilbert, 1928, p. 13). Arrows show directions of shift of underlying crustal blocks.

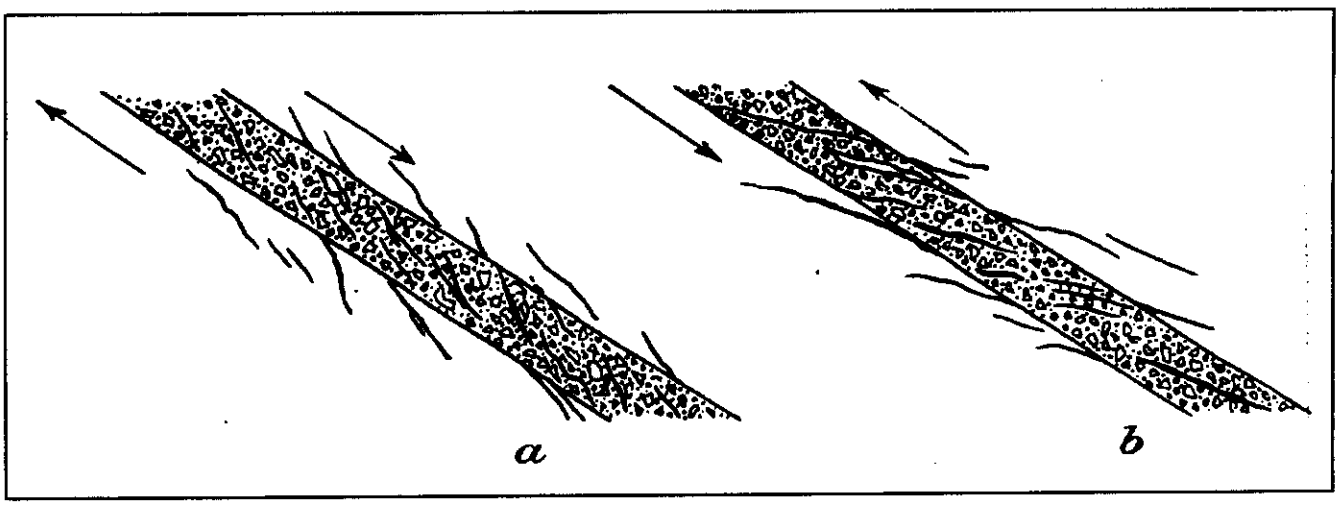

Figure 3. Ideal vertical sections of normal A and reverse B faults and subsidiary slickened partings, illustrating the relations of the attitude of the partings (from Gilbert, 1928, p. 13).

> the fault trace consisted of a system of oblique cracks, as indicated. From the walls of the fault trace ran branching cracks (c, [Figure 2]), the divergence being at various angles but always to the right of one looking along the trace. The trace in places (d, [Figure 2]) swerved to the right and gradually disappeared, to reappear at the left en échelon.

G.K. Gilbert and F.E. Matthes described the feature we have termed a "narrow shear zone" (Johnson and others, 1994) as follows:

> The fault trace is itself in some places inconspicuous.... where one may walk across it without noticing that the ground had been disturbed. Its ordinary phase, however, includes a disruption of the ground suggestive of a huge furrow, consisting of a zone, between rough walls of earth, in which the ground has splintered and the fragments are dislocated and twisted...In many places the fault trace sends branching cracks into bordering land, and locally its effect in dislocation is divided among parallel branches...." (Gilbert, 1907, p. 5)

> [In several places in Sonoma and Mendocino Counties] on fairly level ground, where conditions are simplest and no vertical movement is evident, the sod is torn and broken into irregular flakes, twisted out of place and often thrust up against or over each other. The surface is thus disturbed over a narrow belt...Within such a belt there is seldom, if ever, a well-defined, continuous, longitudinal crack...Rather, there is a marked predominance of diagonal fractures resulting from tensile stresses..." (Matthes, in Lawson, 1908, p. 55).

G.K. Gilbert (in Lawson, 1908, p. 70) (Figure 4) measured the offsets of two fences on Mr. E.R. Strain's property, west of Woodville, California, near the head of Bolinas Bay (Gilbert, 1907, p. 6). The southern fence is crossed by "two visible branches of the fault," represented by short, *en echelon* tension cracks oriented in the usual way. Each of the branches offsets the fence. Gilbert indicates that, on either side of the branches, the fence is straight, meaning that, here, the shear zone is contained between the two branches. Gilbert indicates that "there is more or less diffused shear in the intervening ground" between the two branches, across a zone about 27 m wide. The total offset here is 4.6 m. At a second fence, to the north, the southwest-bounding branch continues, represented by *en echelon* tension cracks, and the shear zone continues, but the northeast-bounding branch is absent. Here, the southwest-branch accommodated 2.6 m of offset; the rest of the shear zone accommodated the additional 3.4 m of total offset. The shear zone here is northeast of the narrow rupture zone.

The fault rupture was not represented by a broad shear zone at all locations, though. According to Gilbert (in Lawson, 1908, p. 71), thirteen kilometers north of this area, "at Mr. Skinner's place, near Olema, the entire fault is apparently concentrated in a single narrow zone." Even at Mr. Strain's place, a large branch of the fault was merely a slip surface (Gilbert, 1907, p. 6): "....the main branch of the fault trace (which is here divided) crosses the foreground from left to right, touching the dissevered ends of the fence, but the shear is at this point so smooth that its surface trace is concealed by the grass." The fence was offset 2.6 m.

Reid's description of broad rupture zones

Reid (1910, p. 33 and 34) also recognized broad shear zones in his part of the report on the 1906 San Francisco earthquake:

> In the general descriptions of the fault-trace it is shown that when the rupture occurred there was a zone of varying width between the shifting sides which did not partake of their simple movements, but was more or less distorted by the shearing forces to which it was subjected. The existence of this zone in alluvium or disintegrating rock may be explained even tho the fault were a sharply defined crack in the underlying solid rock.

Reid goes on to explain that if the mantle over the fault in bedrock is consolidated, the zone of distortion in the mantle will be narrow and most of the shift will be by faulting, whereas if the mantle is unconsolidated, all the shift may be by flowage across a broad zone. Then he concludes,

> ...this seems to be the condition which produces the echelon phase of the fault-trace in very wet alluvium, as described by Mr. Gilbert...

> ...The zone was in some places only 2 to 6 feet wide, in others several hundred yards. Where it was broad the shift was divided in some cases among a number of cracks; in others it was distributed more or less evenly over the zone...

> ...When the shift is concentrated in a narrow zone, only a few feet wide, there is more or less demolition, within the zone, or a fence or other object that may cross it, and the broken ends of the fence receive an offset which gives a measure of the shift. The turf in such a narrow zone is torn in a characteristic way; at the beginning of the movement the turf is rent into strips by cracks formed at right angles to the line of greatest stretching; that is, the cracks and the strips of turf between them would trend about north and south, as the fault runs about northwest...They are frequently described by the word *splintering (Reid, 1910)*.

Since the time of Gilbert's and Reid's studies, some 80 years ago, details of rupturing across shear zones have been documented in only a few situations (e.g. Brown and others, 1967; Philip and Meghraoui, 1983; and Clark, 1972). Because shear zones are the building blocks of larger belts of shear zones, and belts of shear zones constitute fault zones (), we have singled them out for special attention (Johnson and others, 1993, 1994).

The Belt of Shear Zones

Examples of Belts

In many places along the Johnson Valley, Homestead Valley, and Emerson fault zones at Landers, the rupture zones consist of wide belts of shearing, with narrow shear zones, ranging up to a few meters in width, and a few fault surfaces within the belt. We recognize these belts of shear zones as collections of individual shear zones, and we recognize shear zones themselves as collections of fractures and other structural evidence of deformation that forms a distinctive pattern (Johnson and others, 1994). Belts of shear zones have been mapped at Goatsucker Hill ridge; at the Headquarters step; at Wildey Road, as well as at Reche Mountain along the Homestead Valley fault zone (Figure 6, and Plate 1); and at Happy Trail along the Johnson Valley fault zone.

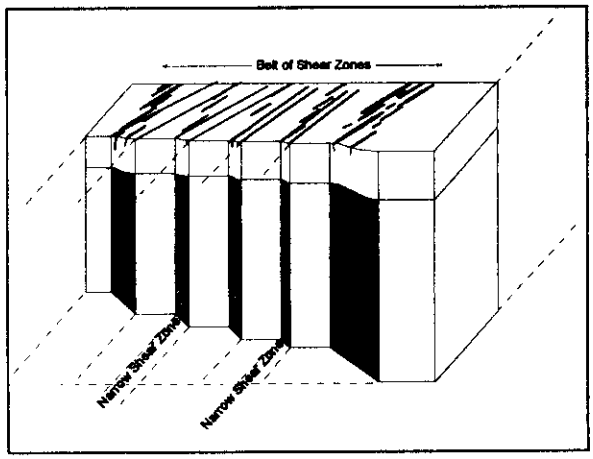

Figure 5. Idealization of a belt of shear zones of the type recognized at Landers. The entire width of the belt consists of a zone of mild shearing which is responsible for broadly distributed tension cracks oriented north–south. Within the belt, though, are narrower shear zones that accomplish most of the shearing across the belt. One of the bounding narrow shear zones, at an outer wall of the belt, accommodates 2/3 to 4/5 of the total shearing of the belt.

The belts of shear zones at Landers range from perhaps 50 to 500 m wide. Some of them are bounded by faults on both sides, some on only one side, and some have no bounding faults. The belt at Happy Trail is about 100 m wide (Plate 1). At the Racetrack Half-Rift, the Johnson Valley and Kickapoo belts branch, forming two belts about 100 m wide. At the Two Ranches Area, the belt is about 200 m wide (Figure 6A). The walls of all these belts are made visible by the roughly parallel, bounding faults. The Wildey Road belt of the Homestead Valley fault zone, north of where the Kickapoo fault zone merges with the Homestead Valley fault zone, is 400 to 500 m wide (Plate 1). The ruptures within the Kickapoo fault zone also form broad belts, 100 to 200 m wide, but the member shear zones within the belts are arranged *en echelon*, and the walls of the belts are delineated not by bounding faults but by the ends of the *en echelon* shear zones. Some of the belts of shear zones along the Emerson fault zone (Plate 6) are intermediate between these two extremes; commonly one wall of the belt is defined by a fault, and the other by the ends of oblique ruptures within the belt.

Figure 6. Aerial photographs of part of 1992 Landers rupture along the Homestead Valley fault zone (about 1:12,000 scale). A. View of rupture zone from near Reche Mountain to south end of Goatsucker Hill ridge in north (see Plate 1). Arrows mark boundaries of belt of shear zones, which ranges in width from about 80 m in south to 200 m in center. B. View of rupture zone from Two Ranches area into exposed bedrock of Goatsucker Hill ridge in north. Arrows mark boundaries of belt of shear zones which passes from consolidated alluvium in southern half of area into bedrock in northern part of area.

Shear Zones

An individual shear zone has a characteristic pattern of fracturing, including long *en echelon* tension cracks, perhaps with some component of left-lateral shift, that are oriented about 20 to 45° clockwise to the walls. Alternatively, there may be a series of opposite–stepping, very narrow shear zones or fault elements oriented about 5 to 20° to the walls of the shear zone (Figure 7) (Johnson and others, 1993, 1994).

We need to explain why we speak of shear zones when, in fact, we observe fractures. Perhaps the most important concept of fracturing and other types of deformation associated with earthquake faulting is that *most of the fractures or other structures one observes at the ground surface are merely guides to deformation at depth. Guide fractures*[3] *indirectly reflect* the deformation and, possibly, the structure beneath the ground surface, generally through the stress state, but also through differential displacements generated by the structure at depth. Guide structures form at the ground surface and include fault elements, thrust faults, folds and *en echelon* fractures above strike-slip faults (Fleming and Johnson, 1989). The most familiar fractures are *en echelon tension cracks*, which occur at the ground surface above the termination of a strike-slip fault or narrow shear zone (Pollard and others, 1982) and generally form in a band of relatively uniform width. Traces of individual cracks are generally inclined 30 to 45° to the trend of the underlying strike-slip structure (Fleming and Johnson, 1989; Nicholson and Pollard, 1985; Olson and Pollard, 1991). Because their formation is relatively well understood, *en echelon* tension cracks are diagnostic guide fractures. The width of the band of *en echelon* cracks reflects the width of the shear zone below, and the orientations provide information about the state of stress at the time of formation.

---

[3] This term derives from Chapter 12 of Hugh McKinstry's textbook, Mining Geology (1948), called "Fracture Patterns As Guides." McKinstry also used the idea in sections on stratigraphic and lithologic guides, and contacts and folds as guides to the location of ore bodies.

A.

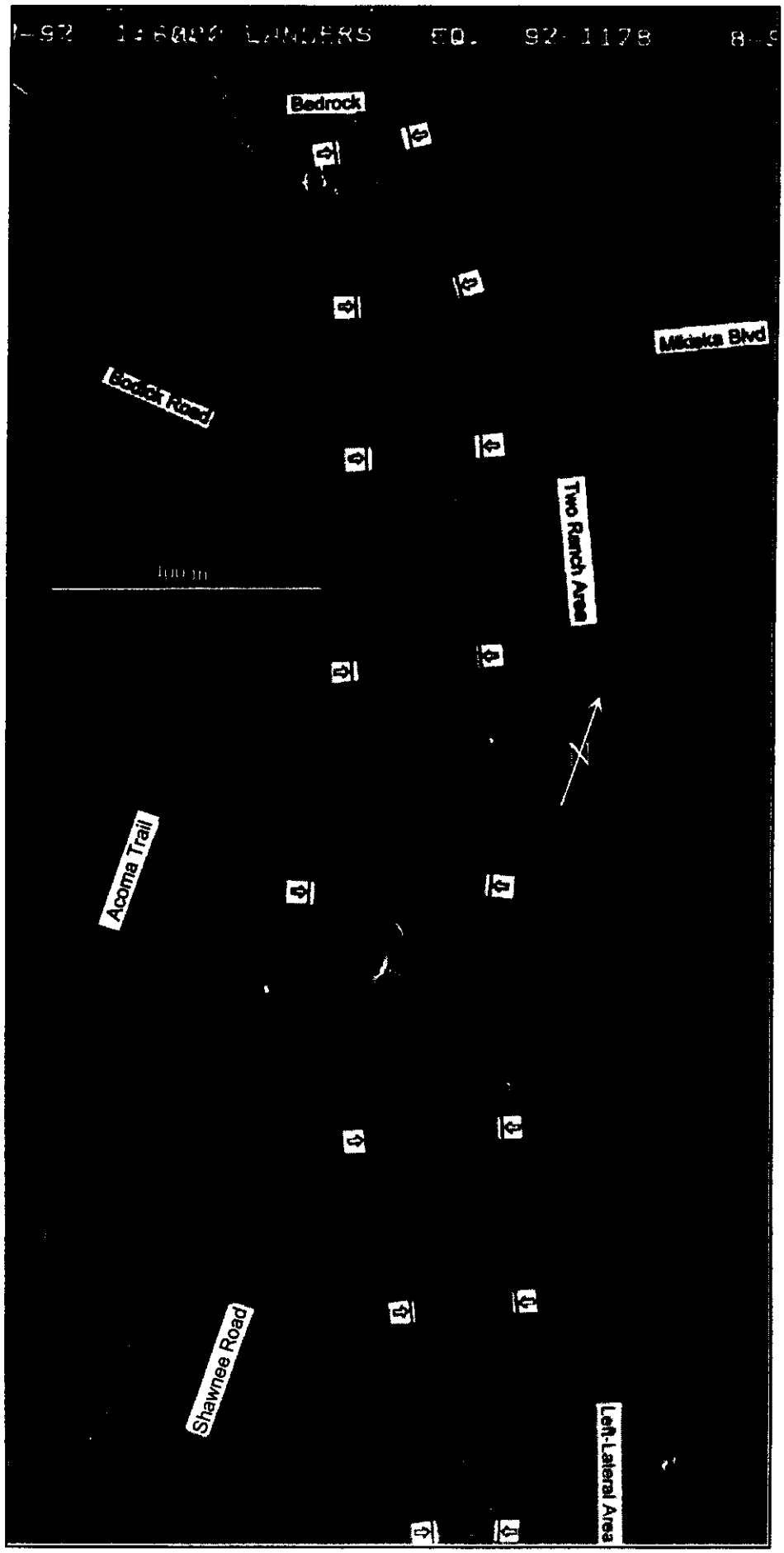
Bedrock
Mikaka Blvd
Two Ranch Area
Acoma Trail
Shawnee Road
Left-Lateral Area

Figure 6

B.

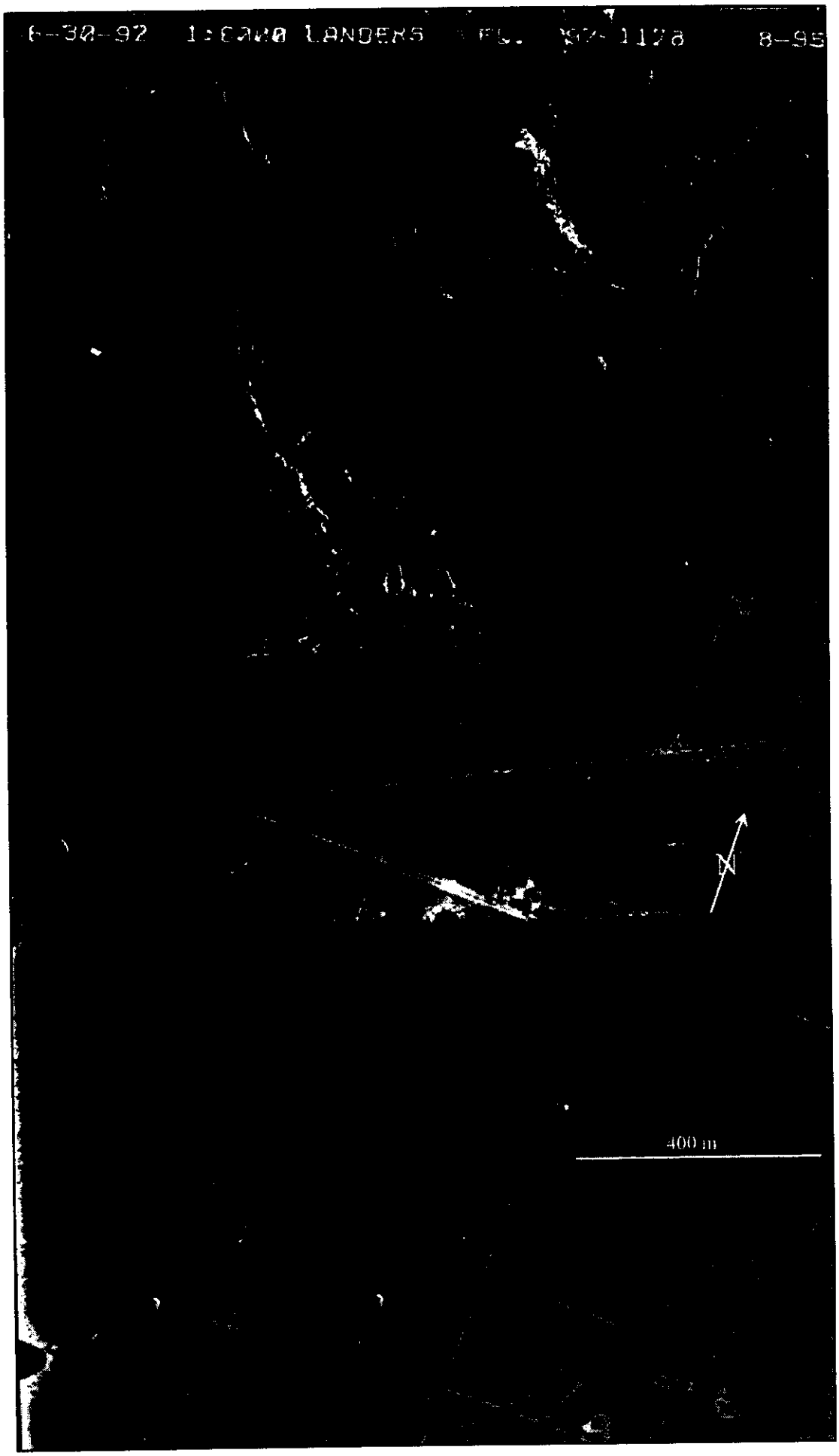

Modes of Rupture

We first described structures in shear zones in a paper on strike-slip faults that bound masses of landslides that moved several meters over a period of three years. (Fleming and Johnson, 1989). We gradually realized that nearly all the fracturing phenomena associated with strike-slip faulting in the landslides are mode *III* phenomena. *The strike-slip structures developed at the ground surface by propagating upward from below, not by propagating horizontally along the fault zone.*

Figure 7. Detailed map of tension cracks, small faults, and right- and left-lateral narrow shear zones along the Homestead Valley fault zone, north of Bodick Road and its intersection with Shawnee Trail. Shapes of individual tension fractures shown schematically with gray lines, but lengths, distributions and orientations are accurate. Some of the fractures that formed as tension cracks subsequently slipped to produce the characteristic open and closed fracture segments that reflect right- or left-lateral shearing. At southwest wall is a shear zone up to 5 m wide that has accommodated 1.5 to 3 dm of right-lateral shift. The band of tension cracks within the broad zone, adjacent to the southwest wall, is about 30 m wide. Much of central third of the belt of shear zones is also characterized by tension cracks oriented roughly north-south. At the northeast wall of the belt is a shear zone that accommodated more than half of the right-lateral shearing of the entire belt. This shear zone is complex and is up to 12 m wide, generally widening from northwest to southeast. Its east side is marked by a scarp, up to 3 dm high, and its west side is marked by thrusts. Within the zone are tension cracks and left-lateral fractures oriented north-south, and right-lateral fractures generally oriented about N.30° W. Components of differential displacement normal to fence line shown along base of diagram. Measurements of offset were from alignment of fence posts.

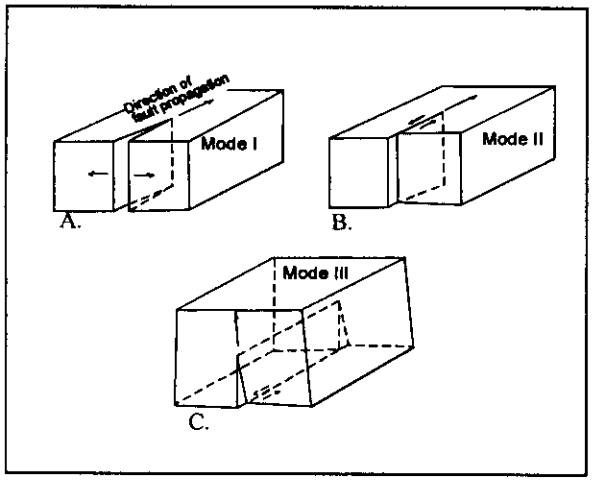

Figure 8. Definitions of mode I, mode II and mode III loading relative to a fracture surface and fracture front. In mode I deformation the fracture surfaces separate normally to produce an open crack. The fracture will propagate horizontally, for the geometry illustrated. In mode II loading of a strike-slip fracture, the fracture front is vertical and the fracture surfaces slip at right angles to the fracture front. If the fracture propagates, it will propagate horizontally. In mode III loading of a strike-slip fracture, the fracture front is horizontal and the fracture surfaces slip parallel to the fracture front. The fracture propagates upward, toward the ground surface.

Because the modes of differential displacement across a fault are important in the description of slip and opening of faults, we will define them (e.g., Lawn and Wilshaw, 1975.). Consider a vertical, strike-slip fault. If the fault is loaded in mode *I*, the walls of the fault might open (Figure 8A), producing a joint, or a graben might form as the walls try to separate. For the other two loading modes, there is horizontal slip. In mode *II*, the fault propagates horizontally along a vertical fracture front (Figure 8B). In mode *III*, the fault propagates vertically toward the ground surface (Figure 8C). It should be clear that faults can also propagate obliquely, in a mixture of modes I, II and III.

During earthquakes, faults apparently propagate outward, from a center, so one would expect mixed-mode rupturing along most of the rupture front. Near the ground surface, however, faults commonly propagate primarily in mode *III*, so we would expect mode *III* rupture to control the formation of near-surface rupture zones regardless of what is happening in the subsurface. We emphasize the difficulties in interpreting the formation of fractures along faults and in shear zones along earthquake ruptures without this understanding. Unfortunately, mode of propagation is widely misunderstood[4].

Two Ranches Belt of Shear Zones

The surface rupture along several of the fault zones at Landers is manifest in *belts of shear zones* of the type described above. There is a broad belt about 180 m wide in the Two Ranches area (Plate 4 and Figure 7). The belt extends for about half a kilometer northwest. To the southwest its eastern side becomes the Headquarters step. The long dimension of the map in Figure 7 is the width of the belt. The belt consists of a broad shear zone, encompassing the entire width of the belt, and several narrower zones of more intense shearing within the belt. Each side is marked by a fault. There are very few fractures outside the belt. The right-lateral shear zones within the belt and the bounding faults are described elsewhere (Johnson and others, 1993, 1994).

The Two Ranches belt of shear zones contains numerous tension cracks (Figure 7). The shapes of individual tension cracks are too convoluted and ornate to show precisely, even at the 1:200 scale of our mapping, so the traces are shown symbolically on the maps. Nevertheless, the

4 For example, lack of understanding of the significance of direction of propagation has flawed an interesting study of faulting within a stepover region at Landers by Zachariasen and Sieh (1995). They speculate that they can determine the direction of horizontal propagation around a step. However, the rupture segments are clearly not connected in plan view, so they cannot be a result of horizontal propagation. They use results of fracture kink theory to explain the orientation of some rupture segments relative to others, whereas, again, the rupture segments are not connected, so they cannot represent kinks. The kinds of structures they describe are a three-dimensional phenomenon of fracturing (Cruikshank and others, 1991a; Scholz, 1992).

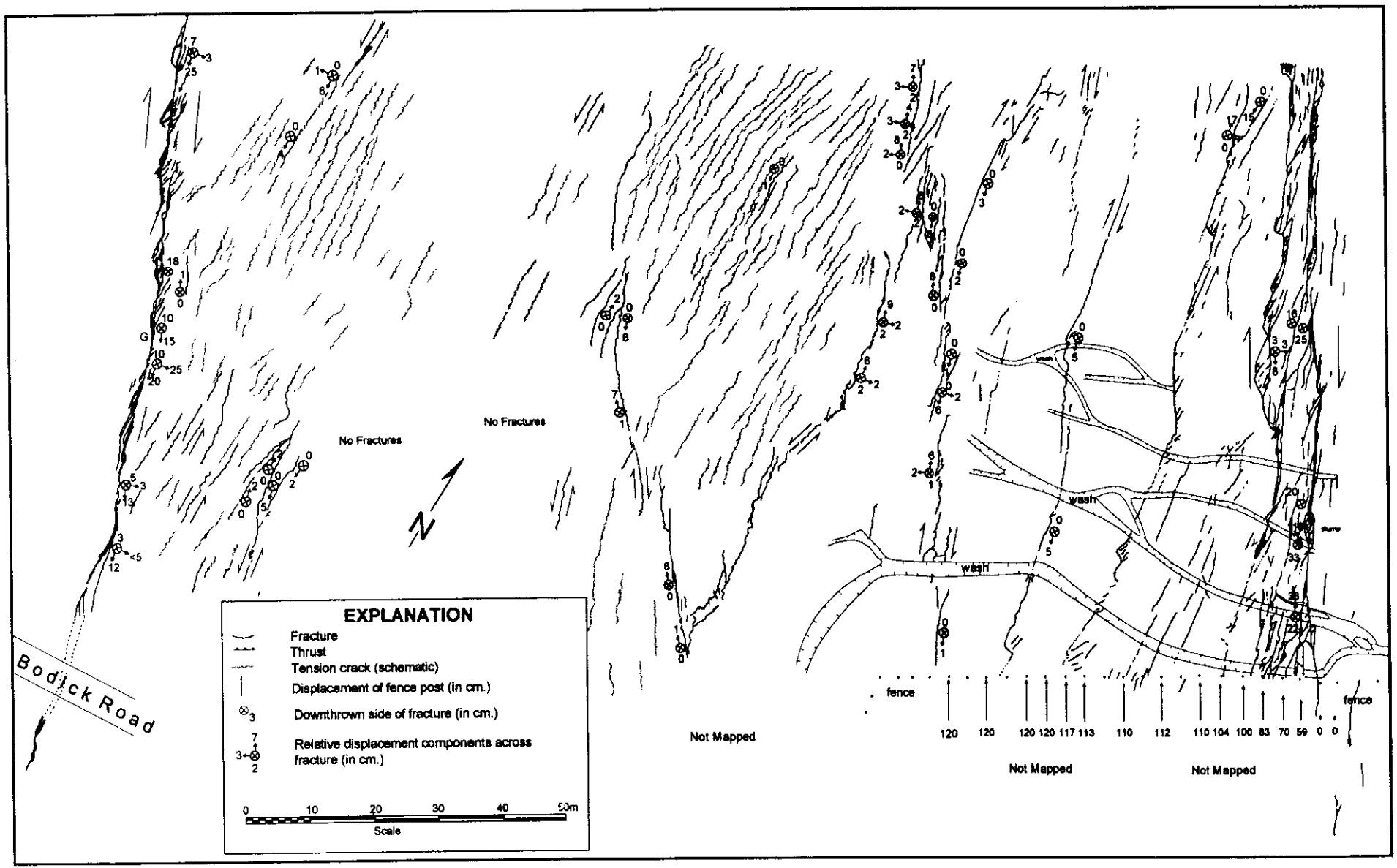
No Fractures
No Fractures
Not Mapped
Not Mapped
Not Mapped
wash
wash
fence
fence
120 120 120 120 117 113 110 112 110 104 100 83 70 59 0 0
Bodick Road
EXPLANATION
Fracture
Thrust
Tension crack (schematic)
Displacement of fence post (in cm.)
Downthrown side of fracture (in cm.)
Relative displacement components across fracture (in cm.)
0 10 20 30 40 50m
Scale

Figure 7

locations, spacing, lengths, and trends of tension cracks are shown accurately. Where tension cracks were absent on the ground, they are absent on the map. The tension cracks are most common in two areas: a belt parallel to the southwest edge of the broad shear zone and in a wedge-shaped zone near mid-width in the shear zone. The distribution of the tension cracks throughout the broad shear zone, and their virtual absence in ground on either side, indicates that the ground within the shear zone was subjected to *localized deformation* vis-à-vis the ground on either side of the shear zone. Characteristically, the orientation of tension cracks throughout the area is north-south. The walls of the broad shear zone in this area (Plate 4)are oriented N30°W, so the tension cracks are oriented about 30° clockwise from the walls of the shear zone.

Scattered throughout the broad shear zone, and not obviously related to any throughgoing structures within the belt of shear zones, are highly irregular left-lateral fractures. Although the left-lateral fractures in the belt are generally parallel to the tension cracks, the primary fractures are the tension cracks. According to our analysis of the formation of left-lateral fractures of this type in the Summit Ridge shear zone (Johnson and Fleming, 1993), the fractures originate as tension cracks (Figure 9A) in response to shearing (and perhaps dilation). As a result of their very formation, though, they change the gross physical properties of the ground being sheared, and immediately begin to act as discontinuities bounding rectangular elements ("dominos") of ground. The "dominos" rotate in a clockwise sense as a result of overall right-lateral shear, and differential displacement between adjacent "dominos" produces the left-lateral offsets (Figure 9B).

Belt of Shear Zones along the Emerson Fault Zone

The same kinds of structures occur within the Emerson belt of shear zones, in the northern part of the Landers rupture (Figure 1 and Plate 2). The belt of shear zones is about 70 m wide and oriented N45° to 50°W. Tension cracks, oriented at clockwise angles from about 30° to 45° from the walls of the belt, are sparse throughout the width of belt; a few of them have minor left-lateral shift. There are a few, narrow, right-lateral shear zones within the broad shear zone in the northwest part of the single-tower powerline area. Most of the right-lateral shift across the rupture zone was accommodated by faults bounding either side of the belt.

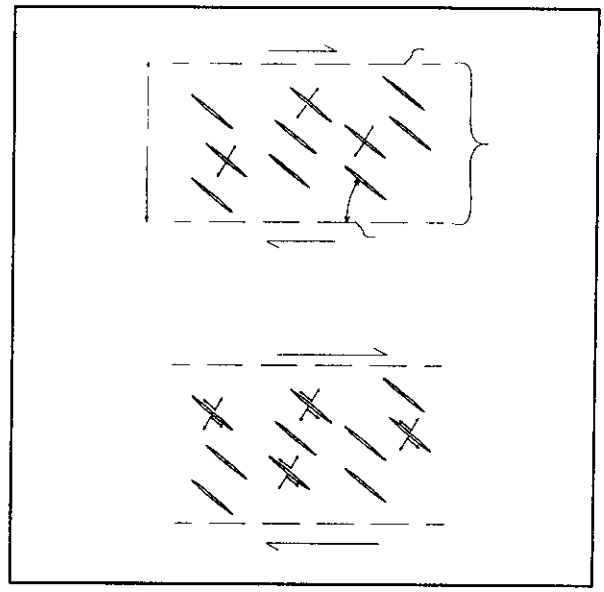

Figure 9. Idealization of rupturing in a broad shear zone. A. Rupture zone is a broad, right-lateral shear zone. Within the shear zone are tension cracks oriented at acute angles of perhaps 20 to 30° to the walls of the shear zone. B. After the tension cracks form, some of the tension cracks become complex fractures, and their modes of deformation change from pure opening to a combination of opening and shearing. The tension cracks become left-lateral, strike-slip fractures oriented at acute angles to the walls of the shear zone.

The fault along the southwest wall of the belt accommodated about 20 cm of right-lateral and 0 to 10 cm of vertical (downthrown on northeast side) relative displacement. Along much of its length it consists of fractures several meters long, oriented north-south, and the blocks of ground between the fractures typically end in low thrusts, directed toward the center of the broad shear zone.

The main fault is along the northeast wall of the belt. It carries about 70 percent of the 2.9 m of total right-lateral deformation across the belt at the Single Tower Transmission Line. The main fault commonly is expressed as a "mole track," with a width ranging from perhaps 0.5 m in the northwest part of its trace to 10 m in the southeast part. It has a beaded, or "pinch-and-swell" structure that is particularly noticeable in the northwest part. The very narrow parts, the pinches, are a few tens of centimeters wide, although along parts of their lengths is a narrower groove, about a 10-cm wide and deep, probably representing a fault surface not far below the ground surface. The broader parts, the swells, are several meters wide and generally have distinctive internal structure. The broader parts contain long fractures oriented at a clockwise angle of about 30° to the trend of the shear zone. Where the fractures bound intact blocks, the blocks resemble the *ramps* that we will describe and illustrate in following pages. Typically, though, one or both ends of the blocks have been thrusted.

Another feature of the main fault is that the ground surface is depressed, perhaps up to 20 cm, along some stretches and

raised, perhaps equally as much, along other stretches, so that, along strike of the fault, there will be repeating elongate basins and domes.

Relevance of Shear Zones

Shear zones are not generally recognized by geologists, except in metamorphic rocks, so one might well ask why we emphasize recognition of shear zones along the strike-slip faults at Landers. Part of the answer, of course, has already been iterated. Shear zones were described by investigators of the northern part of the fault ruptures of the 1906 San Francisco earthquakes, they have been recognized at Landers and at Loma Prieta, and they clearly pose hazards to man-made structures. Besides the existence of shear zones and belts of shear zones, there are six questions about these structures at Landers that can be addressed with our map data:

1. Can the ruptures be mapped analytically with photogrammetry? (Yes, at appropriate scales if one understands fracturing.)

2. Do belts of shear zones appear in bedrock as well as in alluvium? (Yes.)

3. Do belts of shear zones extend to depth, or are they near-surface phenomena? (We have no definitive information.)

4. What are the widths of belts of shear zones? (50 to at least 500 m.)

5. Where is offset accommodated? (In more than half, generally along a fault on one side of belt.)

6. Why is it important to recognize belts of shear zones? (Please read on.)

Can analytical maps of ruptures be made photogrammetrically?

In addressing the question about whether belts extend into bedrock, we made a photogeologic map of the Homestead Valley fault zone from its southern end at Reche Mountain, through the Two Ranches area near the intersection of Bodick Road and Shawnee Road, to Wildey Road (Plate 1), where the Kickapoo fault zone joins the Homestead Valley fault zone. As shown in the previous section, we made detailed maps (1:200 scale) of a small part of the rupture zone during the summer of 1992 while the fractures were fresh. A year later, we made detailed maps of surviving fractures from about 100 m south of Mileska Ranch (Shawnee Road) to about 1 km north of Mikiska Boulevard, including the Goatsucker Hill area (Plate 4).

Although we were generally disappointed with the level of detail that remained one year after the earthquake, several fascinating and previously unrecognized structures were documented. The tension cracks with the left-lateral shift were gone the second year. Only the right- and left-lateral, narrow shear zones composed of fault elements and tension cracks remained, and these were merely as ghosts of their former expression.

It is worth noting for future reference of geologists who decide to do photogeologic investigations of fault ruptures, that the level of detail we were able to map (even at 1:200 scale) in the field one year after the earthquake is comparable to the detail one can map with aerial photos, at a scale of 1:6000, taken immediately after the earthquake (Plates 1 and 2). A significant difference is that more kinematic information may be available in the field than can be obtained with the photos. Displacements can be obtained photogrammetrically, however, by methods described elsewhere (Fleming and others, 1997).

Regardless of scale or method of mapping, though, geologists studying fault ruptures should strive to make *analytical maps*. Analytical mapping of a structure is detailed mapping in which the scale is selected to show the essential features of the elements of the structure. In analytical mapping of fractures, one selects the scale of mapping so that the crucial information required to interpret the fractures is shown on the map. In principal, anyone familiar with fracture mechanics should be able to examine an analytical map and draw the same conclusions about the gross deformation accommodated by the fracturing depicted in the map (Fleming and Johnson, 1989; Johnson and Fleming, 1993; Martosudarmo and others, 1997). The scale of the analytical map is determined by the scale of fracturing, so it is quite different if one is studying the formation of the San Andreas fault zone as a plate boundary than if studying the mechanics of fracturing of ground along a strand of the San Andreas fault that passes through a property being considered for development, or studying microcracks in mineral grains in granite.

Belts in Bedrock?

One of the assertions made by a person in the audience at the 1994 Spring American Geophysical Union meeting, in response to our description of the belts of shear zones at Landers, is that the belts of shear zones are merely manifestations of faulting of soft, unconsolidated sediments and, therefore, are only superficial features.

Our mapping one year after the earthquake, however, showed that the belt of shear zones at the Two Ranches area extends northward at least 1 km, mostly through bedrock. Also, Sowers and others (1994) indicated that the belt of shear zones crosses bedrock in a low hill 200 m north of Mikiska Boulevard, as shown in aerial photos taken shortly after the earthquake (Figure 6A and Figure 6B). The boundaries of the belt can be traced from the left-lateral area (Pipes Wash step) shown near the base of Figure 6A, through the Two Ranch area along Bodick Road, into the bedrock hills of Goatsucker Hill ridge. All of Goatsucker Hill ridge is shown in Figure 6B, which is an unaltered photograph. Dibblee (1967) indicates that Goatsucker Hill is formed in Mesozoic quartz monzonite and diorite. Furthermore, according to our observations and

the mapping of Sowers and others (1994), the Two Ranches area is on consolidated alluvium of Pleistocene to early Holocene age. Thus, at least the walls of the belt of shear zones extend into bedrock.

Maps of the Tortoise Hill area of the Emerson fault zone point to the same conclusion, as documented elsewhere (Fleming and others, 1997; Fleming and Johnson, 1997). Tortoise Hill ridge is underlain by granitic bedrock. According to Dibblee's geologic map (1964), Tortoise Hill ridge is part of a large granitic mass that extends for about 8 km along and 2 to 3 km southwest of the Emerson fault zone. The main break is on the northeastern side of the fault zone. Figure 10 shows Tortoise Hill ridge in the south (bottom) and the Single-Tower Transmission Line road in the north. Near the Single-Tower Transmission Line, the fault zone (belt of shear zones) is about 60 to 70 m wide and widens to about 500 m at Tortoise Hill ridge. The main break is on the northeastern side of the ridge and is alternately in alluvium or granitic bedrock. The rest of the fault zone is in bedrock.

Clearly belts of shear zones are not restricted to unconsolidated alluvium.

Do the Belts Extend to Depth?

We have no first-hand information about the depth the belts of shear zones extend into the earth's crust. If one were to assume that the belts extend half as far to depth as they extend along the ground surface, our compiled map of the Homestead Valley fault zone and Kickapoo stepover provides the following information: The Two-Ranches belt, along the Homestead Valley fault zone, extends over a horizontal distance of about 2 km. The belt in the vicinity of the Wildey Road (Plate 1) along the same fault zone is at least 3 km long. The belt of the Kickapoo fault zone is at least 5 km long (Plate 1). On this basis we might suggest that belts are half-circular elements that extend on the order of 1.5 to 2.5 km deep.

Figure 10. Vertical aerial photograph (about 1:12000 scale) showing belt of shear zones along Emerson fault zone about 6 km northwest of Bessemer Mine Road. Road in upper part of area is along Single-Tower Transmission Line. At south end of photo is north end of Tortoise Hill ridge. Edges of belt shown with arrows. East (right) side of belt is defined by the main fault in this area. The belt is about 70 m wide at transmission line road and 400 m wide in part of ridge shown.

Observations by others, though, suggest that the belts extend much deeper. Low-velocity zones have been recognized along some earthquake faults, including those at Landers (Ben-Zion and Aki, 1990; Hough and others, 1994; Li and others, 1994a, 1994b). Hough and others (1994) reported entrapment of seismic waves in fault-zones within the rupture zone at the southern Joshua Tree earthquake area (April, 1992). Their analyses indicate that the rupture zones are 50 to 100 m wide. Aki, Li and others presented seismological evidence at the 1994 American Geophysical Union meeting in Baltimore, Maryland, that fault zones can be recognized at depth as low-velocity zones 50 to 200 m wide that extend to at least 10 km depths along the Johnson Valley and Homestead Valley fault zones at Landers (Aki, 1994; Li and others, 1994a). Thus, the belts of shear zones probably are not merely near-surface phenomena that extend for many kilometers along the ground surface, but may extend to depths of at least 10 km.

In spite of the geophysical studies by Aki and others, the subsurface form of belts of shear zones is, of course, unknown. Perhaps the belts of shear zones are surface expressions of "flower structures" at depth. Flower structures have been described in seismic images of strike-slip fault zones (Harding and Lowell, 1979; Harding, 1983; Harding and others, 1983; D'Onfro and Glagola, 1983; Plawman, 1983) and in rifts (Genik, 1993; Roberts, 1983). They have a diagnostic branching appearance, from a supposed single branch at depth (generally many kilometers) to two branches above, and then four, and so forth, as the flower structure approaches the ground surface. The branching structures do not appear in vertical seismic sections of simple thrusting or extensional regimes (e.g., Bally, 1983), so they probably are a results of interaction of strike-slip faulting with a free surface. The same may be true for belts of shear zones.

How Wide are Belts of Shear Zones?

In previous papers we have reported that belts of shear zones range from 50 to 200 m in width (Johnson and others, 1993, 1994). We now have, however, additional information that indicates widths of from 50 to 500 m. The Loma Prieta earthquake in northern California produced a belt of shear zones at Summit Ridge characterized by tension cracks and left-lateral faulting across a zone about 500 m wide. A peculiar feature of that belt is that it contained no through-going right-lateral shear zones, and was not bounded by faults, as were most of the broad shear zones at Landers.

The other places we have made observations sufficiently detailed to describe the widths of belts of shear zones are near Landers. The belt of shear zones along the Emerson fault zone at the Single-Tower Transmission Line was about 70 m wide. The belt generally widened southward. If we include Tortoise Hill ridge, the belt of shear zones there was about 500 m wide. The belt of shear zones along the Homestead Valley fault zone ranges up to about 200 m wide. Immediately north of the place where the Kickapoo fault zone and Homestead Valley fault zone join, the belt of shear zones is about 500 m wide.

Where is Offset Accommodated?

It has become common practice in earthquake studies to dig exploratory trenches in order to determine the amount or timing of slip on faults, particularly in developing areas where planners wish to avoid construction of crucial man-made structures on traces of active faults. A fundamental

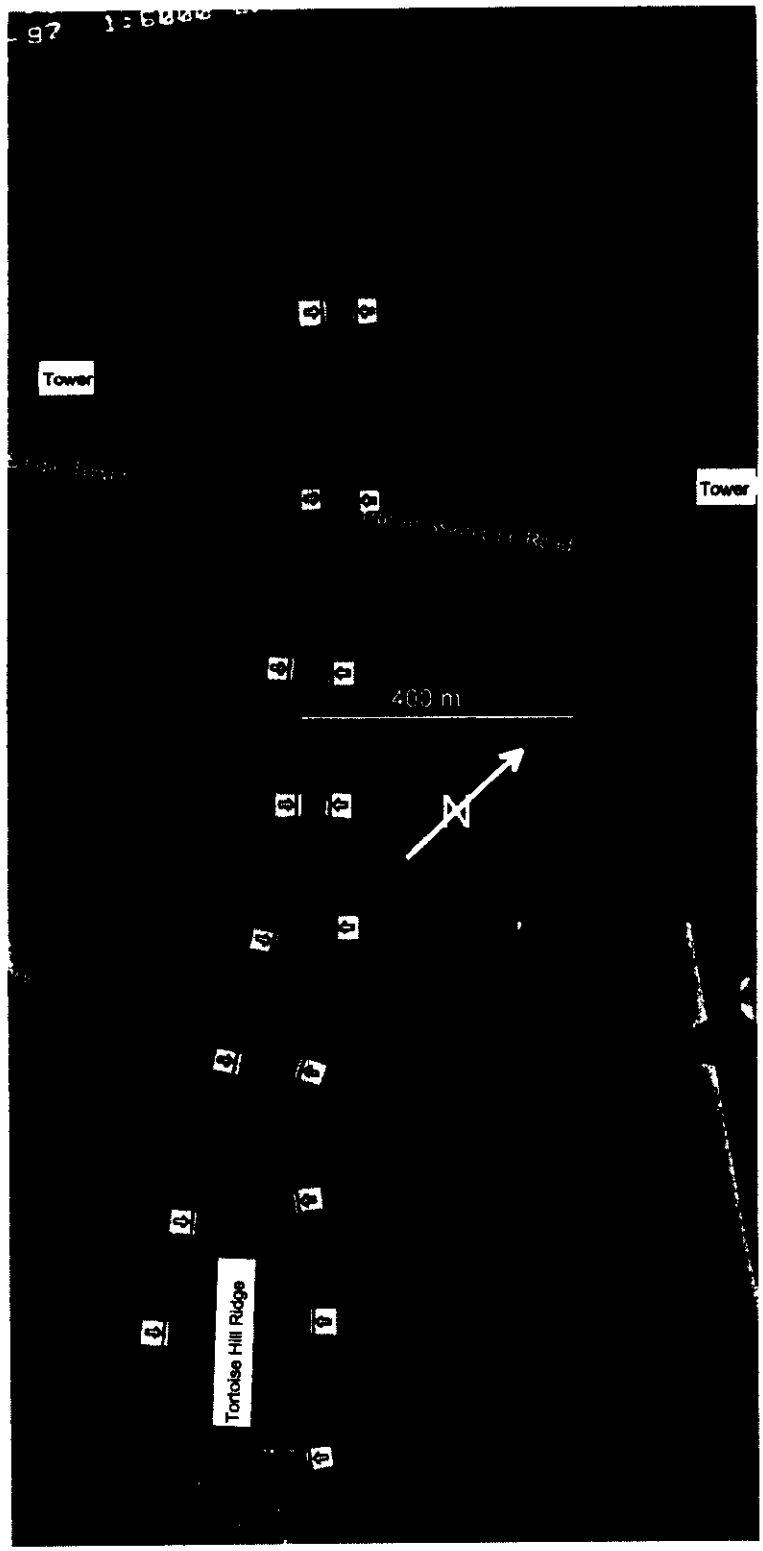

Figure 10. Vertical aerial photograph (about 1:12000 scale) showing belt of shear zones along Emerson fault zone about 6 km northwest of Bessemer Mine Road. Road in upper part of area is along Single-Tower Transmission Line. At south end of photo is north end of Tortoise Hill ridge. Edges of belt shown with arrows. East (right) side of belt is defined by the main fault in this area. The belt is about 70 m wide at transmission line road and 400 m wide in part of ridge shown.

assumption is that the slip of an earthquake rupture is accommodated by a single fracture or a narrow rupture zone that can be exposed in an exploratory trench a few meters long. This assumption turns out to be an unfortunate one. Much of the damage to structures at Landers was a result of position of structures *within* belts of shear zones, not on the bounding faults (Lazarte and others, 1994).

For investigations of siting of structures near fault zones it would be helpful to know how differential displacement is distributed across the fault zone. In general such information is unavailable, for many reasons. In the absence of such information, one might assume that the distribution of strike-slip fault zones will be something like that across the belts of shear zones that we have documented at Loma Prieta and Landers. We have already seen that, at both Loma Prieta and Landers, the offsets are distributed across broad belts of shear zones, ranging from perhaps 50 to 500 m. The distribution of offset, though, is drastically different from place to place. In the epicentral area of Loma Prieta, the right-lateral rupture zones ranged from perhaps 2 to 5 m to 500 m. In the former, the zones presumably represented faults and they accommodated 10 to 20 cm of offset. In the latter, the zone contained left-lateral displacements on the same order, but the offset was rather uniformly distributed; there were no faults bounding the 500-m wide zone.

At Landers there was a wide variety of distributions of differential displacement but, in general, the shift was accommodated primarily by a fault at the wall of a belt of shear zones. At the Emerson fault zone at the Single-Tower Transmission Line, the belt of shear zones is about 70 m wide; about 2.7 of the 3.0 m of shift across the fault zone was along a fault bounding the northeast side of the zone. A fault on the southwest side of the belt accommodated only about 20 cm of differential displacement. Between Mikiska Boulevard and Bodick Road, along the Homestead Valley fault zone, about 60 cm of the total of 180 to 200 cm of shift was across a fault bounding the belt on the northeast. About 100 cm of shift was across a 12-m wide band, including the fault, on the northeast side of the belt. The shift across the fault bounding the northwest side of the belt was 20 to 30 cm. The shift across each of the shear zones within the belt was generally 5 to 10 cm. About 200 m south, at Mileska Ranch, the shear zone on the northeast side of the belt accommodated only 10 to 20 cm. Across about 20 m of the northeast side, 115 cm were accommodated. The remaining 75 to 85 cm of shift were distributed in some way across a belt 200 m wide there.

Our study of the distribution of shift across the Kickapoo fault zone, in the Two Bikers area at Fifth Avenue and the Charles area north of Bodick Road, indicates that there are no bounding faults (Plate 1). Rather, the faults, or narrow shear zones that make up the belt of shear zones, are arranged *en echelon*, and each member fault accommodates much of the total shift at certain points, but that the shift is transferred from member to member.

Clearly one cannot reasonably assume that slip is accommodated only on a single fault trace during an earthquake.

Why is it Important to Recognize Belts of Shear Zones?

There are several reasons it is important to recognize that surface rupture during earthquakes may be represented by belts of shear zones rather than by faults.

1. One is the simple precept of honest scientific description. If an earthquake rupture occurs across a belt 200 m wide and the rupture is mapped as a line (planar fault), reality has been grossly misrepresented.

2. Another important reason was illustrated at Loma Prieta. Detailed mapping in the epicentral area along Summit Ridge revealed that the area is a broad shear zone or belt of shear zones (Johnson and Fleming, 1993; Martosudarmo and others, 1997). This was not recognized by numerous geologists who examined fractures in the epicentral area (e.g., Ponti and Wells, 1991; Prentice and Swartz, 1991; U.S. Geological Survey Staff, 1989, 1990). Neither did we recognize the shear zone at the time of our mapping there; we were puzzled by the left-lateral fractures, but we did not ignore them (e. g., see Aydin and others, 1992). Only later, after experience at Landers, did we recognize the significance of the left-lateral offsets on fractures in a right-lateral zone (Johnson and Fleming, 1993). The outstanding quality of the ground rupture at Landers provided several examples of small-scale models of the fracturing at Loma Prieta.

3. Many fault studies are based on information derived from exploratory trenches. The studies are to determine amounts and timing of "slip" on faults. Derived slip rates for faults are compared to plate motions and recurrence interval of earthquakes, as well as certain characteristics of causal earthquakes. If large fractions of shift during an earthquake occur across broad zones rather than across discrete fault surfaces or the rather narrow zones exposed in trenches, much of the shift will be missed in the trenching. Slip rates would generally be under-stated.

4. Perhaps the most important reason is for theoretical modeling. If we are to develop valid theoretical models of essential mechanisms and mechanics of seismic faulting, our models must include the essential features of the ruptures. Belts of shear zones probably do not occur everywhere along earthquake ruptures, so it might be important to understand conditions under which rupture is across belts, or across one, or more, slip surfaces. Perhaps some aspect of belts is incorporated in recent theoretical modeling of earthquake ruptures by Yehuda Ben-Zion and Jim Rice (Rice, 1993; Ben-Zion, 1995; Ben-Zion and Rice, 1993, 1995).

5. There are also practical reasons. When the senior author was Town Geologist for Portola Valley, California, the town was concerned about the placement of various kinds of structures within the San Andreas fault zone. The

problem is that Portola Valley is largely sited in the San Andreas fault zone. Our chore was to find the traces of the recent breaks and provide narrow zones of setback from those traces (e.g., Hart, 1992; Engineering and Science, 1992; Irvine and Hill, 1993; Hart and others, 1993). The procedure we followed in Portola Valley at that time was flawed. Is it still flawed in California?

The issue concerns whether the pattern of coseismic ground deformation at a site is highly localized along a fault or is dispersed across a belt of shear zones. At Landers, we noted that the main break occurs on one side or the other of the belt of shear zones. Where this occurs, it is important to provide the setback on the correct (undeformed) side of the main break. At Landers, most of the damage to structures was caused by deformation to houses built within belts of shear zones (Lazarte and others, 1994). By sheer luck, very few structures were built across the main breaks. A possible conclusion is that, with respect to ground rupture, one can more–nearly safely ignore the main breaks than the belts of shear zones!

Of course, there is always the question of spatial recurrence. Will the shear zones rupture along the same belt during the next earthquake event on a fault segment? Data from the Loma Prieta and 1906-San Francisco earthquakes (Sarna-Wojcicki and others, 1975; Johnson and Fleming, 1993; Martosudarmo and others, 1997) indicate that there may be a strong correlation between patterns of surface rupture in succeeding earthquakes. In 1989, though, the main break accommodated only a few tens of centimeters of offset in a few patches, whereas there were generally hundreds of centimeters of offset in 1906. The earlier, San Francisco earthquake was several times larger that the Loma Prieta earthquake. Had the timing of the two earthquakes been reversed, the conclusion of similarity of rupturing might be different.

CONTROL OF THE ORIENTATIONS OF TENSION CRACKS WITHIN SHEAR ZONES

Shear zones are expressed in many places by *en echelon* tension cracks, and the primary fractures in broad shear zones are the tension cracks (Johnson and Fleming, 1993; Johnson and others, 1993, 1994; Lazarte and others, 1994). There is significant difference in the angle between the traces of the walls and the traces of the cracks in the shear zones. In this section, we examine the controls on the angle.

Shear-Zone Model

Although the magnitudes of the principal stresses within the belt of shear zones at Landers are unknown, we do know that the deformation responsible for the tension cracks was not pure shear oriented parallel to the walls of the shear zone, as is commonly assumed for simple shear along a fault zone. If the deformation were simple shear, the tension cracks would be oriented 45° (not 30° to 40°) clockwise from the walls of a right-lateral shear zone. The strong preferred orientation of the tension cracks at Landers indicates that the direction of crack propagation parallel to the ground surface was *stabilized* (Cottrell and Rice, 1980; Cruikshank and others, 1991a, p. 875), so the principal stress parallel to the fractures was either zero or compressive. Simple shear parallel to the belt, plus additional pure shear with maximum tension normal to the belt, would provide the orientations of cracks we observe, as well as the necessary compression to stabilize the propagation direction of the tension cracks.

Our interpretation of the stresses near the ground surface, plus the observation that the tension cracks are localized within a distinctive zone a few meters wide, or in a belt a few hundred meters wide, and are absent in ground on either side of the zone or belt, suggest a model in which the ground surface was subjected to localized shearing plus dilation by a broad shear zone at greater depth. This conceptual model is closely related to that which we proposed to explain *en echelon* cracks and thrusts along strike-shift shear zones within the Twin Lakes landslide in Utah (Fleming and Johnson, 1989). At that time, though, we were not attuned to evidence for a zone of combined dilation and shearing, accepting instead the traditional interpretation of a single fault at depth (e.g., Reid, 1910; Pollard and others, 1982).

Our current conceptual model predicts that a combination of shearing and dilation in a shear zone at depth would produce shearing and *tension* in consolidated, near-surface alluvium, so that the tension cracks would tend to be oriented at angles of less than 45° to the walls of the shear zone. There is compression normal to walls of the shear zone below, and tension normal to the walls of the shear zone above. The change in normal stress is a result of the tendency for the shear zone to dilate and the consolidated alluvium to resist dilation. Since the material in the shear zone is coupled in terms of shear to the material in the overlying consolidated alluvium, the deformations and stress states of the two materials are compromised via shear stresses generated at the interface between the shear zone and the brittle alluvium. In this way we can understand the orientations of the tension cracks resulting from a combination of shear stress (which would produce cracks at 45° to the walls of the shear zone) and tension (which would produce cracks parallel to the walls of the shear zone), causing net orientations between 0 and 45°. Thus, the conceptual model qualitatively explains the orientation of the tension cracks.

Two phenomena explained by the conceptual model of a shear zone below and brittle alluvium above are the presence of *numerous* tension cracks at the ground surface between the walls of the belt and the *total absence* of tension cracks on either side of the belt. External loading from the sides of the shear zone at the ground surface—

loading by blocks of ground on either side of the shear zone—would produce only a few tension cracks because the growth of a single tension crack (or a few cracks) would relieve the applied stresses throughout the zone.

To visualize how the shear zone would produce numerous tension cracks, note that the horizontal shear stress vanishes at the ground surface, and that it is the gradient in horizontal shear stress that induces the tension in the brittle alluvium. This is verifiable qualitatively by examining the three-dimensional differential equation of equilibrium for a horizontal direction in terms of stresses (e.g., Johnson, 1970). Because of coupling of the shear zone to the base of the brittle alluvium through an interface, a single tension crack will relieve the tension only locally; and the brittle crust nearby remains in tension, transmitted via a shear stress gradient from the interface to the ground surface. For this reason, many tension cracks can form, side by side (also, see Lachenbruch, 1962).

Using the same arguments, but in counterproof, we explain the lack of tension cracks in ground outside the walls of the belt in terms of insignificant shear stress gradient in that ground because the shear zone is lacking beneath it.

We can proceed one step further, and compute the ratio of the increment of normal strain and the increment of simple shearing, $\delta\varepsilon_n/\delta\gamma_s$, within the shear zone, below, responsible for the orientation of the tension cracks in the consolidated alluvium above. As shown elsewhere, the ratio of strain increments can, in some circumstances, be related to the *angle of dilatancy*, β, of the material in the shear zone (Johnson, 1995). In dilatant shearing, the increment of simple shearing, $\delta\gamma_s$, and the increment of normal strain perpendicular to the shear zone, $\delta\varepsilon_n$, are related through the angle of dilatancy, β.

$$\tan(\beta) = \delta\varepsilon_n/2|\delta\varepsilon_s| \qquad (1)$$

Because the increment of normal strain parallel to the dilatant shear zone, $\delta\varepsilon_t$, is zero, however, the orientation of the principal extension in the shear zone is,

$$\tan(2\theta) = 2\delta\varepsilon_s/\delta\varepsilon_n \qquad (2)$$

In these equations, θ is the clockwise angle between the walls of the shear zone and the trace of the plane across which extension is a maximum, $\delta\gamma_s$, the shear strain is positive if right-lateral, and $\delta\varepsilon_n$ and β are positive if dilative (negative if contractive). Combining these results, we can determine the orientation of maximum extension in the shear zone at depth in terms of the angle of dilatancy:

$$\tan(2\theta) = \cot(\beta)\ \mathrm{sgn}(\delta\varepsilon_s)$$

or

$$\theta = [(\pi/4) - \beta/2]\ \mathrm{sgn}(\delta\varepsilon_s) \qquad (3)$$

in which β is angle of dilatancy and $\mathrm{sgn}(\delta\varepsilon_s)$ is +1 if the shearing is right-lateral, and -1 if the shearing is left-lateral. This is the general case, for right- and left-lateral shearing.

Curiously, this equation (3) for the orientation of tension cracks within shear zones is identical in appearance to the Coulomb expression for orientations of shear bands in a body of granular material,

$$\alpha = \pm [(\pi/4) - \phi/2]$$

in which ϕ is angle of internal friction. Here θ is the clockwise angle between the trace of the wall of the shear zone and the trace of the tension crack (i.e., the maximum compression direction) *within the shear zone*, whereas α is the angle between the direction of maximum compression *within a deforming body* and the trace of the conjugate, Coulomb shear bands within the body.

Example of Dilation

Photogrammetric measurements of displacements and deformations within the Tortoise Hill ridge provide rather detailed information about the horizontal dilation of rock within the ridge and within the belt of shear zones. As described elsewhere (in following pages. Also, see Fleming and others, 1997; Fleming and Johnson, 1997), Tortoise Hill ridge grew about one meter in altitude as the belt of shear zones about 400 m wide, including the ridge, accommodated about 3 m of right-lateral shift. We used aerial photographs (1:6,000 scale) taken before and after the Landers earthquake to determine the kinematics with the ladder of braced quadrilaterals shown in Figure 11 and Plate 5. The horizontal and vertical differential displacements of corners of the quadrilaterals are shown in Figure 11. The vertical differential displacements, du(z), and the components of the horizontal displacements parallel du(y') and normal du(x') to the eastern wall of the fault zone, are shown in Table 1 (original data presented in an appendix paper by Fleming and others, 1997). The displacements are relative to two points of Quadrilateral 2 southwest of the Emerson fault zone. Corners of the quadrilaterals are assigned a letter, A, B, C or D, in a clockwise sequence, starting at the northernmost corner of each quadrilateral. The pattern is shown by the letters in Table 2. Thus, points C and D are the fixed points of Quadrilateral 2. The vectors obtained by (vector) addition of horizontal components du(x') and du(y') are shown in Figure 11.

Figure 11. Map showing fractures bounding margins of Tortoise Hill ridge and differential displacements measured photogrammetically. A ladder of quadrilaterals extends across the ridge. At southeast edge, displacements were measured by land survey of regional grid. Maximum horizontal shift across ridge about 2.65 m. Maximum vertical displacement, relative

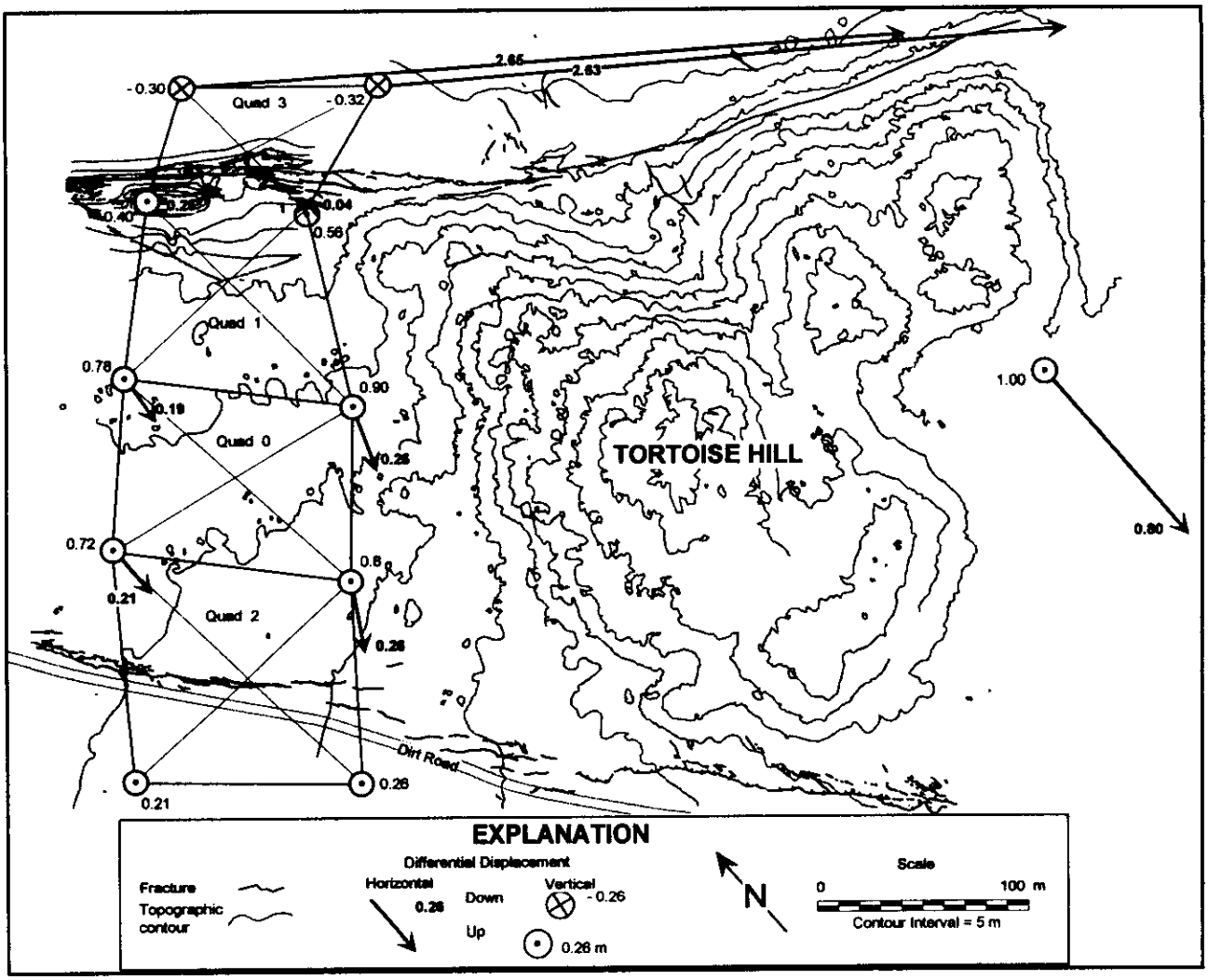

Figure 11. Map showing fractures bounding margins of Tortoise Hill ridge and differential displacements measured photogrammetically. A ladder of quadrilaterals extends across the ridge. At southeast edge, displacements were measured by land survey of regional grid. Maximum horizontal shift across ridge about 2.65 m. Maximum vertical displacement, relative

to an assumed fixed point about 6 km south of ridge, is 1.0 m at center of ridge.

Table 2. Relative Displacements of Corners of Quadrilaterals at Tortoise Hill

(C and D of Quad 2 held fixed)

		du(x',m)	du(y',m)	du(z,m)		du(x',m)	du(y',m)	du(z,m)
	A	2.64	0.18	-0.62	B	2.62	0.21	-0.69
Quad 3					(3)			
	D				C			
		0.24	0.049	0.12		0.01	0.04	0.13
	A				B			
Quad 1					(1)			
	D				C			
		0.11	-0.16	0.54		-0.09	-0.24	0.58
	A				B			
Quad 0					(0)			
	D				C			
		0.13	-0.16	0.49		0.051	-0.26	0.50
	A				B			
Quad 2					(2)			
	D	0.0	0.0	0.0	C	0.0	0.0	0.0

Using this quadrilateral network we found that the walls of the Emerson fault zone (including the ridge) dilated, but the ground within the ridge itself dilated slightly more. The data in Table 1 indicate that there was net dilation of 0.18 to 0.21 m between the most distant points of Quads 2 and 3. That is, the horizontal distance from a point *outside* the ridge on the southwest to points about 350 m away, outside the ridge in the northeast, increased in length by 0.18 to 0.21 m. The dilation is slightly larger, 0.21 to 0.30 m, for the most distant quadrilateral corners *within* the ridge, that is, from the lower corners of Quad 0 to points about 170 m away, at the upper corners of Quad 1. Thus the ground within the ridge is, in effect, spilling over the walls of the Emerson fault zone. Although we have suspected such dilation in fault zones (Johnson, 1995), it had not previously been measured.

The dilation within the ridge is expressed in part by a reverse fault dipping about 45° toward the northeast on the southwest side of the ridge, and a very high angle reverse fault dipping about 86° toward the southwest on the northeast side of the ridge (Plate 5). These faults, though, do not account for the net dilation of 0.18 to 0.21 m for points outside the ridge.

With respect tc the present discussion, the notion is that a dilating body, analogous to Tortoise Hill ridge, lies below a blanket of compact alluvium, and the dilation and shearing are expressed at the ground surface.

Application to Measurements

Unfortunately, we have only three documented examples of orientations of tension cracks within shear zones and belts of shear zones. The examples are in areas we mapped in detail (e.g., 1:200 scale) within a few weeks of the earthquake. The tension cracks soon eroded and filled, and a year later, when we returned to complete the mapping, most of the tension cracks had vanished.

Fortunately, we mapped key areas. Probably the most important is the Two Ranches area (Plate 1) along the Homestead Valley fault zone, which we have described in previous pages and elsewhere (Johnson and others, 1993, 1994). The tension cracks occur throughout the belt, so the entire belt appears to be a broad shear zone. Traces of individual tension cracks within the belt extend irregularly for 1 to 10 m. Although variable, their openings are generally a few millimeters to perhaps a centimeter. They

have rough walls—characteristic of tensile failure—and their traces are extremely irregular. The overall trends of the traces of the tension cracks, however, are remarkably consistently north-south throughout the Two Ranches area. The orientation of tension cracks near the center of the belt of shear zones is 34° or 35° clockwise with respect to the northeast wall of the belt and 30° clockwise with respect to the northwest wall of the belt.

Insofar as the assumptions behind the theory in eq. (3) are relevant to the formation of the tension cracks in the Two Ranches area, we can use the orientation of the tension cracks to assess the state of deformation in the shear zone, below. Thus, if we assume that the maximum tension in the near-surface alluvium corresponds to the maximum extension in the underlying broad shear zone, then for the Two Ranches area $\text{sgn}[\delta\varepsilon_S] = +1$, $\theta = +30°$, and therefore, eq. (3) indicates that the angle of dilatancy is $\beta = +30°$ for deformation in the broad shear zone. This angle of dilatancy is similar to that computed for deformation bands in Entrada Sandstone in Utah (Johnson, 1995).

The tension cracks within the Happy Trail shear zone (Plate 1), described in previous papers (Johnson and others, 1993, 1994), are oriented about 35° clockwise from the traces of the walls of the shear zone. If we assume that the maximum tension in the near-surface alluvium corresponds to the maximum extension in a broad shear zone below, then for the Happy Trail area, we have $\text{sgn}[\delta\gamma_S] = +1$ and $\theta = +35°$, and therefore, the angle of dilatancy is $\beta = +20°$ for deformation in the shear zone.

The surficial materials in the Single Tower Transmission Line area, along the Emerson Fault zone (Plate 3), are much softer than those in the Two Ranches area, indicating that the tension cracks were quite poorly developed, even immediately after the earthquake. As indicated on Plates 2 and 3, though, we were able to map tension cracks in some areas within the belt of shear zones. They are the features shown with short line segments oriented roughly north-south about 80 m southeast, and most of the fractures shown between 40 and 100 m northwest of the Single Tower Transmission Line road. The former are closer to the southwest wall and the latter are closer to the northwest wall of the belt. In both areas, the tension cracks are oriented at clockwise angles of 40 to 45° from the trend of the northeast wall of the belt of shear zones. If we assume that the maximum tension in the near-surface alluvium corresponds to the maximum extension in a broad shear zone below, then we have $\text{sgn}[\delta\gamma_S] = +1$ and $\theta = +40$ to 45°, and therefore, the angle of dilatancy is $\beta = +0$ to 10° for deformation in the broad shear zone. This angle is much smaller than that for the consolidated alluvium. It is similar to that of some kink bands in the Appalachians and in clay at certain water contents (Johnson, 1995).

Thus, the orientation of tension cracks appears to be a function of the physical characteristics of the material in the shear zone beneath the ground surface.

KINEMATICS OF *EN ECHELON* SHEAR-ZONES AND FAULT ELEMENTS

The kinematics of individual *en echelon* fault elements (or cracks) are basic to understanding the structural significance of arrays of cracks and fault elements.

Fault Elements

Fault elements within shear zones are nearly as common as tension cracks, but carry a different kinematic signature. In complex structural situations, they are very useful guides to deformational behavior.

En echelon faults were common in the fault zones of landslides in Utah (Fleming and Johnson, 1989), where they appeared to represent blades of an underlying strike-slip fault that reached the ground surface before the main strike-slip fault. The strike of their traces deviates about 10° from the strike of the fault zone (Fleming and Johnson, 1989, fig. 13). In one landslide, a detailed map of fifteen fault elements over a horizontal distance of 40 m shows that orientations of the fault elements range from parallel to 20° clockwise (for a right-lateral shear zone) with respect to the trend of the fault zone. Traces of the elements range in length from a few tens of centimeters to about 200 cm. At the ground surface, many of the fault elements are open and have thus become complex fractures as a result of continuing displacement of the landslide. We can recognize the complex history and that the fractures originated as mode II or mode III structures (faults) because the surfaces of the fault elements are slickensided to within about 5 cm of the ground surface.

There are two obvious differences between the tension cracks and the fault elements in the landslides. First, the traces of tension cracks tend to be oriented 30 to 45° clockwise, whereas those fault elements tend to be oriented 5 to 20° clockwise to the trend of the walls of the right-lateral fault zones. Second, the surfaces of the tension cracks are rough and irregular, whereas those of the fault elements are smooth and slickensided a few centimeters below the ground surface.

In the coseismic shear zones at Landers, the long tension cracks and the fault elements both have traces of several meters to about 10 m. The traces of right-lateral fault elements are oriented at a small clockwise angle, whereas the traces of the tension cracks are oriented at a large clockwise angle to the walls of right-lateral shear zones. The surfaces of all fractures we could observe within a few centimeters of the ground surface were rough and therefore non-diagnostic. We did not excavate.

The foregoing generalizations about differences in orientations of tension cracks and fault elements would be circular if the orientations were used to ascertain the origin

of a fracture (as pointed out so clearly by Gilbert, 1928). Probably the best method to distinguish between tension cracks and fault elements in the absence of slickensides is at the terminations of the fractures. A strike-slip-fault segment carries displacement parallel to the trace of the fracture. At the tip of the fracture, the displacement is transferred to an adjacent *en echelon* fracture either through compressive structures (buckle folds, thrust faults, domes, etc.) or tension cracks that develop as opening fractures extending obliquely from the ends of the fault elements (Fleming and Johnson, 1989). The compressive structures are expected between tips of adjacent fault elements because of the sense of stepping. Right-lateral segments step left, and left-lateral segments step right. The tips of *en echelon* tension cracks carry no structures at their tips. Continued shear displacement of a group of *en echelon* tension cracks produces further opening and rotation of the cracks into a sigmoidal form.

Gilbert's Law of Oblique Fault (Restraining) Branches

An important type of *en echelon* faulting was recognized by G.K. Gilbert, both along the 1906 earthquake rupture zone north of San Francisco (Gilbert, 1907; Lawson, 1908) and along normal faults near Salt Lake City. According to the latter Gilbert (1928, p. 13):

> "Slipping surfaces of another class are not parallel but oblique to the main fault surface. Their obliquity follows a law, and the law is illustrated by analogous phenomena connected with the California earthquake of 1906. The fault movement which caused that earthquake was horizontal, on a plane trending northwest. .....The visible expression of the faulting was mainly in a surface mantle of earth and included a system of oblique cracks, such as are shown diagrammatically in [Figure 2]. In places (a, [Figure 2]) the fault trace included two walls, with relative displacement as indicated by arrows, and between them a belt of broken earth. The principal cracks within the belt were oblique, as indicated. In other places (b, [Figure 2]) the walls were not developed and the fault trace consisted of a system of oblique cracks, as indicated. From the walls of the fault trace ran branching cracks (c, [Figure 2]), the divergence being at various angles but always to the right of one looking along the trace. The trace in places (d, [Figure 2]) swerved to the right and gradually disappeared, to reappear at the left en échelon.
>
> ...The law, both theoretic and empiric, is that the planes of oblique subsidiary slipping surfaces associated with a fault all deviate in the same way from the plane of the fault. In connection with a normal fault their deviation is toward the vertical; in connection with a reverse fault, toward the horizontal (see [Figure 3]). The law applies to oblique slickened partings within the fault rock, as well as to those in wall rock, and is of service in determining the direction of slip on the principal fault plane."

Thus, *Gilbert's law of oblique fault branching* is a statement, in effect, that faults branch to form what has become known as a restraining step. Indeed, *en echelon* fault elements commonly are arranged with that pattern.

Releasing and Restraining Steps

Examination of any fault system, though, indicates that fault elements step (or jog) in both restraining and releasing configurations. Restraining steps form where right-lateral segments step to the left, or where left-lateral segments step to the right (in short, "opposite-stepping"). Releasing steps form where right-lateral segments step to the right or where left-lateral segments step to the left (in short, "same-stepping").

In a study of strike-slip fault elements in Utah sandstones (Cruikshank and others, 1991a), we found where parts of a single fault had restraining steps and releasing steps along its length. In a study of strike-slip faults bounding landslides in Utah (Fleming and Johnson, 1989), our findings were the same, but most newly–formed fault elements had "opposite steps." Thus the newly–formed segments followed Gilbert's law of oblique faulting. There were, however, some releasing steps as well.

Kinematic Analysis of *En echelon* Zones

Geometry

In order to describe the two-dimensional kinematics of *en echelon* faults or cracks, we need to consider several geometric quantities, including the *walls*, the *width*, and the *spacing*, of the *en echelon* zone (Figure 12A). The walls are imaginary lines, or traces of fault elements, that bound the *en echelon* zone. The walls are oriented at a certain angle, θ, measured (for example) counterclockwise from east. The spacing of the walls is the width, w. The spacing (average, generally) of the *en echelon* segments is s. The (counterclockwise) orientation of the *en echelon* segments relative to the walls is α. These quantities uniquely describe the essential features of a simple pattern of *en echelon* fault or crack elements. We can also relate the geometry of the *en echelon* pattern to the length, ℓ, of an *en echelon* fault element and to the overlap, o, of adjacent fault elements (as defined in Figure 12A). Thus,

$$\ell = w/\sin(\alpha) \qquad (3a)$$

$$o = s/\tan(\alpha) \qquad (3b)$$

$$(o/\ell) = (s/w)\cos(\alpha) \qquad (3c)$$

With these quantities we can completely describe a simple set of *en echelon* fault or crack elements. For example, Figure 12A shows a series of *right-stepping, en echelon* segments and Figure 12B shows a series of *left-stepping en echelon* segments. Whether they are left-stepping or right-stepping depends on the angle α. If α is between 0 and 90° (or between 180 and 270°) (Figure 12A), the segments are right-stepping. If α is between 90 and 180° (or between 270 and 360°) (Figure 12B), the segments are left-stepping. Table 3 contains summary data for structures that we will be describing in following pages.

The ratio of the spacing of the fractures to the width of the fracture zone largely controls the appearance of *en echelon* fractures. The spacing of *en echelon* fractures in the zone is less than the width of the zone in the examples shown in Figure 12A and B, where the zone appears as a compact set of fractures.

The spacing is greater than the width in the example shown in Figure 13A, where the zone appears as offset fault elements or blades. This example resembles *en echelon* fault elements in a strike-slip fault in a landslide flank (Fleming and Johnson, 1989) and in some earthquake fault zones (e.g., Johnson and others, 1993, 1994).

Differential Displacement

Another essential piece of kinematic information concerning a set of *en echelon* faults or cracks is the direction (β) and magnitude (D) of the differential displacement across the walls of the *en echelon* zone (Figure 12A). In general we think of the differential displacement being parallel to the walls, and the only remaining question is whether the displacement is right-lateral or left-lateral, but in fact the problem is more complex. The direction of differential displacement may be oblique to the walls, in which case there might be strike slip as well as normal slip or separation along the *en echelon* segments. The normal slip may be compressional, in which case the fault elements accommodate thrusting as well as strike slip, or it may be extensional, in which case the fault elements accommodate normal faulting as well as strike slip.

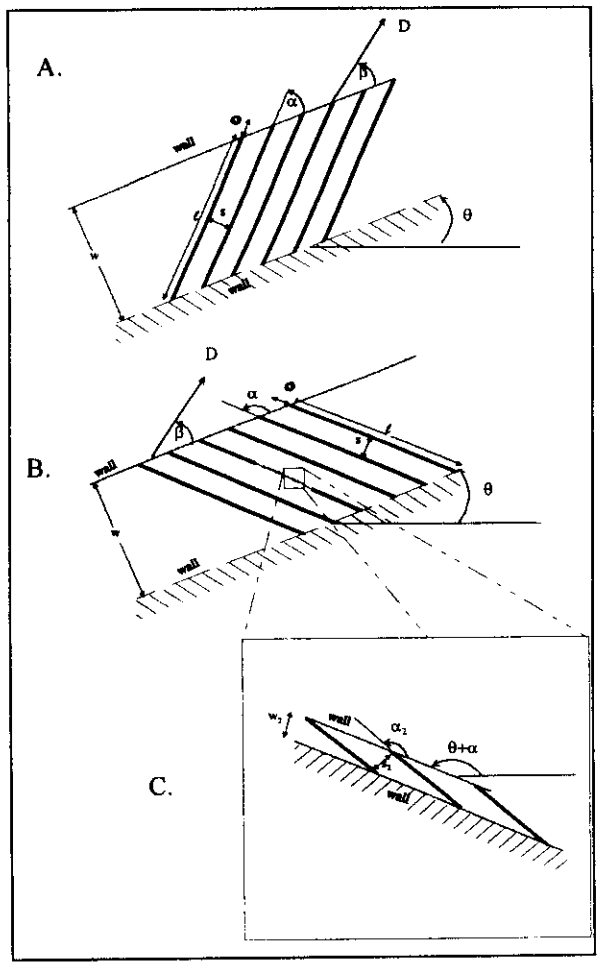

Figure 12. Idealized arrangement of *en echelon* faults or cracks, showing dimensions and angles measured to describe the geometry of such structures. A. Arbitrarily-oriented belt, showing differential displacement vector, *D*, of upper wall relative to lower. The dimensions and angles characterize the geometry of the elements. In this case the *en echelon* fractures are at an acute angle, α, to the walls. B. The *en echelon* fractures here are at an obtuse angle to the walls. Otherwise, the same as in A. C. Each element of an *en echelon* fracture may, itself, be composed of shorter *en echelon* elements, as shown in this detail. Note that the walls for these smaller *en echelon* elements are parallel to the larger elements comprising the larger *en echelon* structure.

Table 3 Geometric Elements of Duplex and *En echelon* Structures at Landers

(lengths in meters)

*Name**	*Width (w) of echelon zone (m)*	*Spacing (s/w) of echelon segments*	*Shift (D/w) across echelon zone*	*Orientation (a) of echelon segments*	*Overlap (o /w) of bounding segments*
STTL	20	0.20	0.140	160°	4
Headquarters	86	0.13	0.014	150°	8.8
Within H.Q.	16	0.18-0.4	—	160°	—
H-E S.O.	560	0.5	0.005	130°	2.1
Kickapoo S.O.	810	0.23	0.004	120-170°	1.6
Within K.fault	230	0.6	0.01	160-170°	
Charles Rd.	100	0.4	—	170°	—
Within C.R.	12	0.2	—	163°	—
Two bikers	45	0.33	0.027	170°	—
Within T.B.	6	0.5	—	165°	—
Pipes Wash (LL)	5.5	0.6	—	15°	—

* Note:
H-E = Homestead-Emerson.
STTL = Single Tower Transmission Line site along Emerson fault zone.
H.Q. = Headquarters
S.O. = stepover
K. fault = Kickapoo fault zone
C.R. = Charles Road
T.B. = Two Bikers
LL = left-lateral (others are right-lateral)

In situations where the *en echelon* fractures separate blocks that are rotating (e.g., Ron and others, 1984), we can describe the slip between blocks in terms of the shift across the rupture zone (e.g., Fleming and Johnson, 1989; Johnson and Fleming, 1993). We have derived the following results (Johnson and Fleming, 1993) for *en echelon* tension cracks: In the derivation, we use the notation in Figure 12, except that δU is the component of shift across but parallel to the *en echelon* zone. δU is negative if shearing is right lateral. Assuming no change in width, w, of the shear zone, the increment of angle is related to the increment of slip through the relation (Johnson and Fleming, 1993)

$$\delta U = - w \csc^2(\alpha)\, \delta\alpha \qquad (4)$$

Further, δu is the increment of differential slip between a block bounded by fractures. As the block rotates, an increment of (left-lateral) slip, δu, between the blocks is proportional to the fixed spacing s of the tension cracks and the increase of angle, $\delta\alpha$, due to right-lateral shear

$$\delta u = s\, \delta\alpha \qquad (5)$$

Combining these results,

$$(\delta u/s) = - (\delta U/w)\sin^2(\alpha) \qquad (6)$$

in which the slip along tension cracks, δu, and the shift across the shear zone, δU, are both positive if left lateral, w and s are fixed, and α is the current angle between the walls of the shear zone and the tension cracks. Note that whatever the angle, if the shift, δU, across the zone is right lateral (negative), the increment of slip, δu, across the tension cracks will be left lateral (positive).

With eq. (6) we can relate the slip across *en echelon* fractures separating rotating blocks to the shift across the zone of *en echelon* fractures in terms of the orientation and spacing of *en echelon* fractures and the width of the *en echelon* zone.

Strike-Slip Duplex Structures

Many *en echelon* fractures or faults are part of a duplex geometry (Boyer and Elliott, 1982; Cruikshank and others, 1991b), in which there are shorter faults arranged *en echelon* between longer, stepping, bounding faults. The shorter faults are oriented at an acute angle to the bounding faults, whether the slip on the bounding faults is right lateral or left lateral. If the bounding faults step in a left sense (determined by looking along the trace of bounding faults), the angle is counterclockwise. If they step in a right-lateral sense, the angle is clockwise. In a *right-lateral duplex structure* of the type we observed at Landers, the bounding faults are right lateral, as are the internal faults within the duplex (Figure 14A).

Thus, whether there are bounding faults (and, if so, the geometry of bounding faults) is yet another important factor that determines the kinematic pattern of *en echelon* faults or shear-zones.

At Landers, duplex structures formed at several places along narrow, strike-slip shear zones or faults where faults

or shear zones step right, and the shift is right-lateral. We previously described duplex structures along strike-slip faults at Arches National Park in Utah (Cruikshank and others, 1991b). A difference is that the duplex structures at Landers formed at the ground surface where the vertical stress was zero, whereas those that formed in sandstone in Utah formed at a depth of several kilometers and, therefore, under large vertical stresses. In the area of Arches National Park there are some rather simple conjugate, strike-slip faults that accommodated a few centimeters of offset, and the faults are in segments that form restraining or releasing steps. For either type of step, there, the steps contain ramp faults and thus have the fault pattern of duplex structures. We have shown that the structures not only look like duplex structures, but that their internal kinematics are those of the classic duplex structure described along thrust faults (e.g. Boyer and Elliott, 1982, Johnson and Berger, 1989; Cruikshank and others, 1991b). Although the duplex structures form at restraining as well as releasing steps, left-lateral faults have predominantly right-steps, and right-lateral faults have predominantly left-steps, so the majority of the steps in the area are of the restraining type.

A. En Echelon Fault Segments

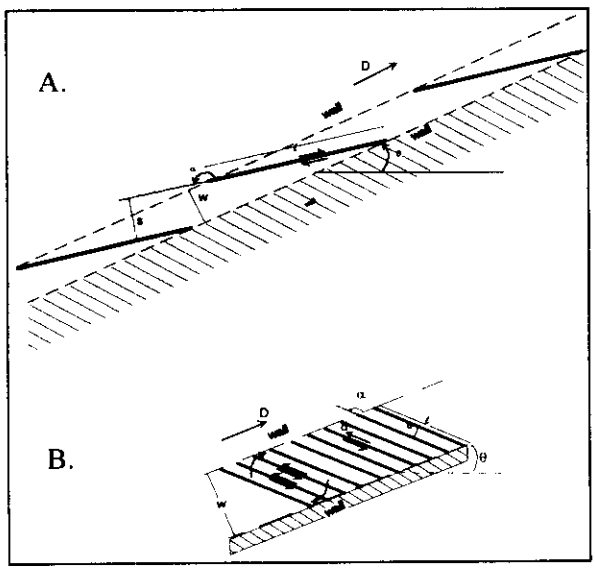

Figure 13. Some of the variation in *en echelon* zones that depends on the ratio of spacing of segments and the width of the zone. A. Typical geometry of restraining *en echelon* faults that slip in a right-lateral sense in a right-lateral, *en echelon* fault zone. B. Typical geometry of *en echelon* cracks that slip in a left-lateral sense as the blades of ground between the walls rotate during overall right-lateral shearing.

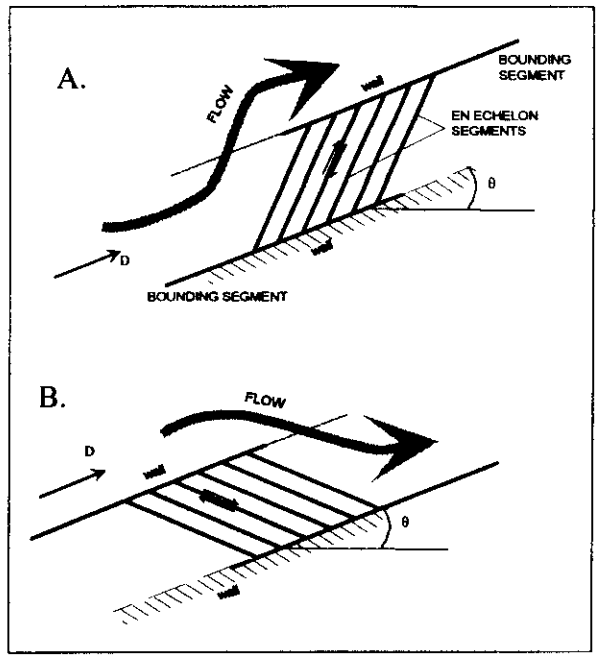

Figure 14. General flow patterns associated with duplex structures, consisting of *en echelon*, bounding faults and *en echelon* fault elements. A. Restraining duplex structure. B. Releasing duplex structure.

The duplex structures that we observed at Landers are all of the releasing type (Figure 14B).

PART II. SETTING OF STRUCTURES ALONG STRIKE-SLIP FAULT ZONES AT LANDERS

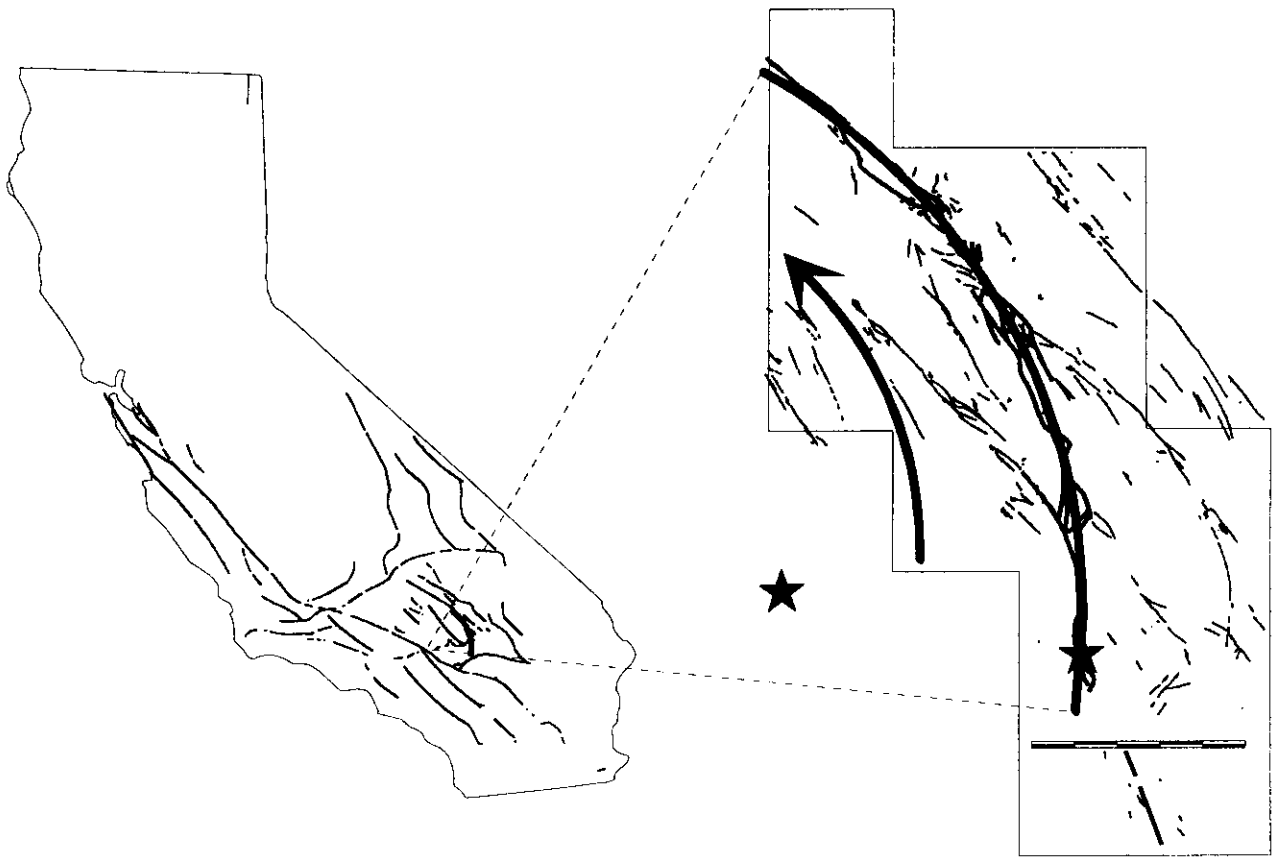

THE LANDERS-BIG BEAR STRUCTURE—A ROTATING BLOCK OR STRUCTURAL VORTEX

The faults that activated during the Landers earthquake are within the eastern California shear zone which, according to Dokka and Travis, 1990), is about 80 km wide and contains several right-lateral fault zones that accommodate 15 to 20 percent of the motion between the Pacific and North American plates south of the Garlock fault zone. The faults that ruptured to the ground surface during the Landers/Big-Bear earthquake sequence included parts of seven named faults within the eastern California shear zone. From north to south (Figure 15), the Camp Rock, Emerson, Maume (not shown), Homestead Valley, Johnson Valley and Eureka Peak faults all exhibited surface rupture along parts of their length. Only the northern third or half of the Emerson fault zone was activated; only the southern half of the Johnson Valley fault zone was activated, but most of the Homestead Valley fault zone was activated during the Landers earthquake.

In the practice of analyzing slip on earthquake faults, the traces of typical faults are considered to be straight. As a first approximation, deformation on faults is considered to be translational. As a result, we can describe the kinematics of faulting in terms of the differential displacement across the fault.

The Landers rupture is not, then, the typical rupture. As shown in the cover diagram of this report, the parts of the faults that produced surface rupture during the Landers earthquake formed a curved, *en echelon* set of right-lateral fault elements about ten kilometers long, stepping right. The east side of the rupture belt moved clockwise (south to southeast). Overall, the longer fault elements form a curve, with a center of curvature perhaps 80-90 km west of Landers near the San Andreas fault zone (Cover and Figure 15). Thus the first approximation to the deformation that was relaxed by the earthquake was not a right-lateral translation, but a counterclockwise rotation of a block or, in effect, a structural vortex, around a center in the San Andreas fault zone.

Figure 15. System of fault elements, totaling about 80 km length, that activated during the 1992 Landers earthquake sequence. A circular arc, with a radius of about 80 km, drawn through the fault elements has a center in area of San Bernardino. The segment has an included angle of about 60°, and cuts across the Pinto Mountain, left-lateral fault. (One could draw other arcs, with different centers that would also closely match the fault elements, but they would be within about 10 km of that shown.) Epicenters of main shocks of Big Bear and Landers earthquake sequences shown with stars.

The actual deformations, of course, could not be purely translational or rotational because fault ruptures end. For this reason the term vortex may be preferable to a rotating block. The rupture at Landers does not produce an entire circle—and the rotating block is joined to neighboring ground. Thus there had to be adjustments between the rotating block and its surroundings. Also, the Landers rupture zone is not a perfect circle, so there had to be adjustments even along the Landers rupture zone. Perhaps the internal adjustments during rotation led to the main shock of the Big Bear earthquake sequence that started shortly after the main shock of the Landers earthquake. The kinematics of stepping faults have been documented in several tectonic situations, but the possibility of rotations seems to have been ignored except at the global scale of plate motions.

The curved pattern of stepping fault ruptures at Landers is accomplished partially by a series of stepovers with their own distinctive patterns of surface rupture. Because the tectonic situation is one of right-lateral faults stepping right, the stepovers were all in a releasing mode. The stepovers between the 10-km fault elements tend to consist of fault elements an order of magnitude shorter, perhaps one to two kilometers long, oriented 30 to 45° clockwise relative to the trends of the longer fault elements (Figure 15).

The stepovers are of different types. The Camp Rock-Emerson fault stepover was principally through a series of tension cracks that are oblique to both fault zones. Two others are releasing duplex structures (Figure 14B). The Homestead-Emerson stepover, where the Emerson fault zone steps to the southwest to the Homestead Valley fault zone, and the Kickapoo stepover, where the Homestead Valley fault zone steps to the southwest to the Johnson Valley fault zone, are characterized by several right-lateral fault zones.

SOUTHERN LANDERS RUPTURE ZONES

Kickapoo Stepover (Releasing Duplex)

Sowers and others (1994) described the surface rupture in the Kickapoo stepover area as well as evidence for earlier faulting along the Johnson Valley fault zone[5]. The section of the fault zone centered on Linn Road, and extending northward to the vicinity of Happy Trail (Figure 16), is characterized by a series of west-facing scarps in older alluvium. In some places fault traces are on both sides of uplifted alluvium and represent tectonic ridges[6]. Vertical components of displacement along this stretch generally

---

[5] See, also, Unrhu and others, 1994; Spotila and Sieh, 1995.

[6] Sowers and others (1994) use the term, "pressure ridge."

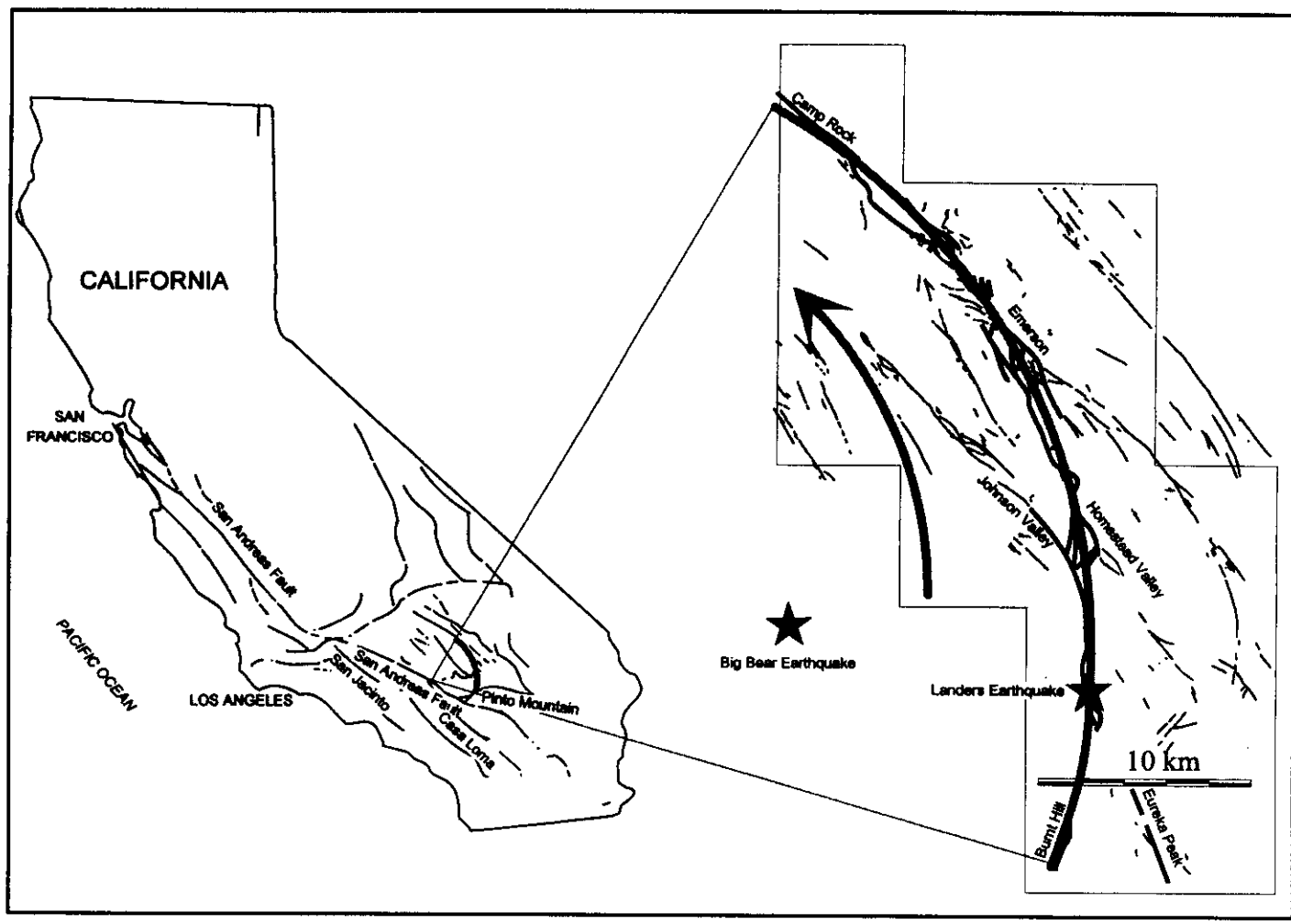

Figure 15. System of fault elements, totaling about 80 km length, that activated during the 1992 Landers earthquake sequence. A circular arc, with a radius of about 80 km, drawn through the fault elements has a center in area of San Bernardino. The segment has an included angle of about 60°, and cuts across the Pinto Mountain, left-lateral fault. (One could draw other arcs, with different centers that would also closely match the fault elements, but they would be within about 10 km of that shown.) Epicenters of main shocks of Big Bear and Landers earthquake sequences shown with stars.

mimic the vertical components in the geologic record (Sowers and others, 1994). In the northern part of the Johnson Valley fault zone, north of Happy Trail (Figure 16), the scarps are east-facing, and the fault zone separates a bedrock pediment on the west from thick alluvial deposits on the east.

The overall fault zone that makes up the Kickapoo stepover is composed of at least three narrow rupture zones that trend acutely to the bounding, Homestead Valley and Johnson Valley fault zones. The rupture zone that forms the west side of the stepover has been termed the Kickapoo fault by Sowers and others (1994). The Kickapoo fault is characterized by one to three main traces within a zone 50 to 100 m wide of dense, *en echelon* fracturing. There is evidence that the Kickapoo fault follows an older structure. Small knolls of late Pleistocene alluvium and bedrock extending through the young alluvium appear to be related to the restraining, left stepovers between fault elements.

Measurements, by Sowers and others (1994), of shift across fault zones throughout the stepover area, combined with data collected by other investigators, provide a good representation of the distribution of slip throughout the Kickapoo stepover area. Most of the shift, about 200 to 280 cm, is on the Kickapoo fault zone. The other two fault zones in the Kickapoo stepover contain 10 to 30 cm of right shift.

According to Sowers and others (1994) the cumulative slip on the bounding, Johnson Valley and Homestead Valley fault zones and the Kickapoo fault zones increases across the stepover from south to north. Their data on horizontal differential displacements across rupture zones (Figure 16) show that there is a progressive transfer of about three meters of right shift across the Kickapoo stepover, from north to south through the region (Sowers and others, 1994). The Johnson Valley fault zone, south of its junction with the Kickapoo fault, is the only large fault and accommodates about 95 percent of the right-lateral shift across the entire rupture zone. North of the junction of the Kickapoo fault with the Johnson Valley fault zone, the shift across the Johnson Valley fault zone decreases as the shift across the Kickapoo fault increases. From south to north, the Kickapoo fault accommodates about 25 percent, then 45 percent, and then 48 percent of the total shift in this area. Right-lateral shift is barely measurable on the Johnson Valley fault zone north of Bodick Road. At Bodick Road, the Kickapoo fault zone and the Homestead Valley fault zone each accommodate about 50 percent of the right-lateral shift. Where the Homestead Valley fault zone and Kickapoo fault join, about one kilometer north of Bodick Road, the net right-lateral shift is about 3.3 m (Figure 16).

Figure 16. Kinematic features of Kickapoo stepover between Homestead Valley fault zone and Johnson Valley fault zone. Horizontal offsets across individual rupture zones are indicated in centimeters. Data mostly from to Sowers and others (1994).

Rupture Zones in Homestead Valley

We have mapped several areas within the Kickapoo stepover, which we examined in Figure 16. We photogrammetrically mapped two areas along the Homestead Valley fault zone, one between Reche Mountain at the southern end of the rupture zone and the Mileska Ranch south of the Headquarters step, and the other north of the Goatsucker Hill ridge (Plate 1). Also, we photogrammetrically mapped two areas along the Johnson Valley and Kickapoo fault zones. One area is the area of the intersection of the Johnson Valley and Kickapoo fault zones. The other is the northern third of the Kickapoo fault zone and its intersection with the Homestead Valley fault zone. As indicted in earlier pages, photogrammetric maps show only traces of fractures, not kinematic information, in these areas. Detailed analytical maps, including kinematic information, were made for three areas on the Kickapoo fault zone and two areas on the Homestead Valley fault zone. Detail was obtained at the Crown and Pickle rift, the Charles *en echelon* zone, the Two Bikers *en echelon* zone, the Race Track half-rift, and the Happy Trail shear zone. The Happy Trail shear zone has been described elsewhere (Johnson and others, 1993, 1994). The Crown and Pickle rift and the Race Track half-rift will be described elsewhere (Fleming and Johnson, in prep.).

NORTHERN LANDERS RUPTURE ZONES

Rupture Zones along Emerson Fault

The Emerson fault zone is in the northern part of the 1992 Landers rupture (Figure 1). The fault was mapped by Dibblee (1964) and Jennings (1973) as extending some 55 km in a southeasterly direction from the vicinity of the Single-Tower Transmission Line road, south along the west side of Emerson Lake, to at least as far south as the latitude of Landers. About 20 km of the fault zone activated in 1992, extending from its northwest end southeast to the vicinity of Galway Lake. At its northwest end, it stepped through a series of ruptures northward to the Camp Rock fault zone. At its southeast end, it stepped through the Homestead-Emerson stepover southward across the mountain to the Homestead Valley fault zone (Figure 17). According to the California fault map by Jennings (1973), the Emerson fault zone is a right-lateral, strike-slip fault; it is a Quaternary fault without historic activity, meaning that it was active during the past two million years but not the past two hundred years. Plate 2 shows traces of fractures within part of the Emerson fault zone, which trends about

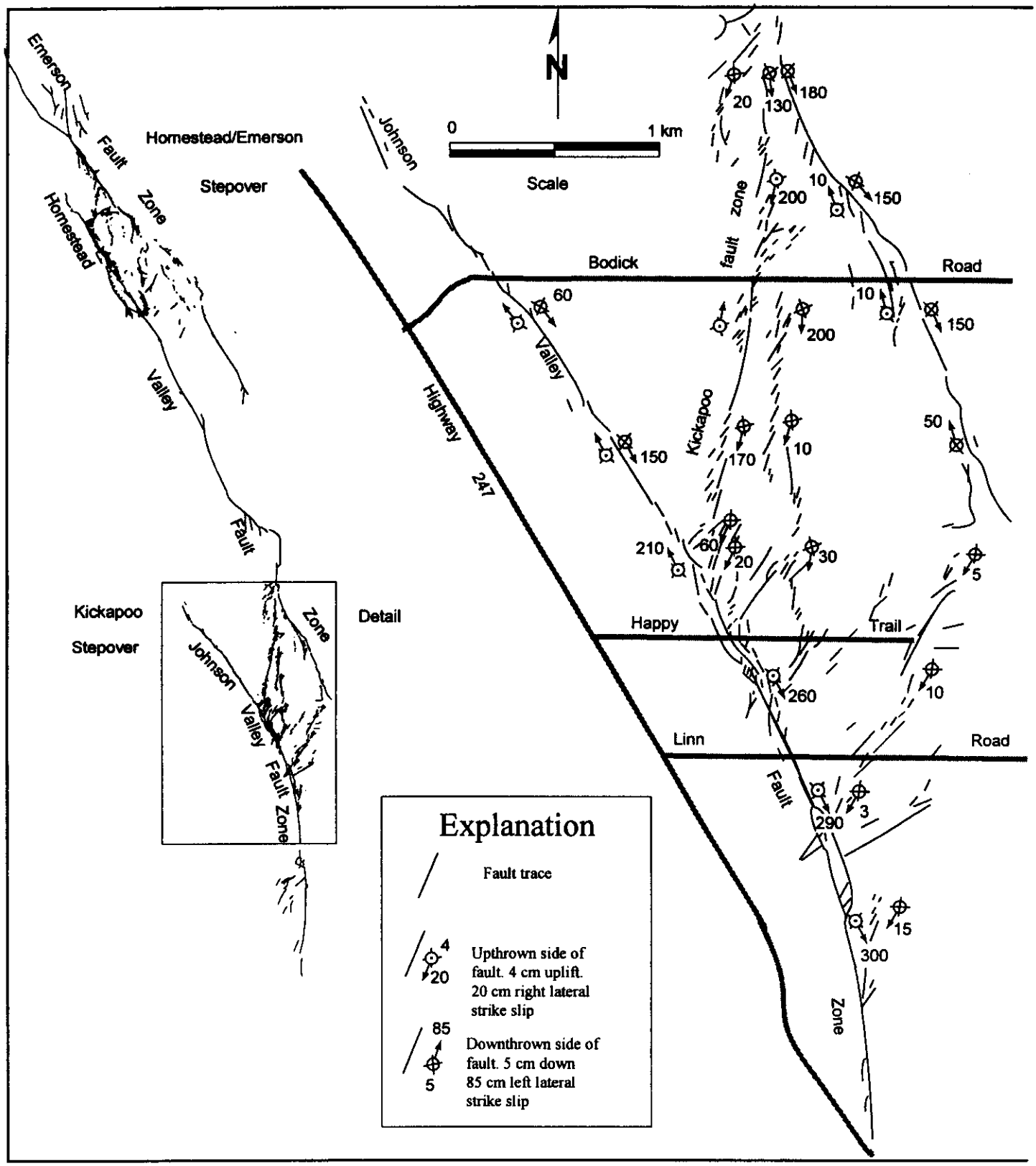

Figure 16. Kinematic features of Kickapoo stepover between Homestead Valley fault zone and Johnson Valley fault zone. Horizontal offsets across individual rupture zones are indicated in centimeters. Data mostly from to Sowers and others (1994).

N30°W between Tortoise Hill in the southeast and the Single-Tower Transmission Line[7] road in the northwest.

The Emerson fault zone accommodated about 290 cm of right-lateral shift at the Single-Tower Transmission Line and 300 to 310 cm at Tortoise Hill ridge. Shift on the Emerson fault zone caused the near collapse of one high-voltage transmission towers whose legs straddled the largest break (Plate 3) in the belt of shear zones. Using the distances between the legs of the deformed tower and the corresponding distances between the legs of a neighboring, undeformed tower, Fleming and others (1997) calculated that the part of the rupture passing beneath the powerline accommodated 270 cm of right-lateral differential displacement parallel, and 2 to 7 cm of dilation normal to the trace of the shear zone within the base of the tower (about 7.3 to 7.8 m sides). By sighting along the towers of the powerline, we determined that an additional 21 cm of right-lateral relative displacement occurred over a distance of about 200 m to the southwest of the deformed tower, making the total 291 cm.

An additional 69 cm of relative displacement of the powerline to the northeast of the deformed tower is attributed to transfer of right-lateral shift through a belt of tension cracks in the stepover between the Camp Rock and Emerson fault zones (Fleming, Johnson and Messerich, 1997).

Homestead-Emerson Stepover (Releasing Duplex)

The Emerson fault zone was mapped by Dibblee (1964) and Jennings (1973, 1994) as extending some 55 km in the southeasterly direction from the vicinity of the Single-tower Transmission Line (Section 15, T6N, R3E), along the west side of Emerson Lake, to at least as far south as the latitude of Landers (to Section 18, T2N, R7E). About half of the known extent of the fault zone activated in 1992; it extended about 25 km from its northwest end to the vicinity of Galway Lake. Near its northwest end it stepped through a series of tension cracks northwestward to the Camp Rock fault zone; and, at its southeast end, it stepped southward through the Homestead-Emerson stepover across a mountain to the Homestead Valley fault zone. According to the California fault map by Jennings (1973, 1994), the Emerson fault zone was recognized to be a right-lateral, strike-slip fault; it was known as a Quaternary fault without historic activity implying active slip between the past 200 and the past 2 million years.

The Homestead-Emerson stepover, between the Emerson and Homestead Valley fault zones (Figure 17), was described by Zachariasen and Sieh (1995) as an *en echelon* stepover, similar to the Kickapoo stepover. The features shown in Figure 17 were mapped on a photographic base at about 1:6000 scale and compiled at 1:12,000 scale. Additional map and kinematic data were obtained in the field. The Homestead-Emerson stepover is between fault elements of the Emerson and Homestead Valley fault zones, which overlap about 5 km and are offset here in a right step of about 2 km. Within the stepover are five right-lateral fault zones that project to, and nearly connect with the bounding fault zones. Thus, the structure is what we have termed a releasing duplex (Figure 14B).

The main trace of the Homestead Valley fault zone deviates from a straight line by only about 200 m over the entire length of overlap with the Emerson fault zone. Most cracks and splays associated with the Homestead Valley fault are on the east side of and within the stepover area. Fractures that have accommodated shearing are typically right lateral, but left-lateral fractures are common as well. The one splay on the west side bounds a long ridge, and the ground within the ridge has uplifted along faults on either side. The northwest part of the splay is a thrust that dips 20 to 25° east, under the ridge (Figure 17).

Figure 17. Kinematic features of Homestead-Emerson stepover between Homestead Valley fault zone and Emerson fault zone. Both vertical and horizontal components of shift across ruptures zones are indicated in cm. Data from Zachariasen and Sieh (1995).

According to Zacharaisen and Sieh, the faults that link the Emerson and Homestead Valley fault zones, forming the releasing duplex, strike north-south, and divide the ground into three slabs about 1 km wide. The largest of these linking faults is in the northernmost part of the duplex, and accommodates as much as 155 cm of right-lateral shift. Other, smaller linking faults accommodate 20 to 40 cm of shift.

The right-lateral shift on each of the faults in the Homestead-Emerson stepover changes in complex ways, according to Zacharaisen and Sieh (1995). The slip of the Homestead Valley fault zone near the southern end of the area (Figure 17) is about 3 m, but ranges from about 2 to 3.5 m. The shift on the Homestead Valley fault zone decreases from south to north, at a rate of about 0.2 m/km, to the intersection of the largest linking fault. At the first intersection, the shift decreases by about 1 m, and then decreases at a rate of about 0.5 m/km. Conversely, the right-lateral shift across the Emerson fault zone increases from south to north, to about 3.2 m where the largest linking fault joins its trace (Figure 17). This is close to the shift of 2.9 m measured at the Single-Tower Transmission Line Road and 3.1 m measured across Tortoise Hill ridge about 7 and 5 km to the northwest, respectively.

Zacharaisen and Sieh indicated that the vertical shift across faults in the Homestead-Emerson stepover is quite variable from place to place, without special patterns. In general, though, the vertical shift on the Homestead Valley fault zone is down on the northeast and that on the Emerson fault zone is down on the southwest, consistent with downdropping of the block of ground within the releasing

[7] Not to be confused with another place, about 2 km northwest, where the fault zone crosses two more powerlines.

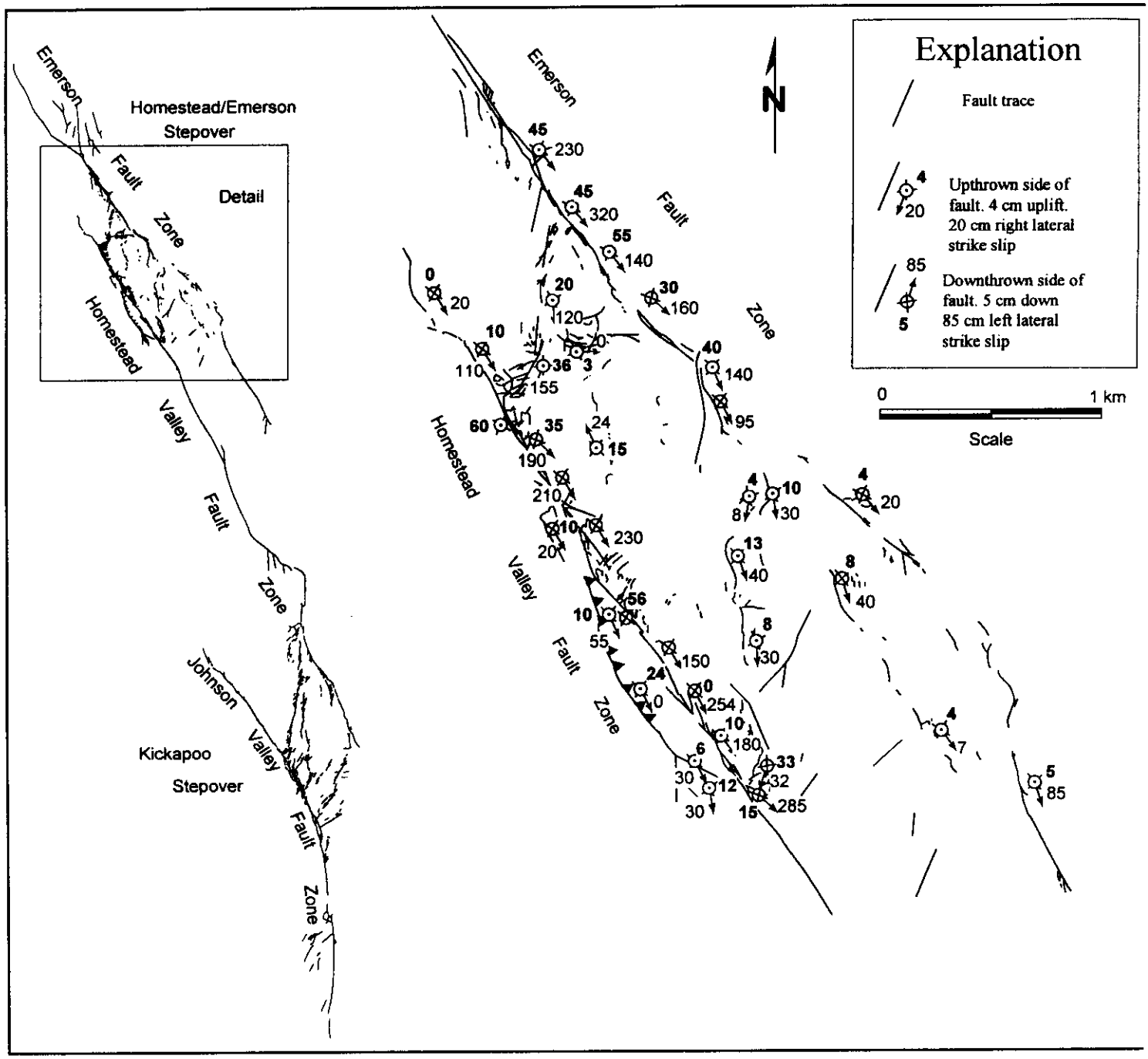

Figure 17. Kinematic features of Homestead-Emerson stepover between Homestead Valley fault zone and Emerson fault zone. Both vertical and horizontal components of shift across ruptures zones are indicated in cm. Data from Zachariasen and Sieh (1995).

duplex. They estimate that the hill containing the duplex subsided an average of 30 cm during the Landers earthquake sequence.

In our view, one of the most interesting results of their study (not mentioned in their paper) is the evidence for *reversal* of vertical tectonic movement that previously dominated in the area of the Homestead-Emerson stepover. We presume that the topographic ridge in the stepover is a tectonic ridge, resulting from some process that causes ridges along strike-slip faults to increase in height (some discussed by Fleming and others, 1997). The astonishing result is that, during the Landers earthquake sequence, the ground in the ridge did not rise; it subsided. This is as expected in a releasing step in a strike-slip system. The ridge has become the site of a developing pull-apart basin, so the present topography is opposite to the topography that was developing as a result of this earthquake sequence. This interpretation suggests that, at this locality, the organization of the faults and the kinematics of faulting during the Landers earthquake are quite different from those previously active along the Emerson and Homestead fault zones. This interpretation is consistent with the idea that, during the Landers earthquake, parts of fault zones were reorganized into a composite fault zone (Figure 15) that accommodated a kind of regional deformation that is not necessarily typical of previous regional deformations in this area. This is contrary to our observations at Tortoise Hill, which we describe in the next part.

THE GALWAY LAKE ROAD ROTATING BLOCK OR STRUCTURAL VORTEX

Whereas measurements of strike-slip offset for a single rupture zone along the Johnson Valley, Homestead Valley and Emerson fault zones indicate generally 3 to 4 m of right-lateral shift[8] (Sowers and others, 1994; Unruh and others, 1994), measurements across the Emerson Fault zone at Galway Lake Road range from nearly[9] 5 to 7 m of right-lateral shift (Sieh and others, 1993; Hart and others, 1993; Irvine and Hill, 1993; Hamilton, oral comm., 1996). The measurements at the road crossing are large relative to measurements elsewhere on the Emerson Fault zone. Displacement at the power-line road crossing of the Emerson fault zone, nearly 6 km to the northwest, was about 2.9 m. Displacement at the Tortoise Hill tectonic ridge along the Emerson fault zone (Fleming and Johnson, 1997), about 4 km to the northwest, was about 3.1 m. Displacements south of Galway Lake Road were reported to be 3.7 to 4.5 m (Hart and others, 1993).

Thus Galway Lake Road is in a region where overall displacement declines from perhaps 4 m in the south to 3 m in the north, and there is no obvious reason for the displacement to jump to 6 m locally.

Fleming and others (1997) investigated the causes of the local, high offset along the Galway Lake Road stretch of the Emerson fault zone, using a special photogeologic study of low- and moderate-altitude aerial photographs of this part of the Emerson fault zone. The purpose of the photogeologic study was to determine the structural setting of the site of anomalous fault offsets. Little did they realize that the study would cast serious doubt on the common practices of measuring offset across faults at the ground surface as well as in trenches. In the process of investigating the anomalous offset of the Galway Lake Road, Fleming and others (1997) discovered the Galway Lake Road rotating block, or structural vortex, a fault-related structure about 3 km long and 1 km wide. The rotating block, or vortex, is not covered by aerial photos at a scale of 1:2,500, which cover a strip only about 0.6 km wide, but it is evident in the aerial photos at a scale of 1:6,000, which cover a strip about 1.5 km wide.

The Fractures

Main Belt of Fractures

The main belt of shear zones along the Emerson fault zone is shown, without details, in Figure 18. Most of the displacement is carried in this main belt of shear zones. The trend of the main rupture belt is curved, but is oriented, overall, at about N30°W. Three places are principal points of reference on the main belt of fractures for the Galway Lake Road rotating block. Near the southern end of the rupture belt is Stanford Hill, a low hill between 40 and 50 m high, that has been described and informally named by Aydin and Du (1995). About 1.5 km to the northwest, the main rupture belt crosses Galway Lake Road. Another 1.6 km to the northwest, the main rupture belt crosses Bessemer Mine Road.

Figure 18 Map of the Galway Lake Road rotated block structure in which fractures that are not believed to be related to the structure have been removed. Remaining features that are shown are index contours (25 m), a few roads, and the belts of fractures. Also shown with letters are locations of a displacement measurement; data are in Table 1. The Galway Lake Road rotated block extends from Bessemer Mine Road to the southeast end of Stanford Hill; rotation contained at least 1.05 m of counterclockwise displacement.

Figure 19 Idealization of Galway Lake Road rotating block along the Emerson fault zone. In A, the photogeologic map shown

[8] This text is based on a paper (Fleming and others, 1997) that accompanies a photogeologic map of part of the Emerson fault zone in the vicinity of the site where the Galway Lake Road crosses the Emerson fault zone (Figure 1). Large slip has been reported for the 28 June 1992 Landers, California, earthquake (Ms 7.5).

[9] The range from 5 to 7 m offset at the crossing of the Emerson fault zone by Galway Lake Road is primarily a result of ambiguity caused by the irregularities of reference lines along Galway Lake Road and by curvature of the Emerson fault zone near Galway Lake Road. Differences in estimates of the angle between the trace of the rupture belt and the direction of the road could account for the entire range of reported offset.

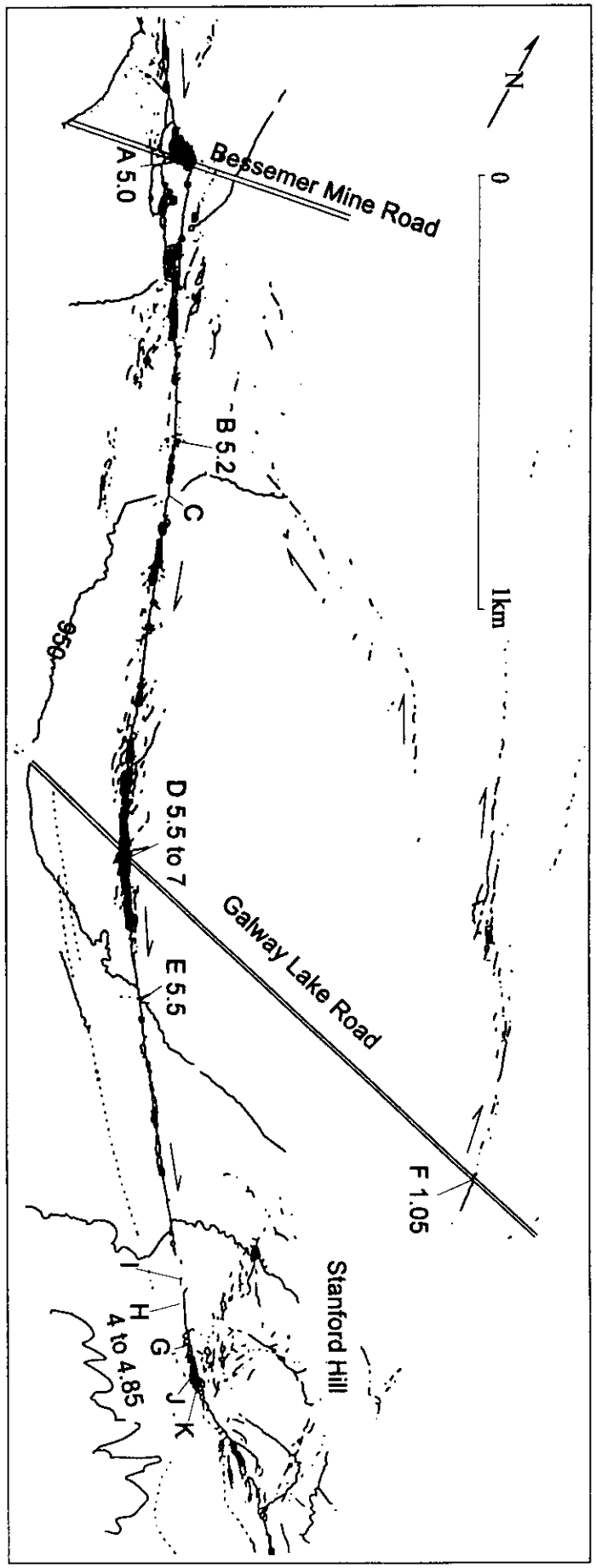
N
0
1km
Bessemer Mine Road
A 5.0
B 5.2
C
950
D 5.5 to 7
E 5.5
Galway Lake Road
F 1.05
Stanford Hill
H
G
4 to 4.85
J
K

Figure 18

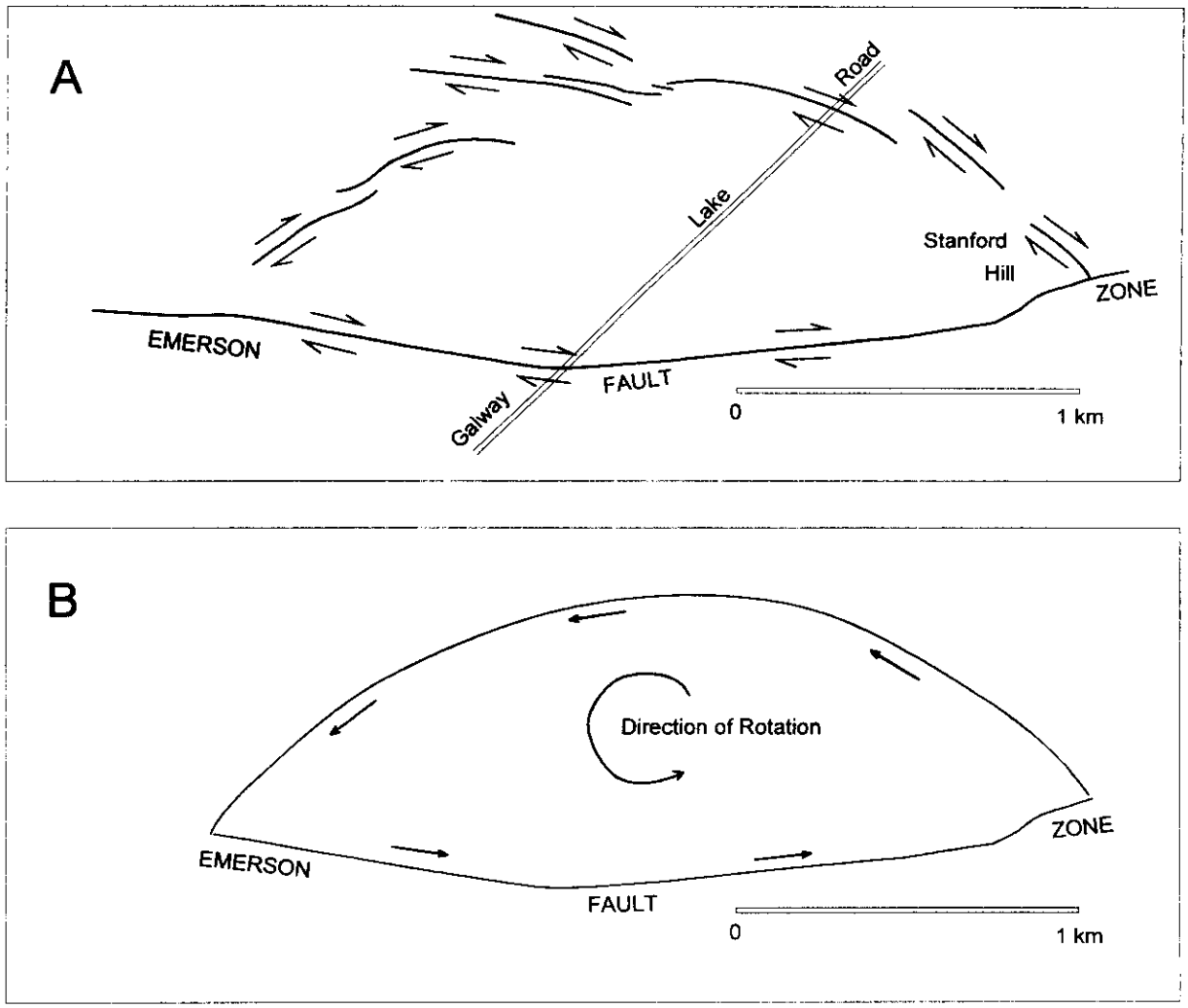

Figure 19 Idealization of Galway Lake Road rotating block along the Emerson fault zone. In A, the photogeologic map shown

in Figure 18 is simplified to a series of simple fault segments, all accommodating right-lateral slip. In B, the fault segments are joined into a football-shaped block that rotates relative to its surroundings because all the fault offsets are right-lateral.

The main fracture belt is intensely broken by a large number of vertical fractures, the traces of which are mostly parallel or oriented 10-20° clockwise with respect to the trend of the belt. The intervening ground between visible fractures is also highly broken, and the rupture belt has a bulged or "mole-track" appearance that is evidently a result of dilation of material in the shear zone. Our experience in detailed mapping in the main belt of fractures (Johnson and others, 1993, 1997) is that all kinematic types of individual fractures may occur within the zone. Most common features are tension cracks and short, right-lateral fault elements that are oriented a few degrees to 45° clockwise to the trend of the fracture belt. There are also thrusts, normal faults, oblique-slip faults, and even left-lateral faults, however, within the right-lateral fault zone.

The main fracture belt varies from a single fault, or very narrow shear zone, about 450 m northwest of Galway Lake road, to a broad zone perhaps 25 m wide at Galway Lake road. Typically, the belt of intense fracturing ranges from 10 to 15 m width. Associated with the main fracture belt are a few groups of fractures that appear to extend away from the main belt at a clockwise angle of about 30°. This type of fracture, which also carries right-lateral shift, was termed "splintering" by H. F. Reid (1910) and was noted by several different investigators in surface rupture produced in the 1906-San Francisco earthquake. Zones of splintering fractures are on the northeast side of the main rupture belt to the northwest of Galway Lake Road, and on the southwest side of the main rupture belt to the southeast of Galway Lake Road. Within the map area, splintering fractures are typically associated with a change in orientation of the main rupture belt.

Peripheral Fractures and Fracture Zones

Peripheral fractures and fracture zones are the indicators or illustrators of the geologic structures. In the absence of peripheral fractures, the main rupture belt would simply contain right-lateral, strike-slip movement. The peripheral fractures that are outside the main rupture belt indicate that more deformation occurred than simple strike-slip motion. These fractures, which typically occur in long narrow zones, are generally tension cracks or right or left-lateral fault zones but can have virtually any kinematic function. Curiously, where the peripheral fractures approach the main belt of fractures, they cannot be traced to intersect with it. This aspect of non-intersection of the fracture traces was noted throughout the Landers earthquake rupture belt, by us as well as others (Aydin and Du, 1995). Most likely, the segmented aspect of these fractures results from the fact that the propagation direction of the deformation was upward and not parallel to the rupture traces.

The way that we interpret geologic structure from the fracture patterns is as follows: The expectable pattern for pure strike-slip faulting is a belt of fractures from a few meters to perhaps 200 m wide that is interpreted to be the fault zone (Johnson and others, 1994). Fractures in the ground surface that are outside of (peripheral to) this simple belt reflect deformation that is related to but not part of pure strike-slip faulting. The additional deformation produces a recognizable geologic structure that is adjacent to but not part of the main rupture belt. Thus, the interpretation of structure is deduced from interpretation of the kinematic function of the zones of peripheral fractures in the overall context of the strike-slip deformation. The differential displacement accommodated by individual fractures is lumped with that of other fractures accomplishing the same deformation, proceeding from detailed to schematic.

The vertical movement within and along the main rupture belt can be inferred from the shape of the contour lines where they cross the zone. Contour lines that cross the main rupture belt are inferred to have been smooth curves before the earthquake. Any disruption of a smooth curve after the earthquake is interpreted to be a result of differential vertical movement during the earthquake. For example, the 885 m contour that crosses the rupture belt about 900 m northwest of Galway Lake Road is apparently bulged over a width of nearly 200 m. This same contour line, about 300 m southeast of Galway Lake Road, is bulged in the same way over a width of perhaps 140 m. The maximum vertical change is less than one 5-m-contour interval and is probably in the range of 0.5-1 m. As the main rupture belt approaches Bessemer Mine Road, the vertical movement changes from bulging to a shallow depression.

Structures on Part of Emerson Fault Zone

Fractures at a Restraining Bend

There is a restraining bend in the main rupture belt about 125 m northwest of Galway Lake Road. The rupture belt makes a bend of 10° to the left. Peripheral fractures occur on both sides of the rupture belt. On the east (or concave) side, there is a complex zone of fractures with two distinct orientations. One set of right-lateral fractures is subparallel to the main rupture belt. The other set makes an acute angle of about 30° with the right-lateral fractures and is roughly parallel to a group of splinter fractures that join the main belt another 100 m to the northwest. These fractures comprise a left-lateral strike-slip fault zone. The two sets of peripheral fractures are a conjugate pair and signify fault-parallel compression (about N5°W) on the concave side of the restraining bend.

The left-lateral fractures and the right-lateral splinter fractures, separated by only 100 m on the concave side of the main rupture belt, have a different sense of slip but approximately parallel orientations. This observation

illustrates why it is necessary to comprehensively map the fractures rather than obtain kinematic information as point quantities along a rupture belt.

On the convex side of the restraining bend are three long zones and another two or three short zones of opening/right-lateral shear fractures that extend to the edge of the map, 400 m west of the main rupture belt. These fractures are indicate right-lateral shear about normal to the main rupture belt. There are a few, weakly developed left-lateral fault zones that make an acute angle of about 40° with the right-lateral fracture zones. Again, the left and right-lateral ruptures apparently represent a conjugate pair. The fracture pattern indicates that the direction of maximum compression is about N85°W or about 80° counterclockwise from the direction of maximum compression on the concave side of the rupture belt. Overall, the structure produced in the 10° restraining bend extends for more than 600 m outside the main rupture belt; lack of low-altitude photographs limits the detection of the extent of fractures on the northeast side and lack of any photographs limits the detection on the southwest side. Minimum dimensions of the peripheral fractures that are associated with the restraining bend are 300 by 600 m. Maximum compression direction on opposite sides of the main rupture belt, as indicated by the conjugate faults, are oriented about 80° apart. Direction of maximum compression on the concave side of the restraining bend is about 20° clockwise from parallel to the main rupture belt. On the convex side of the bend, the maximum compression direction is oriented about 30° clockwise from normal to the main rupture belt. The nearly right-angle difference in orientation of maximum compression on opposite sides of the main rupture belt is strong evidence that the localized fracturing is a result of the small restraining bend in the main rupture belt. There is no indication here that the restraining bend caused any kind of pushup or ridge-like structure. Indeed, the structure formed in a topographic low of the main rupture belt.

The two most significant observations about the fractures at this restraining bend are the lack of vertical uplift and the presence of fracturing on both sides of the main rupture belt. There is no question that localized compression is developed in ground in an area with a restraining bend along a strike-slip fault. The importance of bends in the formation of tectonic ridges and other styles of vertical deformation is not supported by the deformation at the bend at the Galway Lake Road.

The Galway Lake Road Vortex

The Galway Lake Road rotating block, or structural vortex, constitutes much of the remainder of the fracturing shown on the map. To describe the fracturing in the rotating block, we first must identify and mentally discard peripheral fracture zones that are not part of the rotating block structure. On the extreme northwest end of the map and on the northeast side of the main rupture belt is a group of right-lateral fault zones that extend to the edge of the map, and probably beyond. These fractures apparently are the southern limit of stepover fractures to the Camp Rock fault zone that is across the valley to the northeast. Such stepover fractures occur for another 5 km to the northwest along the main rupture belt. There is another, poorly-organized group of fractures on the southwest side of the main rupture belt at the same place. These fractures occur in exposed crystalline bedrock, and their significance is unknown.

There is also a poorly-developed zone of fractures that extends from Bessemer Mine Road nearly to Galway Lake Road on the southwest side of the main rupture belt. These fractures are subparallel to the main rupture belt and are 400 to 500 m southwest of it. These fractures are not part of the main rupture belt, nor are they part of the Galway Lake Road rotating block. The fractures curve toward the main rupture belt on both ends, and all appear to be either tension cracks or right-lateral fault zones.

Finally, the fractures already described in the restraining bend at Galway Lake Road and at another small restraining bend on Stanford Hill (Aydin and Du, 1994) are not essential parts of the rotating block. The deformation on the northeast side of the rupture belt at Stanford Hill is very complex; there are several kinds of deformation superimposed on each other. To understand the deformation, the fractures caused by the presence of the restraining bend need to be isolated and subtracted from the fractures due to other causes. It appears to us that most, if not all of the fractures on the southwest side of the main rupture belt at Stanford Hill are due to the bend. These fractures on the southwest side of the main rupture belt are tension cracks with a component of right-lateral shift. Similar to location on the convex side of the bend at Galway Lake Road , these fractures appear to be the product of fault-normal (about east-west) compression.

If all the previously mentioned fractures are mentally discarded as part of some other structure, the remaining fractures define an oblate or football-shaped structure extending from the northwest at Bessemer Mine Road to the southeast end of Stanford Hill (Figure 19). The block is a little more than 3 km long and a little more than 1 km wide. The main rupture belt bounds the southwest side and several bands of right-lateral, strike slip faulting bound the northeast side. All the peripheral fractures, except for the structures at the ends of the block and the one minor, left-lateral zone that crosses Galway Lake Road at the southeast edge of the map, have right-lateral, strike-slip sense. Thus, the rotation is a required part of the deformation because all the bounding fractures contain the same right-lateral sense of strike-slip motion.

The right-lateral fracture zones that define the northeast side of the rotating block curve into the main rupture belt at both ends. On the Stanford Hill end (southeast), the curving peripheral, right-lateral rupture ends near the base of uplifted Stanford Hill. The termination has a scarp on the northwest side and a thrust fault on the southeast side of the zone; this pattern is consistent with the termination of a right-lateral fracture zone. This zone steps left to a 1.3-km-

long, curved shear zone that offsets Galway Lake Road in a right-lateral sense by 1.05 m (measured in the direction of the fracture zone).[10] The long, curved right-lateral zone contains some complex stepping fractures and another 500-m-long, right-lateral fracture zone at the place where it is about parallel to the main rupture belt.

Farther to the northwest, the long, curved zone steps left to two more curved right-lateral zones that trend a little southeast of a complex knot of fractures at Bessemer Mine Road. These long, curved fractures terminate about 200 m from the main rupture belt.

There are distinctive fracture patterns, representing different kinds of deformation, at each end of the rotating block. The mapping from the aerial photographs does not provide enough detail to fully understand the structures at either end, but the observations do constrain how they formed.

Bessemer Mine Road End of the Galway Lake Road Vortex

The northwest end of the rotating block is a zone along and east of the main rupture belt extending from about Bessemer Mine Road for about 500 m to the southeast. There is no bend in the trace of the main rupture belt there, but the belt widens to about 100 m from the more-nearly typical width of 10-15 m. In other words, the main rupture belt becomes an order of magnitude wider, but the trend of fractures in the main rupture belt extending from both ends of the widened fracture zone is co-linear. What may appear to be a restraining step in the main rupture belt at Bessemer Mine Road is only a widening of the belt, and the widening and unusual fracture pattern may be caused by the junction to the southeast with the arcuate peripheral fractures of the rotating block.

The northern end of the curved right-lateral zones joins five zones of parallel fractures that are 100 to 200 m long. The traces of these fractures are oriented about 20° clockwise from the main rupture belt. In the absence of the curving belt of peripheral fractures on the northeast side of the rotating block, these five zones of parallel fractures might be interpreted as splinter fractures to the main rupture belt. However, the belts of fractures do not show any consistent pattern of stepping that would indicate strike-slip deformation; rather, they appear to be tension cracks that subsequently shifted to produce a down-to-the-northwest offset. They make an acute angle of 45° with the curving right-lateral fault zones of the rotating block described above. These five narrow zones of fractures are all down-dropped between the fracture zones and the main rupture. The downdropping can be inferred from the vertical offset across the belt in three of the zones, and from the deflection of contour lines at the other two zones. The amount of downdropping was measured across a few of the fracture zones, and apparently the total is a few tens of centimeters to perhaps a half meter.

The main belt of rupture, where it widens to about 100 m, contains bounding faults that are right-lateral with a significant normal component. The easternmost fault is down to the west about 0.4 m, and the westernmost fault is down to the east about 0.3 m. Within the zone, fracturing is a complex mixture of left-lateral and right-lateral fault faults and tension cracks. The fractures that are generally parallel to the trace of the main rupture are tension cracks, and those fractures oriented clockwise from the trace of the rupture belt are right-lateral, strike-slip faults. The left-lateral strike-slip faults are oriented counterclockwise from the trend of the main rupture belt. Both the deflection of the topographic contour lines and the vertical shift on the fractures indicate that the belt was downdropped during the fault movement. How the displacement-driven deformation worked in this part of the rotating block is unknown in detail, but the result was principally opening in an east-west direction, i.e., toward the end of the peripheral fractures in the rotating block.

All these kinematic features are predicted in a general way by the kinematic models of intersecting faults described by Gabrielov and others (1996). They show that, where fault blocks are rigid and are bounded by faults with the same sense of slip (all right-lateral or all left-lateral), a geometric incompatibility is necessary. In this case, the geometric incompatibility leads to a divergence of the block corners. Perhaps the knot of fractures at Bessemer Mine Road and the depression near the main break are results of the incompatibility.

Stanford Hill End of Galway Lake Road Vortex

At Stanford Hill, on the southeast end of the Galway Lake Road rotating block, there is a southwest-facing scarp up to 2-m-high along the full length of the uplifted hill. Part of the area of fractures on the northeast side of the main rupture belt was mapped in detail by Aydin and Du (1994), Arrowsmith and Rhodes (1994), and Antonneli and others (1992). Plio-Pleistocene lake beds dip about 30° to the north in the north-northeast end of the hill and 64° to the east in the southeast; slickenlines on the fault plunge 20° to the northwest (Aydin and Du, 1994). No doubt Stanford Hill was uplifted during the Landers earthquake. The increase of dip to the southeast suggests progressively increased tilting as the block was translated along the main rupture belt in this and prior fault-movement episodes. Farther to the southeast, beyond the map area and the rotating block, there are deeply dissected, tilted beds that perhaps represent the displacement of parts of the Galway Lake Road rotating block to outside of the rotating block structure during earlier episodes of fault movement.

The fractures on the southwest side of the main rupture belt appear to be the result of a restraining bend at Stanford

[10] About 150 m farther along the Galway Lake Road is a left-lateral zone that appears to be conjugate to the right-lateral zone. The trace of the road was too irregular here to measure a displacement on the left-lateral fault, but it was less than 0.5 m.

Hill. These fractures are similar to fractures at the convex side of the restraining bend at Galway Lake Road.

With photogrammetric mapping we can identify two additional groups of fractures in the hill that we interpret to be unrelated to the restraining bend. The first is a swarm of tension cracks that strike approximately north-south on the northeast end of the hill. These trend directly toward a group of thrust faults that trend easterly along the base of Stanford Hill. We have seen and described these structures at other locations, most notably the Happy Trail shear zone on the Johnson Valley fault (Johnson and others, 1993, 1994) and Summit Ridge in the San Andreas fault zone (Johnson and Fleming, 1993). The fractures form as tension cracks oriented at a clockwise angle to the main rupture trend. The cracks divide the ground into prismatic blocks that are rotating by further right-lateral shearing. The rotation produces a small component of left-lateral shift on the tension cracks and shortening parallel to their lengths (Terres and Sylvester, 1981). Some of these are shown in Arrowsmith and Rhodes (Fig. 5, 1994) and Aydin and Du (Fig. 6b, 1994).

The other distinctive fracture group in Stanford Hill consists of two north-side-up, curving, bedding-plane fracture zones. In the view of Fleming and others (1997), this part of the fracturing in Stanford Hill is a consequence of the ramp-like shape of the main rupture belt. The main rupture belt trends about N40°W to the northwest of the hill; at the hill, the main rupture belt makes a 20° farther to the west to a strike of N60°W. The main rupture belt maintains this orientation for about 300 m, and it turns back to a trend of N40°W at the southeast edge of the map. The curving bedding-plane fracture zones are sub-parallel to the ramp-like section of the main rupture belt.

Thus, most of the fracturing at the southeast end of the rotating block structure apparently is a result of three causes that are not essential to the rotating block structure. The fracturing on the west and southwest side of the main rupture belt is a local response to the abrupt bend in the main rupture belt. Some of the fracturing on the east and northeast side of the belt may also be due to the bend, but the fracturing there is too complex or insufficiently documented to separate them from fractures due to other causes. The long, straight tension cracks that trend north-south and terminate in a belt of thrust faults are the result of right-lateral shearing (Terres and Sylvester, 1981). And finally, the long, curved north-side-up faults that are parallel to bedding appear to be the result of ramping along an S-shaped bend in the main rupture belt. This alone could account for the movement of Stanford Hill up along the main fault zone. In this view, the all the deformation is displacement driven, and the fracturing is the composite result of a small restraining bend, distributed shear, and the ramp along the main rupture belt.

Differential Displacements Associated with the Galway Lake Road Rotating Block

A horizontal component of differential displacement across fracture zones in the Galway Lake rotating block was measured in two dependent ways on the aerial photographs[11]. First, a horizontal component of differential displacement was measured by the offset of a linear feature across an entire zone of rupture. The component is the normal distance between two line segments that were co-linear prior to the earthquake. This component is always less than or equal to the net differential displacement across a rupture. The orthogonal component that would complete the two-dimensional definition of the net horizontal differential displacement would be at right angles to this one, that is, parallel to the line segments. This component is unknown at Galway Lake Road. At other places at Landers where we had better reference features for measurement, we found that there was dilation or spreading normal to the rupture belt.

The same horizontal component of differential displacement can be calculated by measuring the offset of the linear features in the direction of the trend of the fault zone, again using two line segments that were co-linear prior to the earthquake. One can recover the first measurement with a trigonometric function, so the two measurements are dependent. However, if there were only strike-slip on the fault, this latter measurement would provide the horizontal component of the displacement vector. This is what is typically assumed in measurements of fault offset.

Since Fleming and others (1997) had no way of measuring dilation across the fault zone, they made the usual assumption. Reporting, as they do, a fault-parallel offset, they misrepresent the actual net differential displacement but, unfortunately, they were unable to measure the dilation in the rupture belt photogrammetrically.

Components of relative strike shift displacements measured in the way explained above are shown in Table 1 and Figure 18. At Bessemer Mine Road, the component of strike shift across a zone about 100 m wide was 5.0 m. The component of fault-parallel differential displacement was about the same along the main rupture belt all the way to Galway Lake Road, where they measured 5.2 m across a 75 m wide zone. Point "E," 325 m south of Galway Lake Road, had 5.5 to 7.0 m of right-lateral shift on a motorcycle track across the rupture belt. This was the maximum measured from the aerial photographs; however, the tracks on opposite sides of the rupture belt at point "E" were not

[11] Most investigators ignore the fact that displacement across a fault or any other planar discontinuity is a vector. They implicitly assume that one component adequately describes the vector.

parallel and the minimum value of 5.5 m is probably closer to the actual fault-parallel component of displacement.

Points "G," "H," and "I" were taken from a map—compiled by Cruikshank (unpublished map, 1992) and cited by Arrowsmith and Rhodes (1994)—covering a larger part of the rupture belt at Stanford Hill. The map lists only fault-parallel components of displacement and vertical offset. Amounts vary from 4.0 to 4.85 m. All the measured points at Stanford Hill, "G" through "K," contain significant vertical offset, with the hill uplifted in all cases. Maximum differential vertical uplift was at Point "G," where 2.0 m was measured across one scarp and a total of 2.3 m on two scarps. Other vertical offsets across several smaller scarps were typically sums of 1.1 to 1.5 m.

These results indicate that the main rupture belt along the southwest side of the Galway Lake Road rotating block, between Bessemer Mine Road and Galway Lake Road, contains about 5 m of right-lateral, fault-parallel, horizontal component of shift. From Galway Lake Road, at least 325 m farther to the southeast along the same rupture belt, the rotating block carries 5.2 to 5.5 m of right-lateral, fault-parallel component of shift. Still farther to the southeast, at the northwest end of Stanford Hill, the component of fault-parallel horizontal displacement is in the range of 4 to 5 m.

The maximum vertical shift is 2 m, northeast-side-upthrown, on a single scarp at Stanford Hill. Near Bessemer Mine Road, the main rupture belt is downdropped, a few tens of centimeters to perhaps a half meter, along fractures within, and on both sides of the belt.

The northeast side of the rotating block is depicted by the peripheral fracture zones that cross Galway Lake Road 1.08 km southeast of the main rupture belt (Point "F," Table 1). The road is offset 1.05 m right-lateral in the direction of the fracture zone.

Examining the map with these numbers in mind (Figure 18), we see that the block was rotated on the order of 1 m, which is the value of the fault-parallel differential displacement in the southeastern part of the block where the bounding rupture crosses the Galway Lake Road (Point "F"). Assuming that the same value of rotation applies at the intersection of the Galway Lake Road and the main rupture of the Emerson fault zone, we conclude that the (non-rotational), translational differential displacement is about 5.5 m minus 1 m, or about 4.5 m along the main rupture[12].

The value of 4.5 m is perhaps a little larger, but in the same range as the values of differential horizontal offset measured along strike-slip faults through the Landers area. At the power line crossing and at Tortoise Hill Ridge, 6 to 4 km to the northwest, the differential horizontal displacements were 2.9 to 3.1 m. Differential displacements on the Emerson fault zone south of Galway Lake Road are apparently 3.7 to 4.5 m (Hart and others, 1993).

The value of 4.5 m across the entire structure is significantly smaller than the values of 5 to 7 m reported at Galway Lake Road for the main rupture belt of the Emerson fault zone by Sieh and others (1993), Hart and others (1993), Irvine and Hill (1993), and Hamilton, oral comm. (1996).

Discussion and Conclusions

Recognition of fault-related structures such as rotating blocks, which are like structural vortices, in rupture belts produced by earthquakes presents some opportunities and some difficulties. To those interested in fault-related structures, the notion of rotating blocks or vortices provides an opportunity to recognize new kinds of idealized deformation of fault blocks; blocks may move rigidly by translation and rotation, and masses may move softly by displacement and vortex motions. Some examples are the Big Bear Landers structure described above and of the San Fernando Valley heart structure described in the Northridge area (Johnson and others, 1996).

But the notion of rotating blocks and vortices provides a new difficulty to persons who wish to measure differential displacement across faults. We have shown elsewhere (Johnson and Fleming, 1993; Johnson and others, 1993, 1994; Martosudarmo and others, 1997) that rupture zones are commonly belts of shear zones that distribute the differential displacements, not across individual breaks, but across belts as wide as 50 to 200 m, and even to 500 m wide. We have shown that measurement and summation of shift across single fractures cannot be expected to accurately summarize the deformation (Johnson and Fleming, 1993). Fleming and others (1997) have shown that the measurement across zones of fractures cannot be confidently summed without a knowledge of the kind of structure containing the fracture zones. In the case of the Galway Lake Road rotating block, the right-lateral shift in the peripheral fault zones must be *subtracted* from the right-lateral shift in the main rupture belt to obtain an unexaggerated estimate of the net translational shift across a rupture zone.

If we were to follow the typical practice of adding displacement obtained on the main rupture to that on the rupture that crosses Galway Lake Road 1 km to the southeast of the main rupture, in order to estimate the offset

[12] The net translational displacement may be even less than this value. In a reconnaissance of the rupture zones in March, 1997, we noted seven peripheral, strike-slip fracture zones along Galway Lake Road. The seven zones occurred in two groups. The first group contains the three fracture zones shown on this map. The first zone is at a distance of 1.08 km along the road from the main rupture belt; this zone carried right-lateral shift of 1.05 m. There was another right-lateral zone 90 m farther along the road at 1.17 km. This zone appears to be a continuation of the one mapped farther to the south on the aerial photographs but not visible in the photographs at the road crossing. The stepping sense of the fractures reveal right-lateral shear, but the amount of displacement could not be determined in the field. The next fracture zone was left-lateral at 1.24 km and is shown on the photogeologic map. Therefore, we know that a second right-lateral fault zone crossed Galway Lake Road only 90 m beyond the zone with 1.05 m displacement. The total right shift on this side of the rotated block cannot be measured on the photographs, but the 1.05 m would seem to be a minimum value.

of the ground on either side of the Emerson fault zone, we would be compounding the error. If we added the offset on the main rupture to that on the opposite side of the rotating block, we would markedly overestimate the right-lateral shift as 6 to 6.5 m. By making an appropriate interpretation of the kinematics of the Galway Lake Road rotating block, we have seen that we obtain the much-more-nearly reasonable value of about 4.5 m for the net shift on the Emerson fault zone.

The folly of the typical practice of adding displacements on adjacent faults is illustrated at the Galway Lake Road. If we were to sum the differential displacements on all the peripheral faults that cross Galway Lake Road, there would be five right-lateral faults and two left-lateral faults, in addition to the main rupture belt, producing a differential displacement of perhaps 8 to 8.5 m! This estimate is clearly a ridiculous total in the context of measurements at other places.

Hidden within the overall complex pattern of rupture produced by the Landers earthquake are several other candidates to be recognized as rotating-blocks or structural vortices. The previously mentioned Kickapoo stepover, bounded on four sides by right-lateral, strike-slip faults, contains rotation equivalent to the amount of displacement on the fault with the least movement. The right-lateral zone bounding the southeast end of the stepover structure contains about 20 cm of shift (Sowers and others, 1994). If the structure is considered to be a vortex rather than some sort of duplex, 20 cm of the slip on the sides of the block are due to rotation, and the remainder is translational shift on throughgoing fault rupture and slip transfer between the Johnson Valley and Homestead Valley fault zones.

Fleming and others (1997) suggest that the formation of a rotating block is caused by the geometry of the main rupture. The main belt of rupture of the Emerson fault zone contains a double curve in the area of the rotating block, resulting in a saucer-shaped, rupture belt. Movement of the block opposite the concave side of the saucer-shaped rupture belt would cause a rotation of the material on the concave side of the saucer. At the scale of the Landers-Big Bear rotating block (Figure 15), we also can imagine a saucer-shaped rupture belt along the San Andreas fault, with the bottom of the saucer shape being in the vicinity of San Bernadino (Jennings, 1975 and 1994), associated with the arc of the Landers rupture belt.

Perhaps the most important outcome of the study of the Galway Lake Road area is the recognition that one must know the context of the fault-related feature being studied. Broad shear zones provide a context for individual fractures within the zones. Groups of shear zones interact to produce structures such as duplexes, stepovers, tectonic ridges, and rifts. These structures also need to be placed in their proper context. For example, we noted that rifts formed in areas where two faults with the same kinematics, intersect. Likewise, a rotating block forms where there is a saucer-shaped excursion from a straight trace in the trend of the main rupture belt. The next level of information that we have is at the scale of the Landers-Big Bear rotating block itself. Who knows how many fault-related structures at intermediate scales occur between the Galway Lake Road rotating block, on the order of 1 to 3 km in dimension, and the Landers-Big Bear rotating block, on the order of 30 to 50 km in dimension? There seems to be no alternative to detailed and complete study of a deformed zone.

COMMENTS ON MEASUREMENTS OF SLIP DISTRIBUTION ALONG LANDERS RUPTURE

In conclusion of this section on the background of our detailed studies of structures along strike-slip faults at Landers, we would like to point out another serious problem that we have only started to address (Fleming, 1997) at the end of our joint research on earthquake faulting.

The purpose of measuring offset along faults, as we understand it, is to estimate the relative displacements of the two crustal blocks severed by the fault. Thus the purpose is to obtain not highly detailed information about shift across individual faults or cracks, but rather to collect data that should be relevant to a much larger picture. It is on the basis of this understanding that we see serious problems with the way people have made measurements.

An important part of the problem is the difficulty of determining the displacement across a rupture consisting of discontinuous fault segments rather than a continuous break. The continuous fault is the exception, so it is of little interest. Most faults consist of segments that overlap normal to the trend of the overall rupture belt, commonly but not necessarily in en echelon pattern. Landers is no exception.

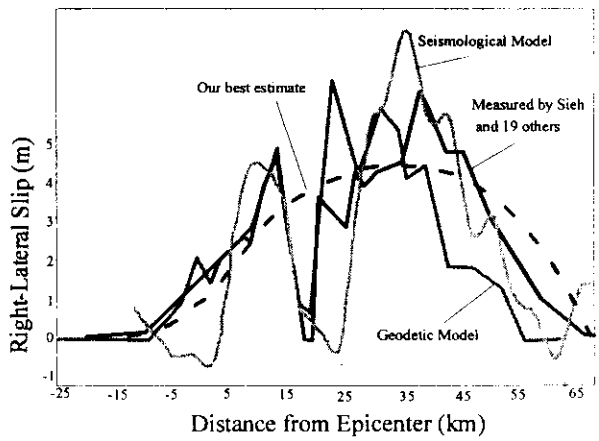

Figure 20 Comparison of slip distributions for the Landers earthquake, according to Sieh and 19 others (1993) (solid black line), according to geophysical modeling by Hudnut and 16 others (1994) (solid gray lines) and according to the two of us (dashed black line). We are outvoted 37 to 2.

Where fault segments overlap, displacement is generally summed to obtain an estimate of the total displacement as a function of distance from the epicenter. An example for the Landers earthquake is shown in Figure 20 (from Hudnut and 16 others, 1994). It is a comparison of slip distributions according to field measurements by Sieh and 19 others, 1993, with geodetic and seismological models. The similarities of the three curves is held up as an example of the wonderful ability of the models to mimic the observations.

There is only one major flaw with this example—the field data are wrong! Is it not remarkable that the theoretical models reproduced even the incorrect results?

The claim that the field data are wrong requires some explanation. Much of the explanation has been presented in preceding pages, where we discussed the Galway Lake Road rotating block. But there is a little more. First consider the measurements of Sieh and 19 others. The right-lateral shift across the Landers rupture was about 1 m at the epicenter and the amount increased toward the northwest for about 15 km where the shift was between 4 and 5 m. From that point, the shift *abruptly decreased to zero* at about 20 km northwest of the epicenter. From there, the shift again gradually *increased to a value of 6 to 7 m* at Galway Lake Road, a point 42 km northwest of the epicenter. Farther northwest, the displacement reduced to zero at 65 km northwest of the epicenter, where the belt of continuous rupture appeared to end.

Our own measurements combined with a few credible measurements by others indicate that the displacement across the Landers rupture is 3 to 4 m, perhaps as large as 4.5 m along most of the rupture zone, reducing to zero of course at each end of the rupture. Thus we do not observe the wild gyrations alleged in Figure 20. Specifically, our observations and measurements contradict the two extreme values reported by Sieh and 19 others (Fleming, 1997).

First, the place that is about 20 km north of the epicenter, where slip reportedly decreased to zero, is in a structurally complex zone. Immediately south of this area the rupture belt is about half a km wide (Plate 1) and accommodates at least 3 m of shift. The area of reported zero shift contained numerous open tension cracks oriented north-south. North-south tension cracks, indeed, occur throughout the Landers rupture belt and typically reflect right-lateral shear oriented at N30 to 45°W (Johnson and others, 1994). Thus, rather than shift concentrated on a strike-slip fault in this area, the shift presumably was distributed across a belt of tension cracks, just as at Loma Prieta. Also, this same area contains a restraining, left step in the right-lateral fault that reportedly produced a thrust fault. The direction of translation on the thrust fault is the same as the shift across the stepping fault segments. The reported value of zero slip, then, is a result of a flaw in the method of determining shift rather than a change of shift of crustal blocks. Indeed, the southwest side of the rupture belt would appear to have moved toward the northwest 3 to 4 m, just like the ground along the narrower belts of shear zones farther to the northwest and southeast where the shift was accommodated by strike-shift shear zones. The report of zero displacement, then, is almost certainly wrong and should not be used in seismological and tectonic modeling of displacement along the long faults at Landers.

The second erroneous result in the profile of "measured" slip is the exaggerated[13] slip value of 6 to 7 m reported for Galway Lake Road, on the Emerson fault zone about 42 km northwest of the epicenter. As discussed by Fleming and others (1997, and herein), the exaggerated slip value is a result of the structural setting of the measurement. There is not simply slip on a fault, but slip on a fault and rotation of an adjacent block. It is the rotation that exaggerates the slip along the fault. When the rotation is subtracted, the remaining slip on the Emerson fault is about 4.5 m, which is roughly the same as elsewhere.

Clearly, the current methods of measurement of slip on strike-slip faults incorporate some serious errors that can overestimate or underestimate the actual amount of shift of the adjacent crustal blocks.

Fleming (1997) suggests that a more generalized, or smoothed, slip distribution be reported because it would better represent the actual slip. At Landers, assuming that the shift of 1 m at the epicenter is correct, we would suggest that the shift increases to 3 to 4 m 10 km northwest of the epicenter. Shift appears to remain relatively constant from there to a distance of 45 km from the epicenter, where it starts to drop. Between 45 and 65 km, the shift apparently drops to zero. The shift apparently decreases from 1 m at the epicenter to zero about 15 km southeast of the epicenter.

---

[13] It is not only at Landers where offsets along faults have been exaggerated. Perhaps the exaggeration is a reflection of the seemingly frantic effort by earthquake chasers to be the one to report the "biggest" offset. In any case, theoreticians such as seismologists and earthquake kinematic modelers should beware of this tendency of the fault measurers. The maximum offset in 1906 across the San Andreas north of San Francisco apparently was about the same as that across the Emerson fault zone at Landers. G.K. Gilbert, a very careful observer, reported an anomalous value of up to 6.4 m of offset in a marshy area, but he also warned that this value is almost certainly exaggerated by special conditions in soft ground, such as lurching or other superficial adjustments. Yet, 6.4 m is the number typically reported for the San Francisco earthquake and used in all kinds of calculations! As indicated above, the maximum displacement at Landers was quickly (Engineering and Science, 1992 and Sieh and 19 others, 1993) reported to be 6 to 7 m based on a single measurement along Galway Lake Road. They did not report that the value of 6 to 7 m belies measurements half as large both north and south of Galway Lake Road. They did not recognize, of course, the complex setting of the Galway Lake Road measurement. But they might have suspected that something must be wrong.

PART III. TORTOISE HILL RIDGE

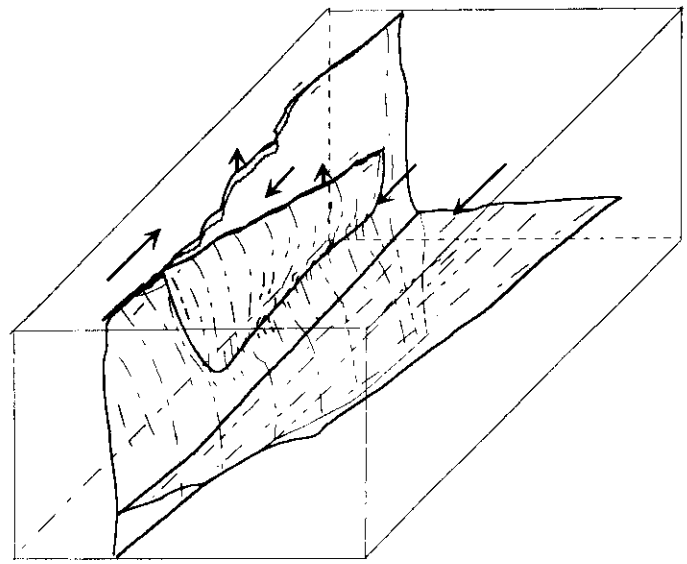

In the process of documenting the surface rupture in different tectonic settings at Landers we began to suspect that, in places, deformation was complimentary to existing topography[14]. Areas of positive relief in the rupture zones appeared to have been uplifted during this earthquake[15]. And, areas that might be tectonically positioned to be downdropped were covered with very young alluvium. In our minds, the landscape began to take on the form of the tectonic deformation that seemed to have occurred during the earthquake. One of these areas, Tortoise Hill, appeared to have been uplifted significantly during the earthquake. We mapped part of the area and decided that the amount of vertical growth was in the range of 0.5 to 2 m. But through mapping alone we could get only hints of how much growth had actually occurred.

During the same period, Fleming was making a concerted effort to locate low-altitude, pre-earthquake aerial photographs of the rupture zone. His search led him to the principal public utility of the greater Los Angeles area, the Southern California Edison Company (SoCalEd), where he learned that Tortoise Hill had been part of a site that had been photographed and surveyed for a potential generating station; and that a relatively dense array of bench marks extends over about 10 land sections, from one side of the Emerson fault zone to the other (Figure 23), that had been surveyed by the utility company in the 1970's. The network of survey monuments crosses Tortoise Hill near the northwest end of the Emerson fault zone, where faulting steps across the valley of Galway Lake to the Camp Rock fault zone. The area is between Bessemer Mine Road in the south and the Rodman Mountains in the north. The Single-tower Transmission Line is in the northwest and the Emerson fault zone cuts obliquely from northwest to southeast in the northern part of the area.

Figure 21. Triangles east and west of the ruptured faults were surveyed by trilateration and show normalized length changes. The direction and magnitude of maximum extension is indicated with double-headed arrows. The measurements reflect left-lateral shearing on the order of 7×10^{-5} that accompanied elastic, right-lateral unloading of the faults. Right-lateral deformations are concentrated in the vicinity of belts of shear zones along the faults.

Figure 22. Fractures at left jog in Emerson fault zone at brow of Tortoise Hill, showing compression features on both sides of the jog. The main rupture of the Emerson fault had a scarp about 65 cm high near center of area shown and right-lateral slip was about 265 cm here. The main rupture trends southeast over the east edge of the elongated dome of North Spine. To the north of the rupture are opposite-facing thrusts, dipping north or south, indicating north-south compression. The brows are up to 10 or 15 cm high. To the south there is a welt marked by numerous tension cracks oriented north-south and bounded on the south by a thrust dipping northward.

The detailed survey information on the benchmarks from the 1970's provided an additional data set that could be evaluated with a resurvey of the same benchmarks, thereby providing access to two somewhat different methods of obtaining near-field deformational data. SoCalEd gave access to the pre-earthquake data and the aerial photographs, and we contracted with them for a resurvey of the bench marks.

In this part we describe the relations between the Emerson fault zone and the Tortoise Hill ridge We present data on the horizontal deformation at several scales associated with activity within the ridge and belt of shear zones and show the differential vertical uplifts. And, we conclude with a discussion of potential models for the observed deformation.

TORTOISE HILL RIDGE AND THE EMERSON FAULT ZONE

In general, the trace of the rupture zone of the Emerson fault is simple and relatively straight for about 2 km to the northwest and 1 km to the southeast of the Single-tower Transmission Line. The fault zone is characterized by a belt of shear zones 60-70 m wide (Plate 3). The overall trend of the belt is N45° to 50° W. The belt contains fractures such as individual tension cracks, en-echelon tension cracks, and right-lateral fault elements. The Emerson fault zone accommodated about 2.9 m of right-lateral shift at the Single-tower Transmission Line and 3.1 m at Tortoise Hill ridge.

Figure 23. Contours of vertical displacement, relative to a point (large shaded circle) near Bessemer Mine Road, showing concentrated uplift at Tortoise Hill ridge, within Emerson fault zone. Land survey control points, surveyed in 1973 and 1994, shown with circles. Circles with cross (arrow moving away from observer) indicate downward movement. Circles with dot (and tips of feathers) indicate upward movement (arrow moving toward observer).

Figure 24. Vertical aerial photograph (about 1:12000 scale) showing belt of shear zones along Emerson fault zone about 6 km northwest of Bessemer Mine Road. Road in upper part of area is along Single-Tower Transmission Line. At south end of photo is north end of Tortoise Hill ridge. Edges of belt shown with arrows. East (right) side of belt is defined by the main fault in this area. The belt

[14] This part is based on a paper by Fleming, Johnson and Messerich (1997).

[15] A fascinating contradiction to this rule is the modern growth of a pull-apart basin centered on a mountain within the Homestead-Emerson stepover, described in Part II, in previous pages. There the basin is not growing at the site of negative relief but, rather, at a site of positive relief. Thus the Landers earthquake is partly reversing what must have been a long-term growth of a large tectonic ridge.

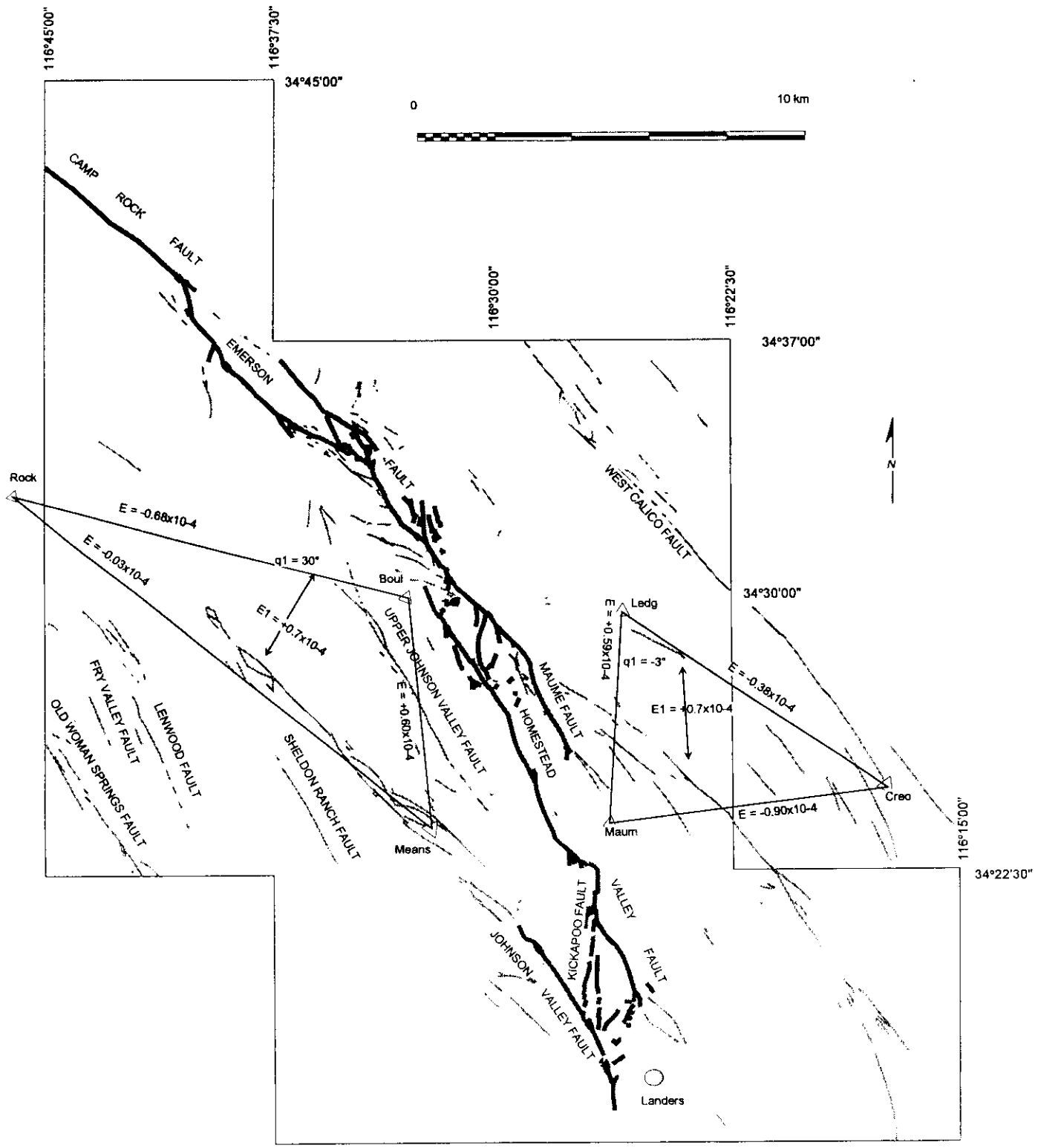

Figure 21. Triangles east and west of the ruptured faults were surveyed by trilateration and show normalized length changes. The direction and magnitude of maximum extension is indicated with double-headed arrows. The measurements reflect left-lateral shearing on the order of 7x10–5 that accompanied elastic, right-lateral unloading of the faults. Right-lateral deformations are concentrated in the vicinity of belts of shear zones along the faults.

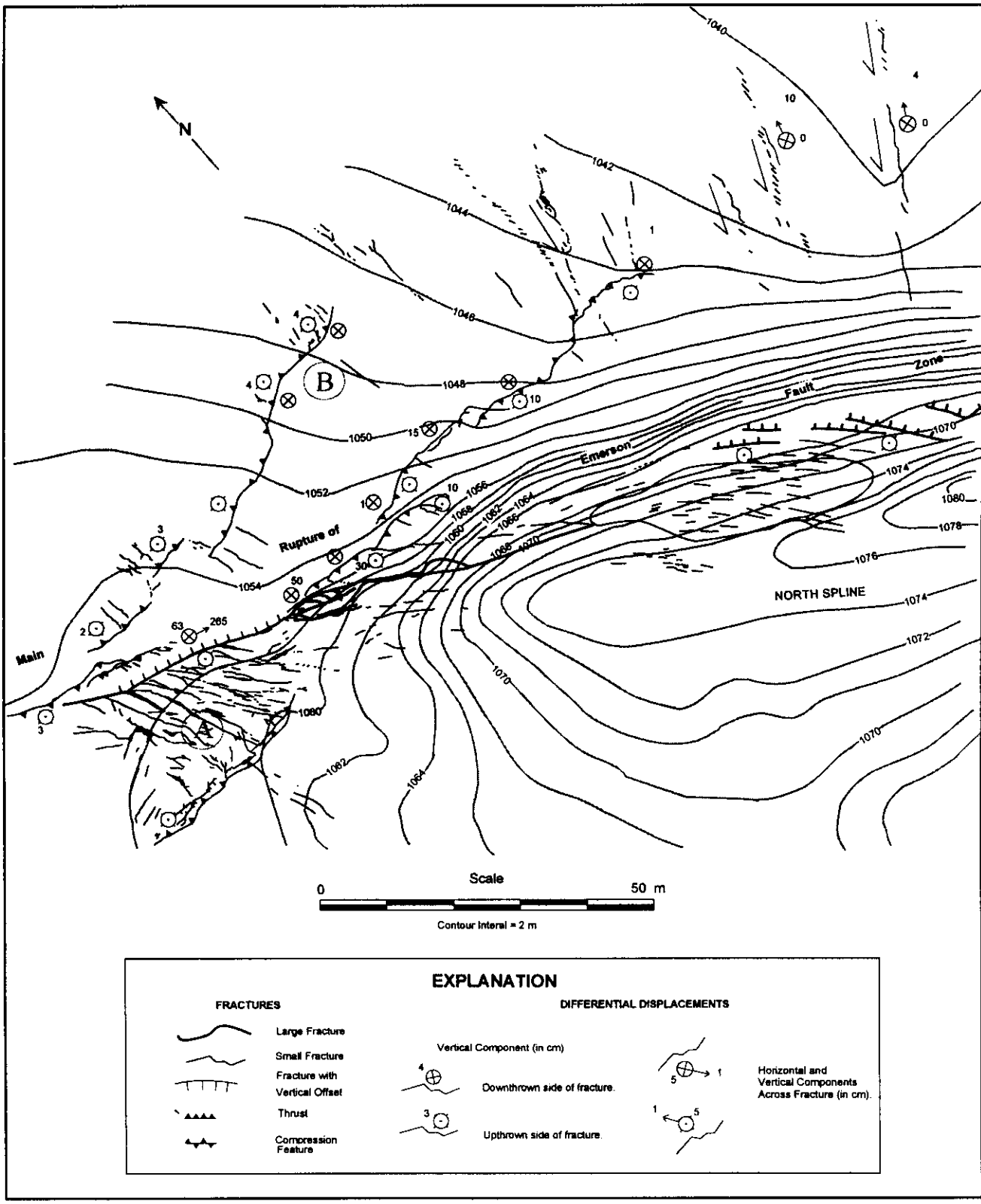

Figure 22. Fractures at left jog in Emerson fault zone at brow of Tortoise Hill, showing compression features on both sides of the jog. The main rupture of the Emerson fault had a scarp about 65 cm high near center of area shown and right-lateral slip was about 265 cm here. The main rupture trends southeast over the east edge of the elongated dome of North Spine. To the north of the rupture are opposite-facing thrusts, dipping north or south, indicating north-south compression. The brows are up to 10 or 15 cm high. To the south there is a welt marked by numerous tension cracks oriented north-south and bounded on the south by a thrust dipping northward.

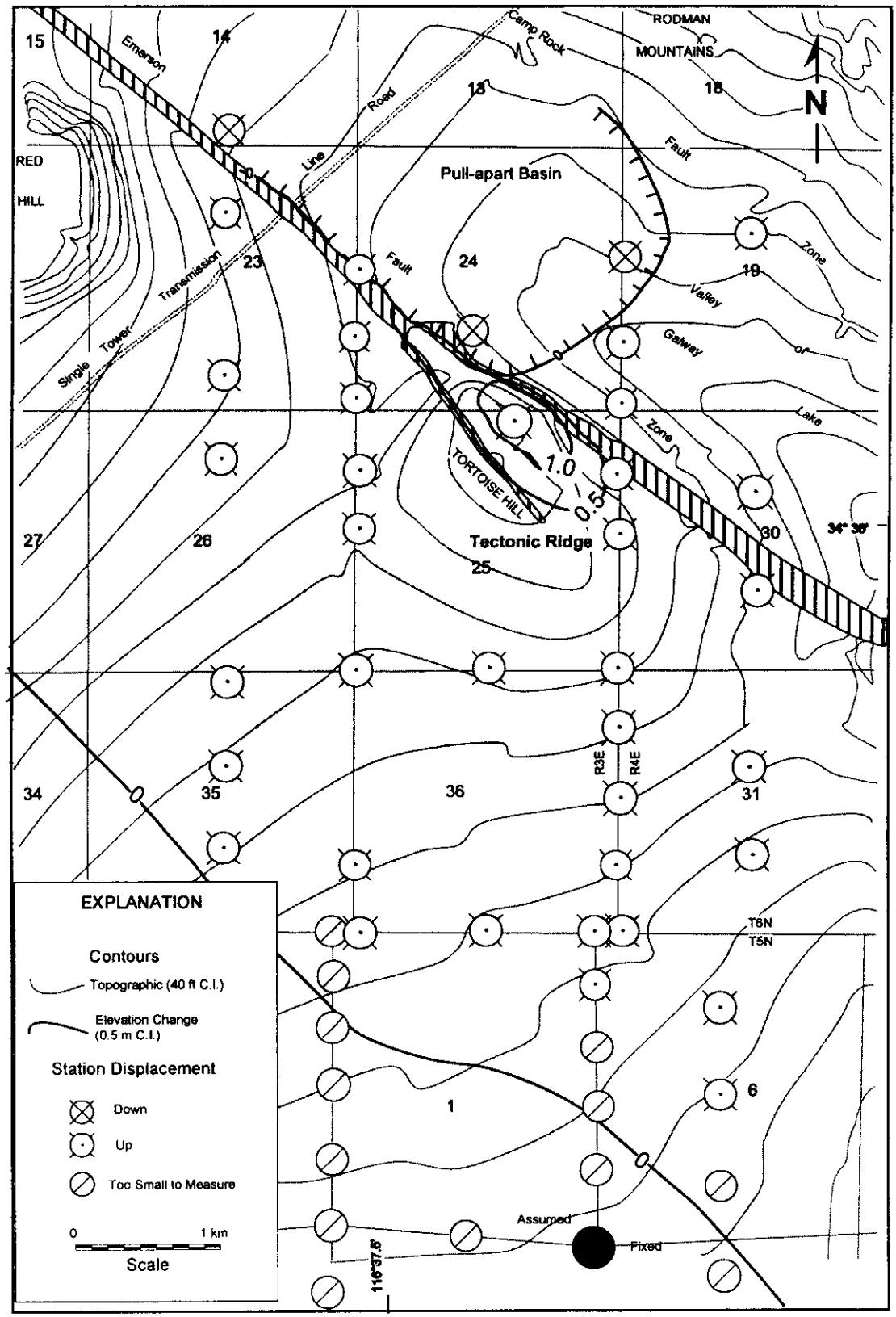

Figure 23. Contours of vertical displacement, relative to a point (large shaded circle) near Bessemer Mine Road, showing concentrated uplift at Tortoise Hill ridge, within Emerson fault zone. Land survey control points, surveyed in 1973 and 1994, shown with circles. Circles with cross (arrow moving away from observer) indicate downward movement. Circles with dot (and tips of feathers) indicate upward movement (arrow moving toward observer).

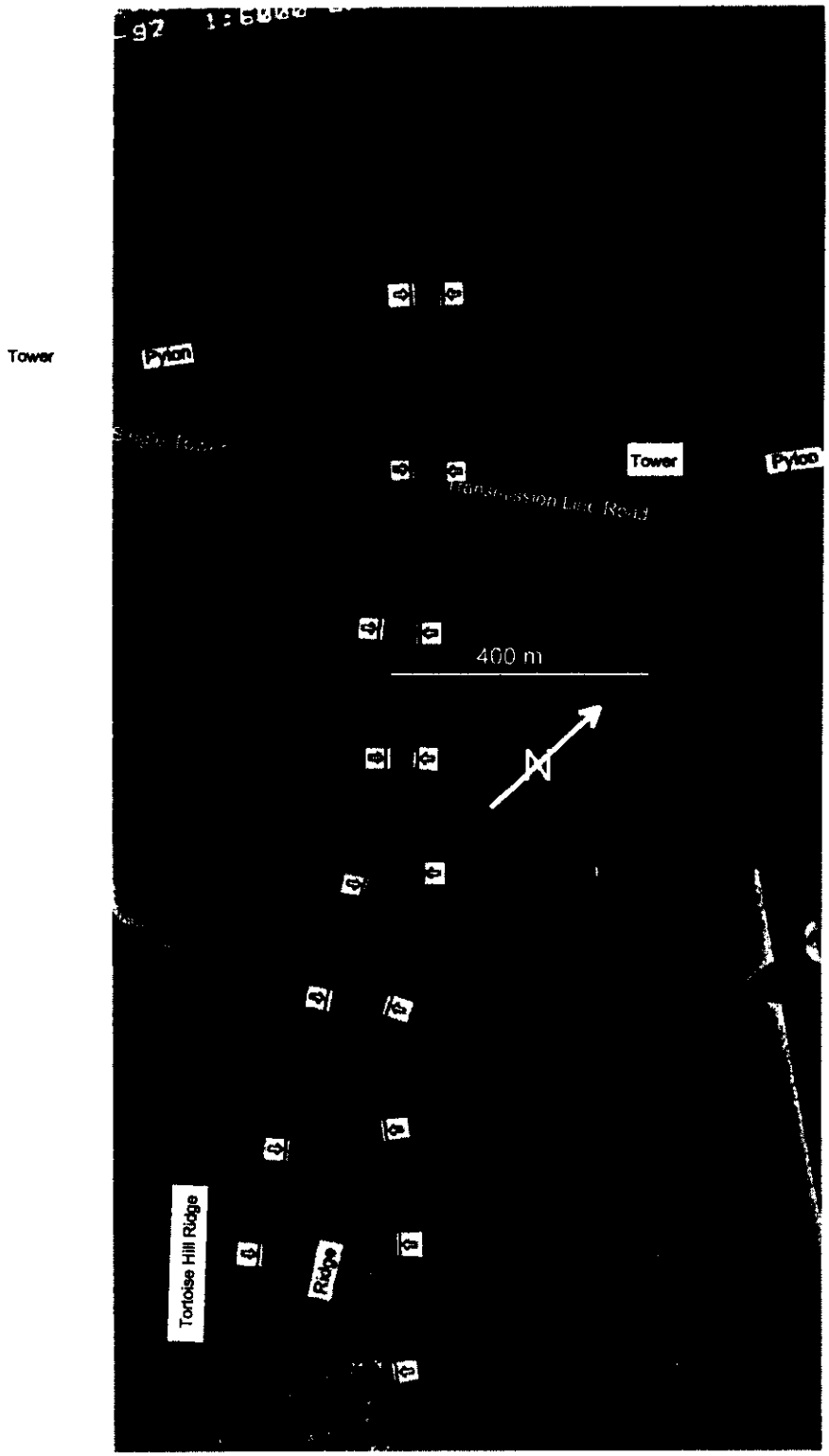

Figure 24. Vertical aerial photograph (about 1:12000 scale) showing belt of shear zones along Emerson fault zone about 6 km northwest of Bessemer Mine Road. Road in upper part of area is along Single-Tower Transmission Line. At south end of photo is north end of Tortoise Hill ridge. Edges of belt shown with arrows. East (right) side of belt is defined by the main fault in this area. The belt

is about 70 m wide at transmission line road and 400 m wide in part of ridge shown.

Tortoise Hill ridge is about 1 km southeast of the power-line crossing (Plate 3). Fractures surround the northwest end of the ridge, apparently as a result of splitting of the belt of shear zones into two, separate shear zones. The pattern of the split belt is like the prow of a Tortoise-Hill-ridge boat, or perhaps a canoe, steaming northwesterly. The bounding zone on the northeast side of the ridge continues to the southeast beyond the map area. The fault zone on the southwest side of the ridge extends only to the southeast end of the ridge and stops. Maximum uplift of the ridge is at about the point where the southwest-bounding fractures end (Plate 3).

The ridge protrudes above the general land surface in an upside-down, keel-shaped outcrop about 400 m wide and 1200 m long. It is about 40 m higher than the valley of Galway Lake on the northeast side and about 20 m higher than the projection of the tilted surface on the southwest side. This southwest side of the ridge is a long, gently sloping surface much like a pediment except that evidence for beveling by erosion is absent. A distinct change in slope is visible about 1 km southwest of the ridge, but the topographic base map on the geologic map of Dibblee (1964) and on Plate 3 indicates that the change of slope is more one of direction than magnitude of slope.

The northeast side of the ridge is very steep and apparently a fault scarp. In the narrow shear zone along part of this scarp, 1 to 1.5 m of differential vertical uplift was evident with the ridge side upthrown. Measurements of offset features indicate that right-lateral shifts of up to 2.65 m were accommodated across the narrow belt of ruptures.

The exposed rock at Tortoise Hill and over several square kilometers of ground to the southwest is Mesozoic monzogranite containing local aplite dikes. The fault-parallel Galway Lake valley immediately northeast of Tortoise Hill is underlain by young alluvium, but small knobs and hills of older igneous and metamorphic rocks project through the alluvium on the northeast side of the valley (Dibblee, 1964).

The fault on the northeast side of the belt of shear zones in the Emerson fault zone throughout the mapped area carries most of the differential displacement across the belt. At the power line, 2.7 of 2.9 m of displacement is on the northeast side. At Tortoise Hill, about 2.65 of 3.1 m is concentrated in a narrow belt on the northeast side. Eight kilometers to the southeast, the concentrated displacement shifts to the southwest side of the shear zone.

Abundant fractures occur on both sides of the northeast-bounding fault (Plate 3). On the northeast side are several long tension cracks oriented about north-south and a group of thrust-fault-like fractures oriented about east-west (Figure 10). The thrust-like fractures have mixed north to south and south to north transport directions and therefore accomplish only shortening (e.g., Fleming and Johnson, 1989) in a north-south direction across the zone. Farther along on the northeast side of the principal rupture zone are about five narrow zones of left-lateral shearing that trend about normal to the direction of the overall shear zone. The left-lateral sense of shear is indicated by the orientations of the *en echelon* fractures. Offset of up to 10 cm was measured at one of these narrow zones.

A zone of tension cracks is shown on the southwest side of the bounding rupture zone, on the left edge of Plate 3. This zone had the appearance in the field of a blister-like structure that had been uplifted and fractured in this small area of perhaps 20 by 30 m. Tension fractures of this orientation were confined to the southwest side of the rupture zone, but arching of a contour line on the northeast side of the rupture zone is perhaps indicative of uplift extending across the bounding shear zone to the other side as well. The zone of tension cracks was bounded on its southern end by a thrust fault. The thrusting is produced when the prisms of rock broken by tension cracks are rotating in right-lateral shear (Figure 10). The blocks are free to rotate on their sides but constrained on their ends; rotation thus produces the thrusting along the boundary of the blister-like structure. The arching of the contour line across the structure indicates that the total local uplift at the blister-like structure is about 1 m (Plate 3).

The shear zone on the southwest side of Tortoise Hill ridge is south and directly across the ridge from the blister-like structure described above. This zone is also broken, and three crude but distinct elements can be identified. Elements are oriented about N45°W, 250-300 m long, and right stepping with 20-40 m of offset on each step. The fractures at the northwest end of the zone are predominantly right lateral with a small component of reverse movement on a surface dipping northeast. Farther southeast, the zone accommodates increasing reverse shift with the ridge side upthrown from a few cm to a few tens of centimeters.

This shear zone on the southwest side of the ridge has lifted the monzogranite in Tortoise Hill above the sloping, pediment-like surface farther to the southwest. Along this side of the ridge, the outcrops of white pulverized rock in zones essentially parallel to the surface-rupture fractures indicate that this side of the ridge has also been the site of repeated faulting.

HORIZONTAL DEFORMATIONS

We have measurements of length- and angle-changes at length scales ranging over three orders of magnitude, from 10 km to 0.1 km. These three levels of information show deformation as a function of position with respect to the surface rupture. Changes in length of long base lines using triangulation and Global Position System (GPS) surveys provide data for far-field strain analysis. Resurvey of a group of pre-earthquake bench marks ranging from about 7 km from the rupture zone to within the rupture zone and across it provides data for close-in deformation determination. Measurement lengths are typically in the range of 500 m to 1000 m. And, analytical aerial photogrammetry provides data on change in lengths of braced quadrilaterals where initial line lengths are in the range of 100 m and where measurement points are within and across the shear zones.

GPS Measurements

Calculations of changes of line lengths and angles using very long baseline trilateration networks and broad-scale Global Position System (GPS) surveys at Landers (Hudnut and others, 1994; and Freymueller and others, 1994) provide regional information about displacement fields on both sides of the rupture zone. Results of these surveys can be used to compute strains a few kilometers from the belts of surface rupture.

Figure 25. Map showing fractures bounding margins of Tortoise Hill ridge and differential displacements measured photogrammetically. A ladder of quadrilaterals extends across the ridge. At southeast edge, displacements were measured by land survey of regional grid. Maximum horizontal shift across ridge about 2.65 m. Maximum vertical displacement, relative to an assumed fixed point about 6 km south of ridge, is 1.0 m at center of ridge.

Trilateration data of Hudnut and others (1994) for monuments surveyed before and after the earthquake provide normalized length changes for triangles spanning relatively large areas on either side of the northern part of the Homestead Valley fault zone and the southern part of the Emerson fault zone. One triangle consists of stations CREO, MAUM, and LEDG, east of the fault zones (Figure 11). The other consists of stations BOUL, MEANS and ROCK, west of the fault zones.

The triangles have legs ranging from about 6 to 20 km long, and at that scale the *normalized length changes*[16] are

$$E_n = (\text{final length} - \text{initial length})/\text{initial length}.$$

The deformations for a triangle west of the Landers rupture are consistent with unloading during the earthquake sequence. For the triangle east of the surface rupture, changes are -0.009×10^{-2} (compression) for MAUM/CREO, -0.004×10^{-4} (compression) for LEDG/CREO, and $+0.006 \times 10^{-2}$ (extension) for MAUM/LEDG. We note that the MAUM/LEDG leg trends roughly north-south, so the deformations are consistent with left-lateral shearing in the general direction N45°W, reflecting unloading of the right-lateral fault zones during the earthquake. If we assume that the deformations are continuous, the direction of maximum extension would be N3°W and the principal extensions would be $E_1 = +0.007 \times 10^{-2}$ and $E_2 = -0.007 \times 10^{-2}$, that is, the deformation is pure shear (or simple shear).

For the triangle west of the fault zones, normalized length changes are -0.7×10^{-4} (compression) for ROCK/BOUL, -0.003×10^{-2} (compression) for ROCK/MEANS, and $+0.006 \times 10^{-2}$ (extension) for BOUL/MEANS. The BOUL/MEANS leg is roughly north–south, again consistent with left-lateral shearing in the general direction N45°W. If the deformations are continuous, the direction of maximum extension would be N30°E and the principal extensions are $E_1 = +0.007 \times 10^{-2}$ and $E_2 = -0.009 \times 10^{-2}$, so there is both left-lateral shearing and slight area decrease.

Qualitatively, the long base-line changes support the suggestion of left-lateral shearing that is generally parallel to the direction of the rupture belt. Both sides of the rupture belt deformed in a manner consistent with unloading of the right-lateral fault zones.

Repeated Land Surveys

SoCalEd established bench marks, surveyed, and mapped an area of about 10 land sections during the mid-1970's as part of the control for photogrammetric surveying of a potential site for a power plant. The plant has not been built, but the survey benchmarks remain. The area included a set of section lines from Bessemer Road in the southwest, across Tortoise Hill

16 We use the term normalized length changes because there may well be fracture discontinuities disrupting the line between the two measurement points. We avoid the closely related term, strain, which is defined only for a continuous body.

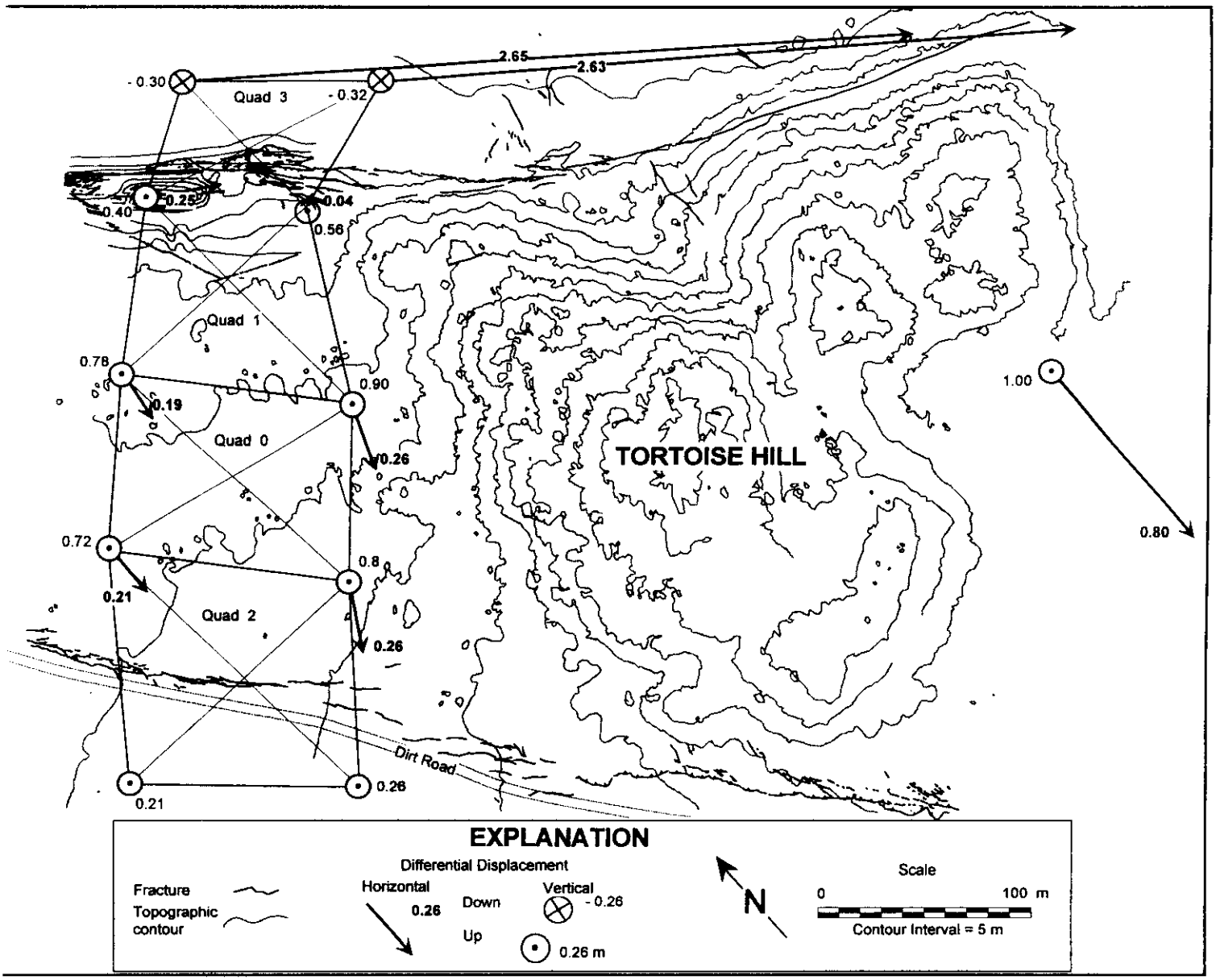

Figure 25. Map showing fractures bounding margins of Tortoise Hill ridge and differential displacements measured photogrammetically. A ladder of quadrilaterals extends across the ridge. At southeast edge, displacements were measured by land survey of regional grid. Maximum horizontal shift across ridge about 2.65 m. Maximum vertical displacement, relative to an assumed fixed point about 6 km south of ridge, is 1.0 m at center of ridge.

ridge and the surface rupture of the Emerson fault zone, and into the alluvial valley of Galway Lake to the northeast. Forty-six bench marks were set as primary *x-y-z* control and an additional 30 wing points were set for elevation control of aerial photography. Using a total station in 1995, SoCalEd repeated angle and length measurements that were made in 1973 and 1976 as part of our investigation of faulting and deformation in the area of the Landers rupture. Plate 3 shows computed horizontal and vertical displacements.

Through examination of normalized length changes, we infer that length changes of about $3x10^{-4}$ and larger should be significant but that inferred length changes of smaller magnitude are masked by survey error. Measurements south of Section 25, T6N, R3E, (Plate 3) which includes part of Tortoise Hill ridge, reflect such small length changes (or errors) that we are unable to obtain meaningful estimates of deformations. According to these results, the normalized length changes are smaller than $2x10^{-4}$ in an area extending 6.5 km south of Tortoise Hill and about 4.5 km southwest the Emerson fault zone (Plate 3). The results suggest that normalized length changes and angle changes are below that level everywhere except where there are control points that span ruptured ground. The small normalized length changes are consistent with the regional GPS and trilateration measurements reported in Figure 11, that the normalized length changes are on the order of $5x10^{-5}$.

Photogrammetric Measurements

In order to determine supplementary length changes in relatively small areas near the rupture zone at Tortoise Hill, we have used a photogrammetric method and sequential aerial photography (see Fleming and others, 1997, for method).

We used the photogrammetric method to measure lengths of legs and braces of a ladder of four quadrilaterals extending across Tortoise Hill ridge from the southwest to the northeast sides. The quadrilaterals, in relation to the fractures that we mapped and the topography of the hill are shown in Figure 11 and Plate 3. The position of the control point in Tortoise Hill that moved horizontally southward is shown near the right-hand end of Plate 3 and with a displacement vector on Plate 3. We determined normalized length changes by comparing lengths of legs and braces in 1973 and 1992. Normalized length changes smaller in magnitude than about $3x10^{-4}$ are negligible (see Fleming and others, 1997).

Starting with the southwest edge of the quadrilateral (Quadrilateral Q2) in the southwest, the normalized length change is marginally significant, but shows a small extension in the northwest direction. The northeast-trending legs cross a rupture zone and both show compression about ten times larger, -1.4 to $-2x10^{-3}$. The compression certainly reflects the thrusting of Tortoise Hill relatively toward the southwest across the southwest rupture belt. The north-south diagonal brace was shortened and the east-west diagonal brace was lengthened, reflecting the right-lateral shear across the southwest rupture belt. Thus the measurements reflect small to negligible extension parallel to the southwest belt, but significant right-lateral shearing parallel and shortening normal to the southwest belt of faulting that bounds Tortoise Hill ridge.

The next quadrilateral to the northeast (Quad Q0) near the center of Tortoise Hill (Plate 3) indicates very small to negligible deformation (normalized length changes smaller than $3x10^{-4}$).

The northeast end of the next quadrilateral (Quadrilateral Q1) to the northeast is within the belt of shear zones on the northeast side of Tortoise Hill ridge. Normalized length changes are generally large, on the order of 10^{-3} and the deformation is clearly inhomogeneous within the quadrilateral. Thus the leg at the southwest edge of the quadrilateral shortened barely significantly, whereas the leg at the northeast edge shortened by $-1.5x10^{-3}$, apparently reflecting the fact that it traverses the right side of the belt of shear zones obliquely. Because the northwest end of the leg is deeper within the belt than the southwest end, the leg is shortened significantly. The shortening of the north-south brace and the lengthening of the east-west brace again reflect the right-lateral shearing in the belt of shear zones.

Another interesting result is that the southwest and northeast sides of quadrilateral Q1 are both extended significantly. Because of the orientations of these sides relative to the orientation of the belt of shear zones, we would expect minor extension in the southwest side and minor compression in the southeast side if there were only simple shearing. We suggest that the significant extension in both sides reflects movement of the center of Tortoise Hill southward relative to the belt of shear zones on the northeast side of Tortoise Hill. We observed this sense of differential displacement for a control point, shown at the left-hand side of Plate 3, that moved 0.8 m toward the south.

The last quadrilateral (Quad Q3) extends from northeast of the belt of shear zones into the belt of shear zones. The northeast side of the quadrilateral stretched significantly, $1x10^{-3}$; the reason is unclear. The northwest and southeast sides also stretched large amounts, 1 to $2x10^{-2}$, apparently reflecting large right-lateral shearing. The minor northeastward thrusting visible in the belt of shear zones apparently was overwhelmed by the right-lateral shearing. The right-

lateral shearing is also reflected in the shortening of the north-south brace and the lengthening in the east-west brace.

In summary, at the three levels of observation, (~10 km, 1 km, 0.1 km lengths), normalized length changes provide insight into the intensity and style of deformation. In the far-field, as measured by trilateration and GPS, principal extensions are in the range of 7 to $9x10^{-5}$. On both sides of the rupture belt in the far field, the deformation is left-lateral shear that is generally parallel to the belt of surface rupture. Re-survey of pre-earthquake bench marks near Tortoise Hill indicates that the deformation is generally below the limit of survey accuracy ($3x10^{-4}$) everywhere except where points cross a belt of surface rupture. The braced quadrilaterals spanning Tortoise Hill gave essentially the same result; normalized length changes were smaller than $3x10^{-4}$ except where quadrilaterals cross faults. Normalized length changes were in agreement with the kinematic expression of fractures in the bounding shear zones.

DIFFERENTIAL DISPLACEMENTS

Horizontal Displacements

The results of the land surveys also determine relative horizontal displacements, assuming that one of the control points and the direction of a line element remained fixed. We selected the southeast corner of Section 36, T7N, R3E to be fixed. The horizontal displacements appear to be smaller than the error level south of Section 25 (T7N, R 3E).

The horizontal displacements are known primarily along the eastern and western section lines. Starting with the eastern section line, and the point farthest north (midheight of Section 24, T7N, R3E), as well as its two neighbors to the south, the displacement is 3 to 3.1 m, right-lateral, roughly parallel to the northeast edge of the Emerson fault zone (Plate 3). This value is slightly larger than the value of differential displacement of 2.9 m we determined by sighting along legs of towers of the Single-tower Transmission Line in Section 23, to the northwest. The next control point along the eastern side is immediately south of the main rupture zone along the northeast side of Tortoise Hill. That point and control points farther south have been displaced horizontally by negligible amounts (less than 20 cm).

The northernmost control point along the western section line is within the belt of shear zones, which, here, is about 50 m wide (Plate 2). The relative horizontal displacement is 0.6 m, directed about 30° east of south. Thus the horizontal displacement is oblique to the northeast wall of the rupture zone but roughly parallel to the southwest wall, which passes around the southwest side of Tortoise Hill ridge. The horizontal displacement of the control point immediately to the south is at the margin of error, about 0.2 m, and is toward the east. The horizontal displacements of control points farther south along the western section line apparently are negligible.

One of the control points is in the center of Tortoise Hill, at mid-length along the southern border of Section 24. The horizontal displacement here, relative to the assumed fixed point is 0.8 m south. This displacement is quite interesting because it reflects the combination of right-lateral differential displacement and southwest thrusting of the block of Tortoise Hill, presumably accommodated mainly by the belt of shear zones that passes around the southwest side of Tortoise Hill.

Differential horizontal displacements were determined relative to quadrilateral points assumed to be fixed immediately southwest Tortoise Hill (Figure 12 and Table 1). The two corners on the southwest end of the ladder of quadrilaterals (Q2-C & D), one of which moved upwards 0.21 m and the other 0.26 m (Plate 3), are points C on the right and D on the left in Table 1. Point A is in the upper left and point B is the upper right of quad Q2. Movement relative to points Q2-C & D is partitioned into components parallel and normal to the fault zone.

According to the bottom part of Table 1, the movement of point A of Quadrangle Q2 was $\delta v = -0.18$ m and $\delta u = 0.13$ m. In combination with the data shown in Plate 3, point A thus moved vertically upward (δz) about 0.72 m, moved to the southeast about 0.13 m (δu), right-lateral, and southwest 0.16 m (δv), thrusting. Point B moved similarly. As indicated in Table 1, point C and D of quad 0 are the same as points A and B of quad 2.

Table 1. Horizontal Displacements of Corners of Quadrilaterals

(Measurements in meters, relative to corners C and D on southwest side of Tortoise Hill ridge).

Quad.	Corner	δu (+SE - northwest) (Parallel to fault.)	δv (+NE -SW) (Normal to fault)	Corner	δu	δv
	A	2.64	0.18	B	2.62	0.21
3						
	D	0.24	0.05	C	0.01	0.04
	A	0.24	0.05	B	0.01	0.04
1						
	D	0.11	–0.16	C	0.09	–0.24
	A	0.11	–0.16	B	0.09	–0.24
0						
	D	0.13	–0.16	C	0.05	–0.26
	A	0.13	–0.16	B	0.05	–0.26
2						
	D	0	0	C	0	0

Thus, according to the photogrammetric measurements (Table 1), the strike-shift across the entire ridge is 2.62 to 2.64 m, and most of this is accommodated on the main shear zone on the northeast side of the ridge. This leaves about 0.4 m of right shift that we measured with our re-survey of bench marks unaccounted for, but presumably it is distributed northeast or southwest the ladder of quadrilaterals.

The photogrammetric measurements also provide rather detailed information about the horizontal dilation of rock within the ridge. According to the photogrammetric measurements, there was net dilation of between 0.18 and 0.21 m between the most distant points outside the ridge, as measured from corner D of Q2 to corner A of Q3 and from corner C of Q2 to B of Q3, respectively. The dilation is somewhat larger for the most distant points within the ridge, between 0.21 and 0.30 m, as measured from corner A of Q2 to corner D of Q3 and from corner B of Q2 to corner C of Q3. The dilation within the ridge is expressed in part by a reverse fault dipping about 45° toward the northeast on the southwest side of the ridge and a very high angle reverse fault dipping about 86° toward the southwest on the northeast side of the ridge. These faults, though, do not account for the net dilation of 0.18 to 0.21 m for points outside the ridge.

Vertical Displacements

Surveyors from SoCalEd re-leveled all the points that could be relocated. This included the network of control points for the northern half of Section 12 near Bessemer Mine Road, through Sections 1, 36, 25, over Tortoise Ridge, to the middle of Section 24 northeast of the ridge as well as all the wing points (wooden stakes) that we could find on either side of the line of sections (Figure 13 and Plate 3).

We have contoured the changes in altitude of control points and wing points, assuming that the point at the southeast corner of Section 1, T5N, R3E did not change altitude. The changes in altitude are marked beside the diamond-shaped symbols representing the control or wing points in Plate 3. We have put three contours on the map with heavy lines, for 0 m, 0.5 m and 1.0 m of vertical uplift. According to our results, the entire area south of the 0 m contour changed altitude insignificantly(changes smaller than 2 cm).

The map with three solid contours of vertical uplift (Plate 3) is the main result of the regional leveling. In this contour map we see a highly localized uplift of Tortoise Hill ridge. The ridge was pushed upward about 1 m as about 3 m of right-lateral shift was accommodated across the Emerson fault zone during the Landers earthquake.

We can see more details of the uplift if we interpolate some intermediate contours, especially if we add some data from the photogrammetric analysis of quadrilaterals shown in Plate 3. Using both sets of data, the regional survey, and the photogrammetric survey of part of the ridge, we have constructed the map of contours of uplift shown in Plate 3.

The regional pattern is an abrupt uplift of the ridge within the bounds of the surrounding belts of shear zones. Where the belt of shear zones on the southwest side of the ridge ends, the uplift of the ridge is less spectacular, but not absent. Thus, the greatest growth of the ridge is an elliptically-shaped domical area centered on the high ground of Tortoise Hill ridge. There the differential growth relative to the tilted surface to the southwest is about three-quarters of the total, or 0.7 to 0.8 m.

There is significant uplift (0.33 to 0.35 m) at wing points east and southeast of the ridge, suggesting that an area of unknown shape extends from Tortoise Hill in that direction. There is another topographic ridge about 3 km southeast of Tortoise Hill Ridge, bounded on the east by the Emerson fault zone, but we do not know whether it grew during the 1994 earthquake.

Another striking feature of the map of contours of altitude change in Plate 3 is a broad trough underlying the valley northeast of Tortoise Hill, between Tortoise Hill and Rodman Mountains to the northeast. The trough probably is a reflection of a pull-apart basin forming where the shift across the Emerson fault zone is decreasing and the shift across the Camp Rock fault zone is increasing.

DISCUSSION

The repeated land survey determined that 3.0 to 3.1 m of right-lateral, horizontal differential displacement was accommodated across Tortoise Hill relative to a fixed point southwest the ridge. It showed that the center of the ridge moved upward 1.0 m relative to the same reference. The same point moved about 0.57 m in a right-lateral sense. A point within the narrower belt of shear zones northwest of Tortoise Hill moved about 0.6 m in a right-lateral sense and was uplifted about 0.3 m.

The photogrammetric survey with a ladder of braced quadrilaterals shows how the vertical and horizontal displacements are distributed across Tortoise Hill, and show that the ground in the valley to the northeast moved downward, as much as 0.3 m, presumably reflecting the growth of a pullapart basin in that area (Plate 3).

The subsurface form of the belt of shear zones and tectonic ridge at Tortoise Hill is, of course, unknown. We know of only two sets of observations that are relevant to subsurface conditions here. One is indirect evidence of zones 50 to 200 m wide at depths as great as 10 km that trapped seismic energy along the Homestead Valley and Johnson Valley belts of shear zones at Landers (Aki, 1994; Li and others, 1994a, 1994b). The other is the documentation of *flower structures* along some strike-slip faults. Flower structures have been described in seismic images of strike-slip fault zones (Harding and Lowell, 1979; Harding, 1983; Harding and others, 1983; D'Onfro and Glagola, 1983; Plawman, 1983) and in rifts (Genik, 1993; Roberts, 1983). They have a diagnostic branching appearance, from a supposed single branch at depth (generally many kilometers) to two

branches above, and then four and so forth as the flower structure approaches the ground surface. The branching structures do not appear in vertical seismic sections of simple thrusting or extensional regimes (e.g., Bally, 1983). Flower structures appear to be complex in vertical sections because a vertical section of a strike-slip fault that is normal to the trace of the fault is a secondary view. A map view of a strike-slip fault is the principal view.

Observations Relevant to Mechanisms of Tectonic Ridge Formation

Several mechanisms have been suggested for the formation of tectonic ridges (and push ups) as well as analogous ridges known as *flank ridges* in large landslides. Tectonic ridges have been described many times (e.g., Sibson, 1980; Segall and Pollard, 1983; Aydin and Page, 1984; Sylvester, 1988; Bilham and King, 1989; Scholz, 1990). Flank ridges were described in several landslides in Utah by Fleming and Johnson (1989) and by Baum and others (1988a and 1988b) and the Slumgullion landslide in Colorado (Fleming and others, 1996).

Our observations at Tortoise Hill ridge at Landers provide some detailed information about the growth of a tectonic ridge:

1). Fractures define a broad belt of shear zones along the part of the Emerson fault zone that ruptured during the Landers earthquake, extending from somewhat north of the Single-tower Transmission Line to at least the southern end of Tortoise Hill (Plate 3). The amount of right-lateral shift ranges from 2.9 m at the single-tower powerline to about 3.1 m at the southeast end of Tortoise Hill ridge.

2). Horizontal deformations in the vicinity of the Emerson fault zone show left-lateral shearing in rocks even a few hundred meters on either side of the belt of shear zones, representing stress drop and elastic rebound, and right-lateral shearing and probably dilation within Tortoise Hill ridge, reflecting permanent ground deformation within the belt of shear zones.

3). Differential vertical displacements show that Tortoise Hill ridge grew about 1 m in height much as an elongated dome centered on the highest point within the ridge as the Emerson fault zone accommodated about 3 m of right lateral shift.

4). The elongate-dome-shaped region of growth is bounded on the northwest and southeast sides by belts of shear zones, accommodating both right-lateral and differential vertical shift.

5). Although the uplift of ground was largely concentrated in the ridge, the ground extending for at least 3 km southwest of the ridge was bent upwards. The ground is not merely tilted because the slope of the change in elevation increases as the southwest side of the ridge is approached from several kilometers away.

6). The present topography and geology of Tortoise Hill reiterates and echoes the growth that occurred during the 1992 earthquake (Figure 4). The northeast face of the ridge is steep and rugged where it rises abruptly above the valley of Galway Lake. The southwest face is much lower and extends only about 20 m above the pediment-like rock surface farther to the southwest the ridge. Most of the differential vertical displacement was on the steep, northeast side of the ridge. Sub-vertical scarps there are up to a meter high. The scarps of the low-angle reverse faults on the southwest side of the ridge are only a few tens of centimeters high.

7). Tortoise Hill contains spines of granite near the northeast-bounding shear zone that appear to have been pushed upward differentially.

The measurements and observations at Tortoise Hill can be supplemented with data from landslides to identify potential mechanisms of ridge formation. Observations of map and cross-sectional views of flank ridges in landslides, documentation of differential displacements and strains within one ridge in the Aspen Grove landslide in Utah, and examination of maps of other ridges in that area suggest that there are several potential mechanisms of ridge formation (Fleming and Johnson, 1989).

Steps, Jogs or Bends

Tectonic ridges and push ups have been widely reported (e.g. Aydin and Page, 1984) to occur at opposite steps, jogs or bends along faults (i.e. restraining structures). An opposite bend or step would be a left step, jog, or a left bend in a right-lateral and would be a right step, jog, or a right bend in a left-lateral strike-slip fault. Our observations of structures that form at opposite steps at various places at Landers and in large landslides, however, suggests that the main phenomenon of restraining steps is not ridge formation on one side of a restraining bend, but rather near-surface compressional phenomena such as folding or thrusting on both sides. Representative examples are the structures that formed at the small restraining bend near the northwest end of Tortoise Hill. Adjacent to the restraining bend was a small dome and tension cracks on the southwest side and thrust faults on the northeast side of the rupture belt (Figure 10 and left side of Plate 3).

The case is similar in landslides. We generally saw low domes or thrust faults at opposite or restraining steps; we did not see ridges at such places (Fleming and Johnson, 1989). The structures that formed at restraining bends in flanks of landslides are different from those along faults; they were restricted to the moving ground. Non-moving ground outside the flanks did not contain the compressive structures. The ridges we saw in the landslides were fault-parallel and typically along straight stretches of rupture zones.

Although there is no question that localized compression will be developed in ground in an area with an opposite step or restraining bend along a strike-slip fault, the importance of opposite steps and restraining bends in the formation of tectonic ridges remains to be demonstrated. In the references cited above, e.g., Sibson, 1980; Segall and Pollard, 1983; Aydin and Page, 1984; Sylvester, 1988; Bilham and King, 1989; Scholz, 1990; the relation was merely assumed.

Dilatancy

The ridges, both in landslides and along faults, could result from dilatancy of rocks in shear zones (Johnson, 1995). We note that strike-slip faulting commonly occurs in belts of shear zones rather than across single fault surfaces, so ridges could be associated with the belts of shear zones rather than individual fault strands.

Our observations and inferences (Fleming and Johnson, 1989; Fleming and others, 1996) of ridges in landslides and along strike-slip faults lead us to suggest the following:

1). Ridges occur within belts of shear zones along faults with predominant strike-shift differential displacements. In the case of landslides, the belts of shearing are within the active landslide debris as are the ridges, but they are adjacent to the bounding or internal fault zones, not within non-deforming debris. In the case of tectonic ridges we have examined, the ridges are within a belt of shear zones.

2). The belts of shear zones occur at depth as well as at the ground surface.

3). Ridges are a result of localized increase in pressure and volume within the belts of shear zones beneath the ground surface. The increase in pressure and volume at depth pushes the ground upward within the ridge.

4). The increase in pressure and volume can be a result of positive dilatancy of the fractured rock within the belt of shear zones beneath the ground surface (e.g., Johnson, 1995).

5). Some ridges form in certain materials that occur within belts of shear zones. The materials that produce ridges translate along the fault zone as the ridge grows, carrying the causative mechanism with them, and growing as a dome that presumably has roughly the area of the horizontal area of the mass of dilatant materials below. Where ridges are a result of dilatation, they have a finite period of growth because the material eventually dilates to a constant state volumetrically.

In contrast, if ridges were a result of a step or similar irregularity in the shape of a single fault, they would grow essentially at a point and then be translated away from the causative step and be dormant thereafter. The causative mechanism would be static. The active part of the ridge should be at one end of the ridge.

Wedging

Another mechanism for producing ridges is suggested by three observations: Faults typically are straight in the direction of fault slip but are highly curved in the direction normal to the direction of slip. Tortoise Hill and some other tectonic ridges in the Landers area have an enveloping belt of shear zones. Flower structures at depth have been identified along some strike-slip faults with seismic exploration techniques.

Figure 26. Idealizations of ruptures along Emerson fault zone suggesting mechanisms for growth of Tortoise Hill ridge and tilting of ground southwest of fault zone. A. Idealization of canoe structure, consisting of a main fault, a splay fault, and a tilted floor of the wedge between the main and splay faults. If the wedge moves more slowly than the blocks to either side, the sloping floor will cause the wedge to rise, as an idealized ridge. B. Idealization of a twisted splay. The part of the block above the splay moves more slowly than the blocks on either side of the main fault. As a result of the twist in the shape of the splay, part of the block near the fault tilts. C. Idealization of proposed canoe structure beneath Tortoise Hill ridge. D. Idealization of proposed twisted splay at deeper level beneath Tortoise Hill ridge.

Normal and reverse faults are characterized by highly irregular and sinuous surface traces, but strike-slip faults are characterized by relatively straight surface traces. Thus we would expect the Emerson fault zone to have a highly sinuous trace if we would examine it in vertical section. A change in the sinuous trace with horizontal position near the ground surface could cause the ground to rise or fall near the trace of the fault.

The overall form of Tortoise Hill ridge is a wedge-shape, both in plan and, presumably, in cross section (Figure 14C). The dip of the bounding faults near the ground surface indicates that they would converge at depth. As shown in Plate 3, or especially Plate 2, the plan view of the northwest part of Tortoise Hill is a wedge, bounded on the northeast by the main rupture zone and on the southwest by the thrust/right-lateral rupture zone. The latter rupture zone is a splay that diverges from the main rupture zone. The trace of the trace of the splay is oriented with a clockwise trend with respect to the trend of the main, right-lateral, rupture zone on the northeast, in the sense that G. K. Gilbert noted for faults along the surface rupture north of San Francisco following the 1906 earthquake and along normal faults in Utah (Gilbert, 1928, p. 13).

Figure 14C shows Tortoise Hill interpreted as a simple flower structure, a wedge, within a belt of shear zones. The idealized mechanism of growth is illustrated in Figure 14A. The mechanism has two essential parts, one geometric and the other kinematic. The geometric part is a sloping base or bottom of the wedge. The kinematic part is that the wedge moves more slowly than the block of ground on the same side of the main rupture. Specifically applied to Tortoise Hill, the block of ground to the east (left in Figure 14A) has a relative displacement toward the south. The block of ground to the west, except for the wedge, has the same

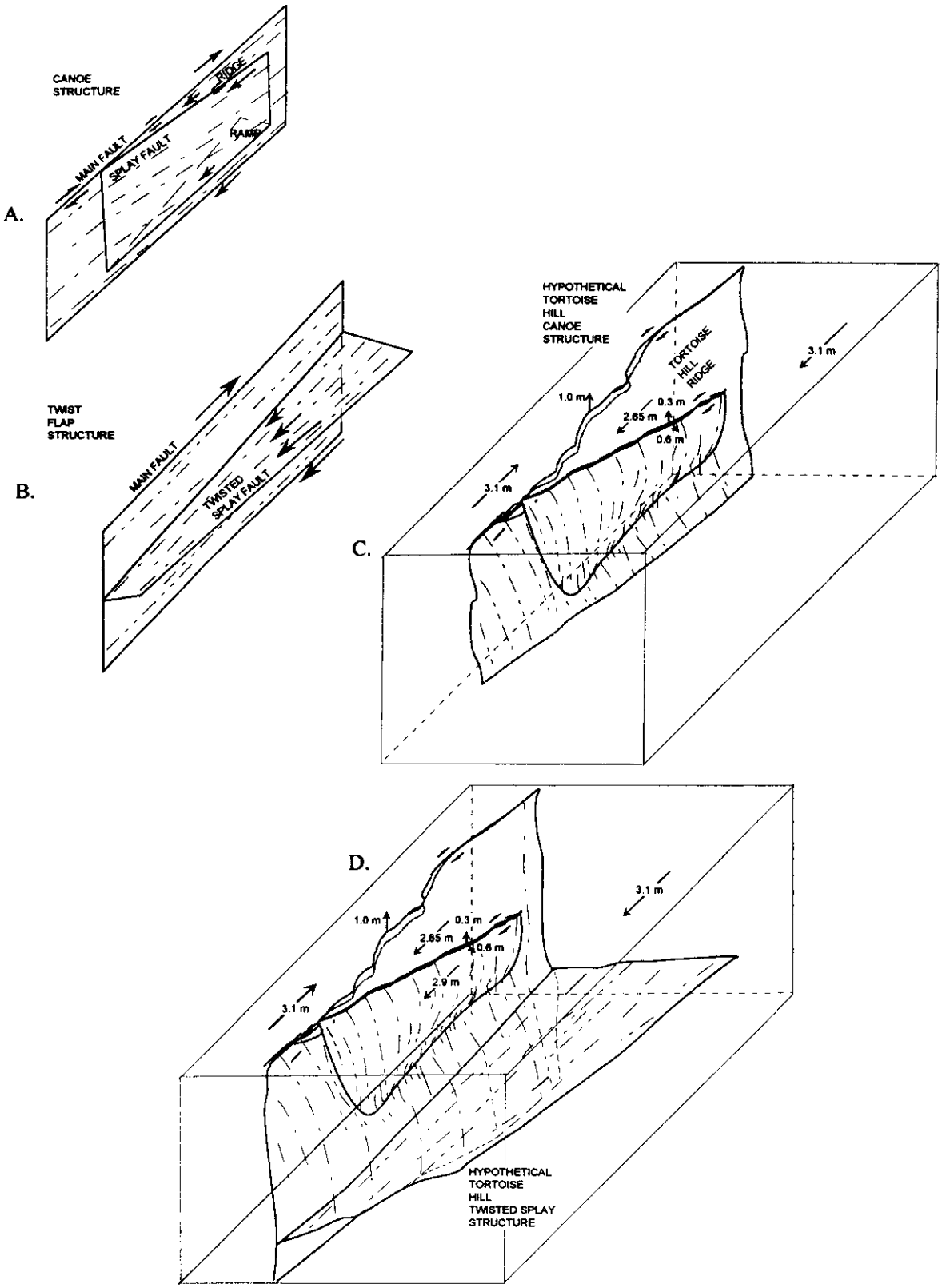

Figure 26. Idealizations of ruptures along Emerson fault zone suggesting mechanisms for growth of Tortoise Hill ridge and tilting of ground southwest of fault zone. A. Idealization of canoe structure, consisting of a main fault, a splay fault, and a tilted floor of the wedge between the main and splay faults. If the wedge moves more slowly than the blocks to either side, the sloping floor will cause the wedge to rise, as an idealized ridge. B. Idealization of a twisted splay. The part of the block above the splay moves more slowly than the blocks on either side of the main fault. As a result of the twist in the shape of the splay, part of the block near the fault tilts. C. Idealization of proposed canoe structure beneath Tortoise Hill ridge. D. Idealization of proposed twisted splay at deeper level beneath Tortoise Hill ridge.

relative displacement, but toward the north. The wedge has a smaller relative displacement toward the north. Thus the wedge is lifted as the block to the west moves beneath it.

At Tortoise Hill, the wedge is imagined to be shaped like half of a sway-backed canoe, with the front of the canoe deeper than the midlength. Thus, since Tortoise Hill moves more slowly, relatively, northwesterly, than the ground to the southwest, the hill rises, forming a tectonic ridge.

An appealing feature of this explanation of the growth of Tortoise Hill ridge, besides that it is consistent with the field observations and measurements, is that the same basic mechanism can explain the tilting of the pediment to the southwest of the ridge. If there is a deeper splay within the flower structure, perhaps nearly horizontal, but twisted about an axis parallel to the main fault, the same differential displacements discussed above would produce a tilting of the ground. The basic mechanism is illustrated in Figure14B and its application to Tortoise Hill is suggested in Figure 14D.

Other reasons we favor this mechanism for some ridges is that ridges within wedge-like intersections of a main fault and a splay fault along right-lateral, strike-slip faults have been mapped throughout the Landers area. There are several along the Emerson fault zone next to Emerson Lake, one along the Calico fault zone about 8 km northeast of Tortoise Hill, and two along the Johnson Valley fault zone near Melville Lake (Dibblee, 1964, 1967a, 1967b). Finally, the proposed splay faults are similar to simple flower structures observed in seismic profiles of strike-slip and rifting areas throughout the world (e.g., Harding, 1983; Harding and Lowell, 1979; Harding and others, 1983; D'Onfro and Glagola, 1983; Genick, 1993).

Final Comments

We have identified geometric and material property conditions that could produce tectonic ridges. An opposite step or bend in a fault produces compression that may produce a dome and thrust faults and perhaps even a ridge. A dilative material in a broad shear zone near the ground surface could develop sufficient pressure at depth to intrude more mobile material at depth and extrude some material onto the ground surface. This is an important mechanism of ridge-formation in landslides, and may well be important along some faults. Simple flower structures within strike-slip fault zones that change shape along strike could produce tectonic ridges and tilt the ground on either side of a fault zone.

Presumably ridges can form in all these ways and it would be foolish to think there are not other ways. There is no reason to believe that structures with the one name can be produced by only one mechanism. In landslides, for example, we have not noticed ridges that have formed at splays of the main bounding shear zone. At Landers, many of the tectonic ridges occur between a splay and a main rupture zone. Perhaps many of these formed by wedging. But not all tectonic ridges occur adjacent to a splay.

Only the splay mechanism specifically addresses the tilting of the ground to form a pediment-like slope southwest the fault zone (Plate 3).

PART IV. STRUCTURES FORMED IN RELEASING STEPS

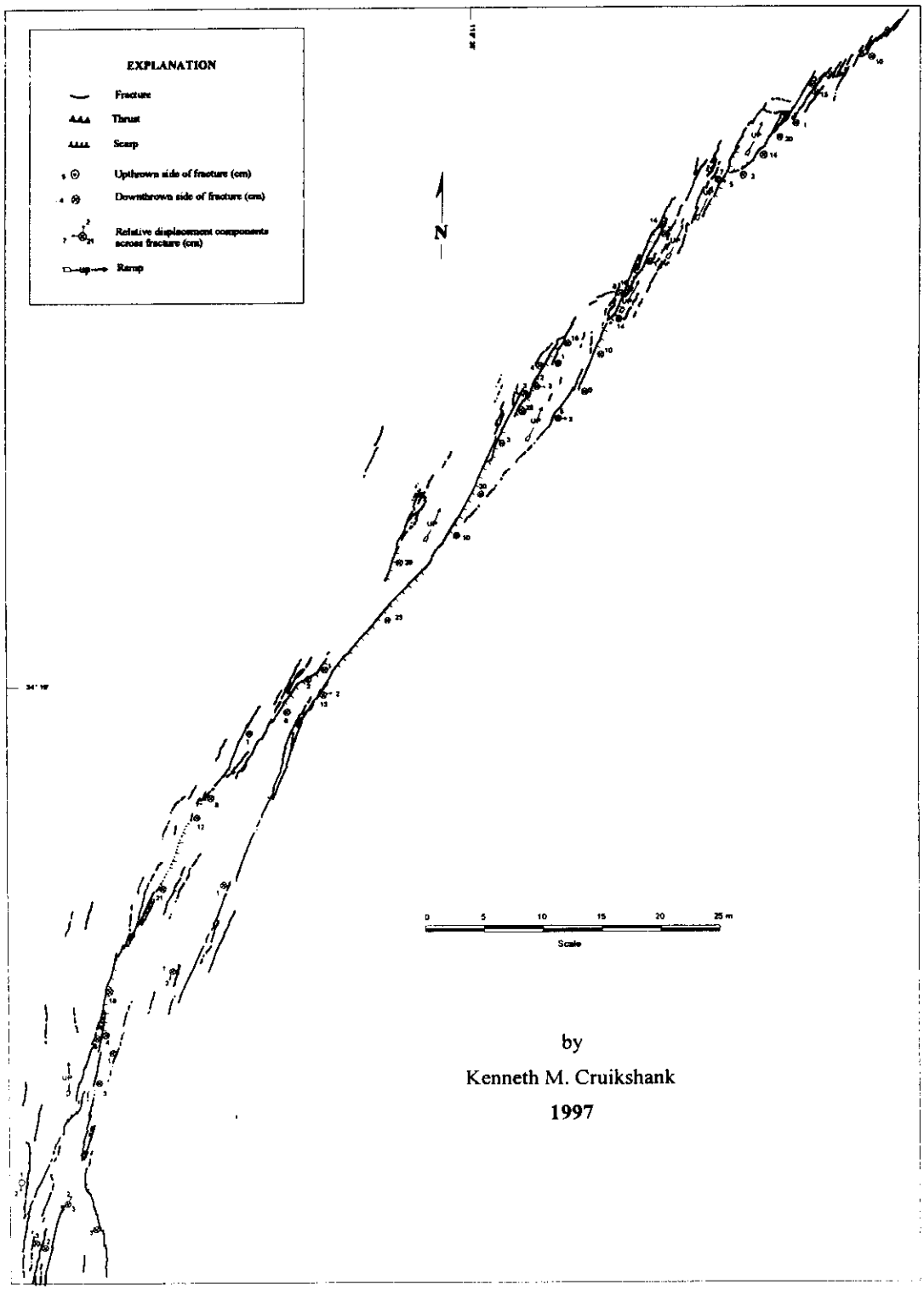

by

Kenneth M. Cruikshank

1997

SMALLER DUPLEX STRUCTURES

In previous pages we described two large duplex structures that form the Homestead-Emerson and Kickapoo stepovers. Here we describe a well-documented structure in the Two Ranch area along the Homestead fault zone and an incompletely documented duplex structure along the Emerson fault zone.

Headquarters Duplex in Homestead Valley Fault Zone

The Headquarters duplex is along the northeast side of the rupture zone of the Homestead Valley fault zone (Plate 1 and Plate 3). Between Goatsucker ridge in the northwest and Reche Mountain in the southeast, the fault on the northeast side of the rupture zone consists of three *en echelon* elements about one kilometer long. The segments step right in releasing steps. Different structures form in the two intervening steps between the segments. At the Headquarters step, there is a duplex structure; at the Pipes Wash step, farther south, there is a left-lateral rupture zone bounding a rotating block.

We set control points for our maps of the Headquarters duplex (Plate 4) with a Total Station (Theodolite with electronic distance meter). The duplex begins near Mikiska Boulevard, north of Bodick Road, and extends about 400 m south to Mileska Ranch, on Shawnee Road (Plate 4). We mapped the part of the duplex structure south of Bodick Road a year after the earthquake, yet its essential features were still well defined (see Plate 4). The features south of Bodick Road are nearly as clear as those north of it.

The duplex structure is about 400 m long and 90 m wide. It consists of diagonal, shear-zone segments that form the internal elements of the duplex structure plus the bounding faults. The bounding fault on the east extends southward, to near the building marked "Headquarters" in Plate 4, about half the length of the duplex. The bounding fault on the west extends northward to near Bodick Road, about two-thirds the length of the duplex.

The shear zones within the duplex are right lateral, as are the bounding faults. Individual shear zones are spaced about 10 m apart, are 100 to 150 m long, and are oriented at a clockwise angle of 20 to 30° to the bounding faults. The shear zones within the duplex are, themselves, short, right-lateral, *en echelon* fault elements 5 to 10 m long. Between many of the fault elements are short thrusts (Plate 4) that shift displacement across from one fault element to another.

The Headquarters step consists of a hierarchy of stepping elements (Plate 4). The Headquarters duplex itself forms a releasing step (Figure 14B) because the bounding faults are right lateral and they step right. Within the duplex, though, the fault elements have restraining steps, at two different scales. The shear-zone elements within the duplex have restraining steps because they are right lateral and step left (Figure 12B and Figure 14A). Furthermore, many of the shear zone segments are composed of short fault elements also arranged as restraining steps (Figure 12C).

The lateral shift in the internal shear zones in the northwest part of the duplex, between Bodick Road and Mikiska Boulevard, was evident in the deformation of the fence on the north side of the Northern Ranch (Plate 4). The lateral shift there was generally 5 to 10 cm. In the southeast part of the duplex there were few markers, but we would estimate an average of 30 cm accommodated by each short shear-zone segment, about 5 to 10 m long. We could measure vertical shift, generally a few cm, with downthrowing on either side (Figure 11). The openings of cracks along the internal shear zones were similarly on the order of a few centimeters (Figure 11), indicating some dilation in the releasing duplex.

Offsets of fences with different orientations at the North Ranch indicates that the bounding fault on the east side of the duplex accommodated 1 to 1.2 m of right lateral shift (Johnson and others, 1993). Offset of fences with different orientations at Mileska Ranch indicates a net shift of 1.6 m across the bounding fault segment on the west side of the duplex. This later number was determined as follows. The bounding fault accommodated about 1.4 m of right-lateral shift in the south fence and 70 cm of right lateral shift in the west fence of the Mileska Ranch. Thus the net shift was about 1.6 m. Besides the lateral shift, the ground to the west of the west fence of the Mileska Ranch was relatively downdropped about 10 cm.

Table 3 compares the geometric elements to those for other duplex structures at Landers. Nothing about this duplex is remarkable, geometrically.

Duplex at Single-Tower Transmission Line Site

In preceding paragraphs, we have described the belt of shear zones at the Single Tower Transmission Line area along the Emerson fault zone. Starting about 40 m southeast of the collapsed tower (Plate 3), the shear zone bounding the northeast side of the belt broadens from about 3 m width to 15 - 20 m width over a horizontal distance of about 200 m. Then it abruptly narrows to 1 - 2 m width. We made only a photogeologic map of the fractures in this area, but the widening appears to define a narrow duplex structure of right-lateral fault elements. The duplex accommodates a shift of perhaps 2.7 m. Table 3 compares the geometric elements of this duplex structure (STTL) with those of others in the Landers area.

PIPES WASH ROTATING BLOCK IN RELEASING BEND

The right step between fault elements along the Homestead Valley fault zone at Pipes Wash has an internal structure that is quite different from that at the Headquarters step. Rather than a group of right-lateral ruptures connecting the stepping right-lateral bounding faults, there is a left-lateral rupture, plus some associated normal or oblique faults (Figure 27). In many respects, the left-lateral rupture plays the same role as the left-lateral fractures between rotating blocks in the Summit Ridge shear zone at Loma Prieta (Johnson and Fleming, 1994), and the left-lateral fractures within the Happy Trail shear zone along the Johnson Valley fault zone at Landers (Johnson and others, 1993, 1994). The rotating block at Pipes Wash is, in some ways, reminiscent of the Landers/Big Bear rotating block mentioned in earlier paragraphs.

Figure 27. Fractures in Pipes Wash stepover in Homestead Valley fault zone as mapped one year after Landers earthquake. The main rupture of the Homestead Valley fault zone is defined by en echelon swarms of tension cracks oriented north-south and thrusts at the southwest ends of individual swarms. As indicated in Plate 1, the main trace turns clockwise near the ranch, so most of rupture shown here is within the stepover. The stepping segment to south is out of view. Within the stepover is the left-lateral/normal rupture zone shown near the center of the figure. It extends from near the ranch southwestward about 150 m to right-lateral/normal faults. Details of the left-lateral rupture are shown in Plate 7.

Along the Homestead Valley fault zone, south of Virginia Avenue (Plate 1), the belt of shear zones is about 300 m wide. The rupture bounding the northeast side of the belt of shear zones forms a double bend, by turning clockwise and proceeding laterally about 100 m over a horizontal distance of about 200 m, and then turning counterclockwise back to its original orientation. Thus, the structure forms not in a step, but in a double bend. Within the belt of shear zones, fractures are oriented north-south in the area north of the bend where the wall is oriented about N25°W. The fault elements are a few meters long and bound blocks that have been thrusted, suggesting that the blocks were rotating (accommodating left-lateral slip between blocks). The amount of shift across this part of the northeast side of the Homestead Fault zone was 1.65 m, according to measurements of offset of fences on two sides of the property shown in Plate 4. Farther south, the northeast side of the Homestead Valley fault zone turns clockwise about 25°, to roughly a north-south orientation. It continues to be composed of *en echelon* fault elements (and tension cracks) bounding blocks that have rotated and thrusted. The fault elements are oriented about N20°E, a clockwise change of orientation of about 20°, roughly the same as the change of orientation of the walls. We have some kinematic information for individual faults and tension cracks within this zone. The differential vertical displacements across the faults within the right-lateral *en echelon* zones are small, generally 3 cm, to as large as 5 cm. The downthrown side is typically on the inside of the belt of shear zones, although there is a small, shallow graben near the channel of soft alluvium.

On the western side of the short, misoriented segments of the bounding shear zone is a left-lateral rupture zone. It is in the position of duplex structures in many of the other releasing steps at Landers. The detailed maps of the Pipes Wash area illustrate fractures formed at the first bend in the wall of the Homestead Valley fault zone and in the left-lateral fault zone that formed at the northwest end of the structure. Although much of the detail of deformational structures was gone, because we mapped the area about a year after the earthquake, we could still see that the bend in the wall of the Homestead Valley fault zone consists mainly of *en echelon* fault elements.

At the northeastern end of the left-lateral shear zone its walls are oriented about N30°E, and fault elements within it are oriented about N20°E. Thus, the angle between the walls of the right-lateral *en echelon* zone north of the bend and the walls of the left-lateral *en echelon* zone is about 80°. The trend of the left-lateral zone curves and then, at its southwest end, turns north-south and is replaced by tension cracks. The downthrow across the left-lateral rupture is much larger than on the right-lateral ruptures, on the order of 10-20 cm, and as large as 25 cm along the left-lateral *en echelon* rupture. We have no information about the magnitude of the left-lateral shift across the left-lateral zone.

The geometric features of the *en echelon* zone are unremarkable. In Table 3 we have listed the geometric information that we use to compare and describe *en echelon* fault structures. The walls of the *en echelon* zone are separated by about 5.5 m and the spacing of the faults is about 3.5 m, so the ratio of spacing to width is about 0.6, and the length of the fault elements is about 18 m, at least in the northern part of the map area. The angle, α, between the walls is about 15°. A geometrically–similar symmetric right-lateral rupture zone would have an alpha value of 175°. Table 3 indicates that, although this left-lateral zone contains some of the shorter fault elements, the relative spacing of fault elements and the equivalent orientation (of 175°) of the fault elements relative to the walls are quite similar to those of several right-lateral *en echelon* zones.

We view the left-lateral rupture as a boundary of a block rotating clockwise within the right bend of the main break of the Homestead Valley fault zone in this area.

TENSION CRACKS AND GROWTH OF A PULL-APART BASIN

Another type of accommodation within a stepover formed at the Single Tower Transmission Line site along the Emerson fault zone (Figure 1). A swarm of tension cracks, shown near the collapsed tower in, extends across the valley of Galway Lake from the east wall of the Emerson

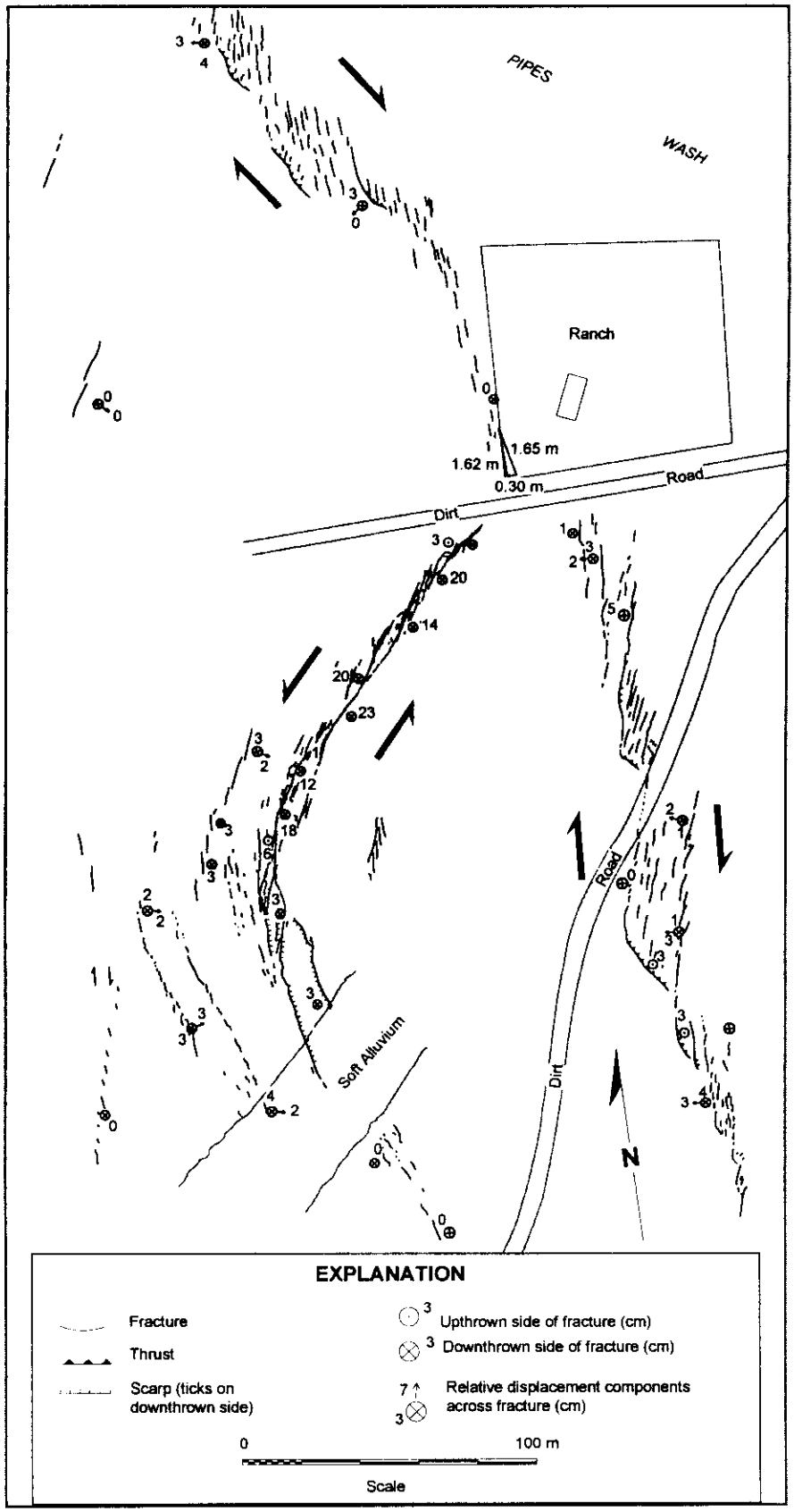

Figure 27. Fractures in Pipes Wash stepover in Homestead Valley fault zone as mapped one year after Landers earthquake. The main rupture of the Homestead Valley fault zone is defined by en echelon swarms of tension cracks oriented north-south and thrusts at the southwest ends of individual swarms. As indicated in Plate 1, the main trace turns clockwise near the ranch, so most of rupture shown here is within the stepover. The stepping segment to south is out of view. Within the stepover is the left-lateral/normal rupture zone shown near the center of the figure. It extends from near the ranch southwestward about 150 m to right-lateral/normal faults. Details of the left-lateral rupture are shown in Plate 7.

fault zone toward the Camp Rock fault zone on the east side of the valley. The Single Tower Transmission Line site is one of several places along the valley of Galway lake where rupture connections have formed between the Emerson fault zone and the Camp Rock fault zone. The swarm of tension cracks occurs in a belt about 50 or 60 m wide, trending N 20° to 30° E, and extending at least 500 m toward the Camp Rock fault zone. Although we traced the tension cracks only a few hundred meters across the valley, they probably extend to the Camp Rock fault zone, about 1.5 km to the northeast. As such, they are an expression of the deformation in the transfer zone—between overlapping segments of the Emerson and Camp Rock fault zones that ruptured during the earthquake. By sighting between the supports for the formerly–aligned transmission towers we found that 69 cm of offset was contained within the transfer between the Emerson and Camp Rock fault zones.

The orientations of the tension cracks within the transfer zone are distinctly different, by 20° to 30°, from those of the tension cracks within the broad shear zone along the Emerson fault. The tension cracks in the shear zone are oriented at a clockwise angle of 30° (to as much as 45°) to the walls of the shear zone, whereas those within the transfer zone are typically oriented at a clockwise angle of 60° to 70° to the walls of the shear zone.

A consequence of the two different orientations of tension cracks is the difference in direction of maximum tension within and outside the shear zone. The tension direction was about N60°W within the transfer zone, but about E-W within the broad shear zone. This marked difference in stress state over a relatively short horizontal distance supports our interpretation that the tension cracks within the broad shear zones result from shearing and dilation within a zone of *localized* shearing at depth; because the shearing and dilation are localized below, the stresses generated in the near-surface materials are localized. In contrast, the stresses responsible for the fractures within the transfer zone are a result of *interaction between two relatively widely spaced fault zones*, in this case interaction across the valley. Studies by Pollard and his students (e.g., Segall and Pollard, 1983; Martel, Pollard and Segall, 1988; Martel and Pollard, 1989; Martel, 1990) have clearly illustrated and documented the formation of tension cracks in similar transfer zones between interacting faulted joints in granitic rocks. Interestingly, they observe that the traces of tension cracks form at 50° to 90°, perhaps with a strong tendency for angles of 60° to 70°, counterclockwise with respect to traces of stepping, faulted joints. The angle for bounding right-lateral fault zones at the Single Tower Transmission Line site is equivalent—60 to 70° clockwise.

The tension cracks presumably formed in response to pull apart, and we have some evidence that a pull-apart basin subsided at least 0.3 m during the Landers earthquake described elsewhere and illustrated in (Figure 23) is a broad trough of differential vertical displacement underlying the valley northeast of Tortoise Hill, between Tortoise Hill and Rodman Mountains to the northeast. The trough of vertical displacements in the Valley of Galway Lake is probably a reflection of a pull-apart basin forming where the shift across the Emerson fault zone is decreasing and the shift across the Camp Rock fault zone is increasing. More detailed data indicate that, near the northeast side of Tortoise Hill ridge, the ground has dropped at least 0.3 m, and a control point between Sections 19 and 24 dropped 0.2 m. Thus, this pull-apart basin subsided at least as much as that in the Homestead-Emerson stepover, described by Zachariasen and Sieh (1995).

PART V. *EN ECHELON* FAULT ELEMENTS

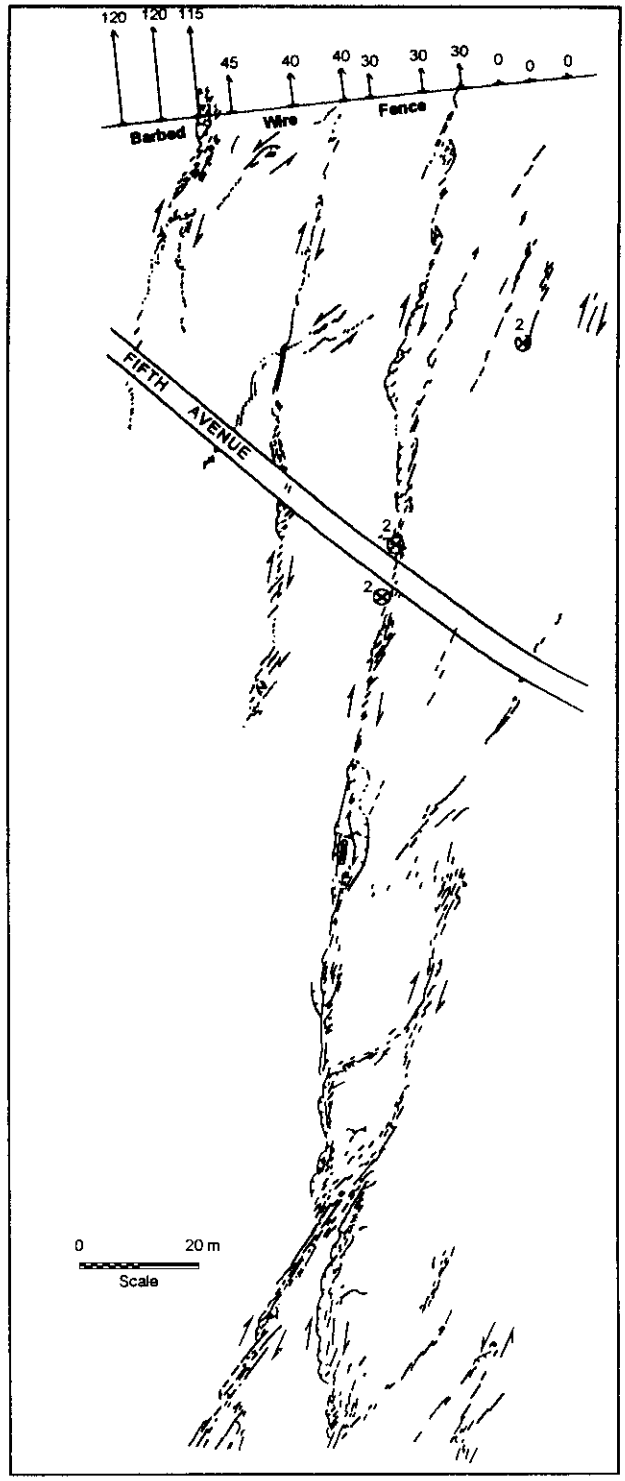

EN ECHELON FAULT ELEMENTS IN LANDSLIDES

Fleming and Johnson (1989) described *en echelon* fault elements at landslides in Utah, where elements were well expressed and where movement was sufficiently slow that we could observe their formation. The principal difference between fractures produced by earthquakes and landslides is that the earthquake fractures are the result of sudden movement. There is no opportunity to observe the formation of a fracture produced by an earthquake, and fractures must be interpreted as a snapshot in time. Strike-slip-fault segments bounding landslide masses typically dip 80-90°, differential displacements are subparallel to the surface traces, the surfaces are generally slickensided, and the slickenlines generally plunge at the average slope angle of the ground surface, indicating slope-parallel movement. The faults are segmented into elements, and adjacent elements have different orientations or step laterally. The strike-slip faults we studied in the Aspen Grove landslide propagate toward the ground surface in mode III (Figure 8), 1975); they do not propagate parallel to the ground surface after they reach the surface. The fault elements appear to represent fingers of an underlying strike-slip fault that have reached the ground surface (Fleming and Johnson, 1989, fig. 13).

The fault elements typically are *en echelon*, and continued displacement of the landslide produces folds, thrusts, and tension cracks between the elements. Along one part of the Aspen Grove landslide, the fault elements are parallel to the walls or are oriented 10 to 20° clockwise with respect to the walls of the right-lateral *en echelon* zone. The traces range in length from a few tens of centimeters to about 2 m. Many are open but have slickensided surfaces. The obliquity of the fault elements relative to the walls of the *en echelon* zone causes the elements to open and form compound cracks with continuing displacement across the walls.

The *en echelon* fault zone in the flank of the Aspen Grove landslide in Utah appears to have developed above a propagating strike-slip fault that initiated at depth, along the base of the landslide, and turned upward and propagated toward the ground surface in fingers or blades. As it approached the ground surface, it separated into a series of fault elements whose new surfaces twisted as they propagated toward the ground surface. Near the ground surface the fault traces are typically oriented about 10-20° clockwise with respect to the trend of the fault surface at depth (Fleming and Johnson, 1989).

Fault elements of *en echelon* zones in the landslides are analogous, at least superficially, to the fault elements in *en echelon* zones that formed during the Landers earthquake. In a landslide, the slip rate on the continuous fault at depth is presumed to be constant. There is, however, typically a gradual change in slip amount and rate along the trend of a landslide flank, from a value of zero above the head, to zero below the toe. In between, the rate, and hence the amount of slip increases to some maximum value and decreases to zero. This change in slip rate or amount occurs on the flanks of large landslides over distances of hundreds or thousands of meters. For example, displacement on a flank of the 3.7-km-long Slumgullion landslide in southern Colorado increases gradually from zero at the head, to about 6 m/yr about 2 km from the head, and decreases gradually to less than 2 m/yr at the toe. Along any given stretch of a few hundred meters, the change in displacement rate may be 0.1-0.2 m/yr.

At the scale of fault elements produced by earthquakes or in landslide flanks, the displacement underlying an element can also be assumed to be a constant. The displacement on each fault element that is viewed at the ground surface, however, must change from zero at the element tip to a finite value along the element, and to zero again at the other tip. Displacement is transferred from one element to another by thrusting or buckling the material between the tips of the elements or in the zones where the elements overlap.

EN ECHELON RUPTURE ELEMENTS OF KICKAPOO FAULT ZONE

The Kickapoo fault zone is a right-lateral fault zone that connects the right-lateral Homestead Valley and Johnson Valley fault zones. It is highly segmented into elements at several levels. The elements are stepped *en echelon*, and the individual elements themselves are divided into smaller *en echelon* elements. Furthermore, the largest elements accommodate vertical shift as well as right-lateral shift, and the overall morphology of the stepping structures reflects the complex shift.

Two areas of the Kickapoo fault zone were mapped in detail; each contains interesting structural details. The elements in the Kickapoo fault step left so there are restraining steps at their terminations that are similar to fault elements in landslides. In the case of the elements in the Kickapoo, there is a broad bulging or uplift of the areas between the overlapping elements.

Two-Bikers Area

The Two Bikers area is at Fifth Avenue, about 500 m north of the intersection of the Kickapoo fault zone with the Johnson Valley fault zone (Plate 1) and east of Kickapoo Trail. We selected the area for analytical mapping, at a scale 1:200, because there is a wire fence at the north end to measure the lateral-shift distribution, and there are several fault elements in the area. The geometric elements of the *en echelon* zone in the Two Bikers area are given in Table 3. The orientation of the Kickapoo fault zone, within the Kickapoo stepover, is about $\alpha = 140°$ (Table 3). The walls

of the Kickapoo stepover are oriented about N35°W, so the Kickapoo fault zone is oriented about N5°E. The walls of the *en echelon* ruptures in the Two Bikers zone are oriented about N5-10°E, and the angle of the elements within the Two Bikers zone is α = 170°. The walls of the small *en echelon* zone within the long element in the Two Bikers area are oriented about N20-25°E, and the orientation of the elements is α = 165°. Thus, at each level, the elements are oriented farther toward the east. According to Table 3, for the three levels of *en echelon* ruptures, the ratio of spacing to width ranges from 0.2 to 0.5.

Figure 28. *En echelon* shear zones along the western side of the Kickapoo fault zone near intersection of Kickapoo Trail and Fifth Avenue. Each longer element of the zone consists of several smaller elements in a restraining orientation with respect to the longer element. Thrusts reflect the restraining steps or bends. Shift on the longest element nearly dies out before the element reaches the fence line at the northern end of the area. The element offsets the fence about 30 cm. Total shift recorded by the fence line for the *en echelon* shear zones is 120 cm. Another right-lateral rupture zone enters the south end of the map area with an orientation of N30°E, crosses the longest element of the north-south rupture, and then turns roughly north-south on the east side of the longest element. The two rupture zones seem to share tension cracks.

In the Two Bikers zone, a right-lateral shear zone appears to merge with another shear zone (Plate 1). A zone with a trend of N30°E is shown to join the Kickapoo fault zone at the southern end of the detailed map (Figure 28). This shear zone extends across open ground for several hundred meters to the southwest, nearly reaching the Johnson Valley fault zone. The rupture zone that enters from the west crosses the long element and then turns to become subparallel with, but about 17 m east of the longer element, where it ends. There is no other evidence of interaction of the two right-lateral rupture zones.

Although the two shear zones superficially appear to be conjugate (one right-lateral and the other left-lateral), the kinematic signatures show that both zones are right lateral. It is difficult to understand how intersecting faults could have the same sense of shift if they occurred simultaneously or how the stress state could change enough during the earthquake sequence to sequentially produce two right-lateral shear zones. As mentioned above, however, the map view does not show the direction of propagation of the surface rupture. The situation at depth may be a product of misalignment of the fault zone, similar to the Kickapoo fault zone relative to the Johnson Valley fault zone, and to the Sargent and San Andreas fault zones in the Loma Prieta earthquake (see Johnson and Fleming, fig. 4, 1993).

The Two Bikers area includes parts of three *en echelon* rupture zones, trending about N10°E, that is, 10 to 20° clockwise from the overall north-south orientation of the walls of the Kickapoo fault zone. The longest element extends for about 250 m and ends in the vicinity of the fence. The right-lateral shift across this long, narrow zone was about 30 cm at the fence, as compared to a shift of 120 cm for the entire *en echelon* zone (Figure 28). To the west of the long shear-zone element shown in Figure 28 is another shear-zone element about 80 m long that accommodated about 10 cm of right-lateral shearing at the fence line. Still farther west, starting at Fifth Avenue and extending for at least 200 m to the north (well off the map area) is a third shear-zone element. This shear zone accommodated the most shift, of the three, at the position of the fence line, offsetting the fence an additional 70 cm (Figure 28).

Each of the narrow shear zones consists of the same fracture elements described elsewhere at Landers (Johnson and others, 1993, 1994). The fracture elements are dominated by diagonal tension cracks oriented about 30° clockwise with respect to the overall trend of the zone. Some of these have accommodated subsequent, left-lateral offset of a few cm. There are small thrust faults, generally marked by low lobes, at one or both ends of the blocks of ground bounded by the tension cracks. There are a few right-lateral ruptures parallel to the narrow shear zones, but distinct fault surfaces are lacking. A striking difference between the orientation of tension cracks in the narrow shear zones in the Two Bikers area of the Kickapoo fault zone and the narrow shear zones elsewhere at Landers is that the tension cracks, rather than being oriented north-south, are oriented N30-40°E in the Two Bikers area.

Whereas the Johnson Valley and Homestead Valley fault zones step in a releasing mode (right step of right lateral elements), the individual elements within the Two Bikers area and the individual short elements within the longer element both step in restraining modes (left step of right-lateral elements).

Charles Road *En echelon* Zone

The Charles Road *en echelon* zone, part of the Kickapoo fault zone, extends north from Bodick Road about 800 m to a small ranch (Plate 6). The right-lateral shift across the fault zone is about 2.8 m, as determined by sighting along a line of power poles.

Even at the scale of the location map (Plate 1), we can see that the Charles *en echelon* zone has a well-defined west wall and an ill-defined east side. The west wall is not a continuous fault, but rather is defined by the southwest ends of numerous *en echelon* fault elements. The Kickapoo fault zone is 200-300 m wide in this area and its walls are oriented about N7°E. The Charles *en echelon* zone is about 800 m long and is oriented N17°E. As indicated in Table 3, the width of the *en echelon* zone is about 230 m and the angle α (Figure 13) is about 170°.

The left step of the Charles *en echelon* zone is abrupt. It extends from Bodick Road to Charles Road, where it ends, between houses east of Charles and a small ranch west of Charles. We could see no damage to the houses or deformation of the fences east of the road. Neither could we could see any distortion of the southern fence bounding the small ranch west of the road. The next element to the left (north) is roughly in line with the ranch house. There are a

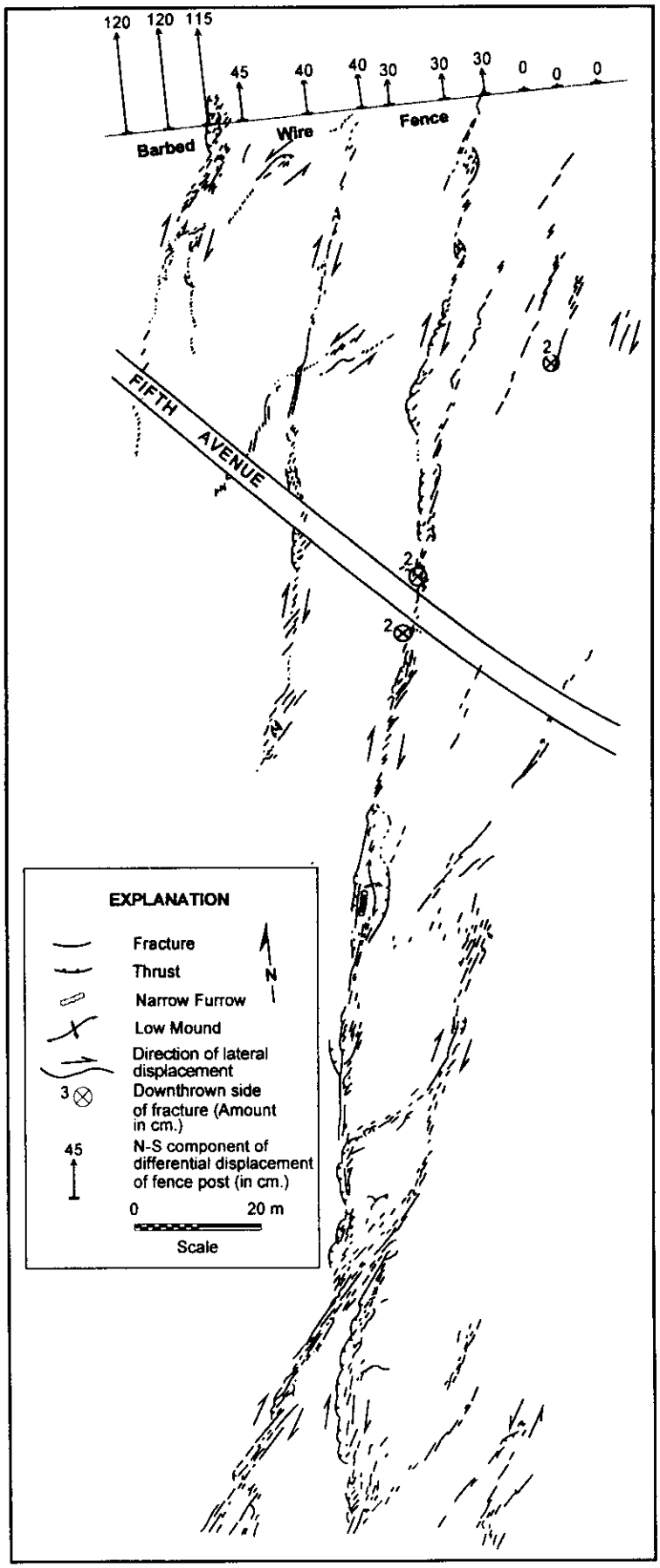
120 120 115
45 40 40 30 30 30 0 0 0
Barbed
Wire
Fence
FIFTH AVENUE
2
2
2
EXPLANATION
Fracture
Thrust
Narrow Furrow
Low Mound
Direction of lateral displacement
3
Downthrown side of fracture (Amount in cm.)
45
N-S component of differential displacement of fence post (in cm.)
0
20 m
Scale
N

Figure 28

few cracks in the vicinity of the house, and we were told that there was minor damage to the house. Thus, the elements of the main rupture of the Kickapoo fault zone stepped through this area of relatively dense housing, almost miraculously, without seriously damaging any of them! Houses in other places along Charles were not so luckily sited; they were directly underlain by fault elements (Lazarte and others, 1994).

A compilation of three detailed maps (1:200 scale) of the Charles *en echelon* zone is shown in Plate 6, and part of the central of the three maps is shown in even greater detail. The northern part of the map of the Charles Road area was constructed photogrammetrically, and no kinematic information is available. The other maps show kinematic information where such information could be determined in the field. The maps also show scarps and, in places, rubble on the downthrown side of scarps. The surficial debris in this area was quite sandy and friable, and we mapped the area a year after the earthquake, so the fractures were neither well formed nor well preserved, and kinematic information was difficult to obtain.

The most distinctive feature within the Charles *en echelon* structure is the zone of lower-order, *en echelon* shear-zone elements. The roughly 250 m–long elements are oriented N24°E and bound the Kickapoo fault zone on the west. The elements define a restraining, *en echelon* zone with a width of about 100 m, and the ratio of spacing of individual elements to width is about 0.4 (Table 3). The shear-zone elements are uniformly downthrown on the southeast side, generally 30 to 60 cm to as much as 1 m. We could measure strike-shift offsets of some of the smaller fractures, but not along the main rupture zone, where it must be on the order of 2 to 3 m. The vertical shifts are normal, not reverse, so the net shift is right-lateral strike-shift and normal-shift, with the southeast side downthrown.

The detailed map in Plate 6 shows that the second-order elements (about 250 m long), arranged in a restraining configuration, are themselves composed of third-order, *en echelon* elements about 25 m long, which also arranged in a restraining configuration. Whereas the 250 m elements are oriented about N24°E, the 25 m elements are oriented about N45°E.

It is interesting that, at each scale, the fault elements trend further in the clockwise direction. The Kickapoo fault zone trends, overall, N7°E. Within it, the first-order shear-zone elements are oriented about N17°E. The second-order shear zone elements along those are oriented about N24°E, and the third-order shear zones are, in turn, oriented about N45°E.

Although the configuration of the shear-zone elements appears to be fractal-like, we believe it is not. Only in some places are the 800-m elements broken into 250-m elements. Neither are all of the 250-m elements broken into 25-m elements; the 25-m elements occur only locally. We suggest that the various elements simply reflect the vertical dimension of the element. The 25-m elements are exposed only where they are near the ground surface, and extend only a few tens meters into the subsurface. These, though, are like fringes locally on the larger, 250-m elements. Likewise, the 250-m elements are exposed only where they are near the ground surface, and extend only a few hundred meters into the subsurface. They are like fringes locally on the larger, 800-m elements. We suggest that they are analogous to—but not of the same mechanical origin—the "twists" described along joints in Arches National Park (Cruikshank and others, 1991a; Scholz, 1992).

SOME SUMMARY REMARKS

The object of this document has been to describe and explain several of the structures along the rupture zones at Landers. We have been fortunate to have been involved in detailed mapping of ground ruptures that formed in three large earthquakes in California—1989 Loma Prieta, 1992 Landers, and 1994 Northridge. From these studies and other descriptions of earthquake ruptures and descriptions of landslide structures, we have become infused with the similarities in surface rupture and deformation styles caused by earthquake and large-landslide ruptures. Single fractures of the types described in Utah by Fleming and Johnson (1989) and at Landers by Johnson and others (1993, 1994) are the basic building blocks of these structures.

We have learned that, if we are to understand the structure underlying a fractured area, we must first learn to interpret the fractures. In such interpretations there are two basic principles. First, groups of fractures in surficial materials are *guide fractures*, and as such provide insight into the growth of the structures (Johnson and Fleming, 1993; Martosudarmo and others, 1997). They reflect what is happening at depth, where we cannot directly observe the conditions or processes. Second, the work accomplished by the formation and further displacement across a fracture is defined in terms of its orientation and kinematics as a function of position. One can describe a piece of a fracture as a point quantity—the orientation of a fracture plane and a vector of differential displacement—as was done by most investigators at Loma Prieta (e.g., U.S. Geological Survey Staff, 1989, 1990; Spittler and Harp, 1990; Prentice and Schwartz, 1991). As Ponti and Wells (1991) and Martosudarmo and others (1997) have demonstrated, however, such descriptions are incomplete, misleading and confusing. Descriptions of fractures without the spatial distribution of orientation and differential displacement are inadequate for deducing the kinematics of a deformation.

In one place at Loma Prieta, we showed that two blocks of ground are separated by a rupture that is right lateral in one place, left lateral in another, and pure opening in a third, plus transitions in between. Without recognizing and mapping the orientation of the rupture and the distribution of differential displacement, we would not have been able to determine that the blocks of ground were simply moving apart, more or less like tectonic plates. The faulting appeared to be very complicated because the trace of the rupture was complicated. The block kinematics, however, were simple.

We have come to these realizations gradually as we have tried to make sense of the information on various maps. In many cases we made detailed maps, not because we knew where the mapping would lead us, but believing that, if we mapped carefully and faithfully, we would later be able to understand what had happened. When asked at the time why we were mapping in detail, we answered that we really did not know, yet. In our landslide mapping, we eventually interpreted most of the structures represented by the guide fractures shown on the maps. It turns out that, in this way we inadvertently found ridges, broad shear zones, structures at fault bends, and pull aparts at right-stepping right-lateral faults. We also mapped ruptures in detail at Loma Prieta. Again, we were initially puzzled by the map patterns, especially the left-lateral fractures (Aydin and others, 1993). As it turned out, our subsequent mapping and analysis of fractures at Landers showed that we had mapped part of a broad right-lateral shear zone at Loma Prieta (Johnson and Fleming, 1994) that had gone unrecognized by ourselves and others.

And now at the conclusion of these studies of surface rupture at Landers, we once more realize that our map information, alone, is largely insufficient to carry these observations to an understanding of structures much larger than the areas we mapped. In general, our detailed mapping and structural measurements will probably be investments in the future. As we examine other structures, and return to the observations at Landers preserved in the maps of this report, we will be able to recognize the significance of map patterns that have thus far been obscure. The recognition of the left-lateral fractures at Loma Prieta as a common feature of broad right-lateral shear zones is an example; the understanding of the left-lateral rupture in the Pipes Wash step as a reflection of rotation of blocks is another. At the time we did the mapping, we saw these structures in sufficient detail to map them, but did not understand their meaning. The recognition of the Landers-Big Bear rotating block is yet another example. We understood the significance of the crude arc of fault traces at Landers only after working out a theory of faulting in flowing materials, and considering the general kinematics of slip on curved and straight faults (e.g., Johnson and others, 1996).

One can hardly avoid drawing broad conclusions about these structures. A striking feature of rupture zones, whether produced by landslides or faulting during an earthquake, is the structures' independence of form and scale. For example, the *en echelon* fault elements that follow Gilbert's law of obliquity are beautifully developed, at scales of 1 to 10 m, in the Aspen Grove landslide and, because of their slickensided surfaces, are clearly faults. Many of the freshly-formed fault elements at Landers, at scales ranging from 1 m to 500 m, also follow Gilbert's law. There are many other examples: The *en echelon* tension cracks, a few centimeters to a meter long, above an upward-propagating strike-slip fault in the Aspen Grove landslide, appear to be analogous to *en echelon* tension cracks, 1 m to perhaps 10 m long, within shear zones and

belts of shear zones at Landers. The rifts we mapped at Landers that were a few tens of meters wide are clearly analogous to the rifts, a few meters wide, that we mapped in Utah landslides. The long thrust faults at restraining steps are clearly analogous to short thrust faults at restraining steps in Utah landslides.

Fleming and others (1997) point out that their investigation of the Galway Lake rotating block further emphasizes that coactive, *fault-related structures* form at different scales in a variety of settings along earthquake ruptures. The Landers earthquake rupture produced more than 80 km of spectacular ground rupture. The rupture area consists of fault-related structures on at least five levels of scale. At a regional level, the largest structure is the Landers-Big Bear rotating block, discussed above. The second level of structures are the active parts of various fault zones, including the Emerson, Homestead Valley and Johnson Valley fault zones. These active parts of fault zones are composed of smaller, third-level structures that include releasing duplex structures and pull-apart basins that are present in stepovers between fault zones, including the Kickapoo stepover and the Homestead-Emerson stepover described above. The third-level also includes *en echelon* fault elements, tectonic ridges, twisted flower structures, and rotating blocks that occur within the fault zones. An example is the Galway Lake Road rotating block of this study. Still-smaller structures at the fourth level include rotating blocks, belts of shear zones, releasing duplex structures and small basins in releasing bends, and thrusts and domes at restraining bends (Johnson and others, 1993, 1994; Fleming and Johnson, 1997). At the smallest scale, the fifth level, we mapped and described en echelon tension cracks and faults, complex and compound fractures, and shear zones (Johnson and others, 1993).

The mechanical behavior of rock should produce surface rupture that follows pre-existing faults as long as the orientation of the faults is compatible with the tectonic deformation that is relaxed by the earthquake. Instead, the Landers rupture zone utilized only those parts of the pre-existing faults that were connected at the second level by stepovers to form the broad curve of the Landers rupture. The stepovers contain distinctive internal patterns of surface rupture. The stepover between the Johnson Valley and Homestead Valley fault zones was a releasing duplex, or perhaps a rotating block, where relatively long right-lateral strike-slip faults were connected by shorter right-lateral faults oriented 30° to 45° clockwise to the longer faults (Johnson and others, 1997). The stepover between the Homestead Valley and Emerson fault zones was apparently a duplex structure. The stepover between the Emerson and Camp Rock fault zones was at least partly accomplished through a series of tension cracks oriented about 60° clockwise to the trends of the two fault zones; the structure is a pull-apart basin (Fleming and others, 1997).

In the process of analyzing fault-related structures at Landers, we now realize that the full understanding of fault-related structures not only requires study of individual fault-related structures at the next lower level, but must also study of structures at the next higher level. Detailed mapping is required to understand fracture kinematics and a larger, more general map view is required to understand boundary conditions. This is true whatever the level of an investigation.

Our own failure to determine the context of fault-related structures as we mapped rupture zones at Landers has been a learning experience. In 1992, shortly after the Landers earthquake, we made detailed maps by plane-table methods, at scales of 1:200 and 1:500, for interesting parts of the different faults that produced surface rupture (Johnson and others, 1993, 1994). One of the maps, at the Two Ranches area, illustrated what appeared to be typical surface ruptures within a shear zone (Figure 7). The following year, the adjacent area to the south of the "typical" area was mapped and we learned, to our surprise, that part of the previously mapped area contained a distinctive fracture pattern associated with a duplex structure centered about 200 m south of our earlier map (Plate 4). A photogrammetric map of an even larger area confirmed the context for the duplex structure. In the study at the Two Ranches area, the maps of individual fractures provided information on fracture kinematics, but the map of a larger area provided information required to understand the boundary conditions of the fractures in the smaller area. The same is true for the Galway Lake Road rotating block where a lack of context led to an incomplete interpretation of the geologic structures at the site as well as exaggerated estimates of offset of crustal blocks.

REFERENCES CITED

Aki, K., 1994. Seismological expressions of the fine scale structure of fault zones. ABSTR., Program of American Geophysical Union Spring Meeting, Baltimore, p. 106.

Antonellini, M., Arrowsmith, J. R., Aydin, A., Christiansen, P., Cooke, M., Cruikshank, K., Du, Y., and Wu, H., 1992, Complex surface rupture associated with the North Emerson Lake fault zone, caused by the 1992 Landers, CA earthquake: results of detailed mapping: *EOS*, v. 73, p. 362.

Arrowsmith, J. R., and Rhodes, D. D., 1994, Original forms and initial modifications of the Galway Lake Road scarp formed along the Emerson fault: Bulletin of the Seismological Society of America, v. 84, p. 511-527.

Aydin, A. and Du, 1995, Surface rupture at a fault bend: the 28 June 1992 Landers, California, earthquake: Bulletin of the Seismological Society of America, v. 85, no. 1, p. 111-128.

Aydin, A. and Page, B.M., 1984. Diverse Pliocene–Quaternary tectonics in a transform environment, San Francisco Bay region, California. Geological Society of America Bulletin, 95:1303–1317.

Aydin, A., and Nur, A., 1982. Evolution of pull-apart basins and their scale dependence. Tectonics, 1:91-105.

Aydin, A., Johnson, A.M., and Fleming, R.W., 1992. Right–lateral/reverse surface rupturing along the San Andreas and Sargent fault zones during the October 17, 1989 Loma Prieta, California, earthquake. Geology, 20, 1063–1067.

Bally, A.W., 1983. Seismic expression of structural styles—A picture and work atlas. American Association of Petroleum Geologists, Studies in Geology, Series 15, four volumes.

Bateman, P.C., 1961. Willard D. Johnson and the strike-slip component of fault movement in the Owens Valley, California, earthquake of 1872. Bulletin of the Seismological Society of America, 51:483-493.

Baum, R.L., and Fleming, R.W., 1991. Use of longitudinal strain in identifying driving and resisting elements in landslides. Geological Society of America Bull., 103:1121-1132.

Baum, R.L., Fleming, R.W., and Ellen, S.E., 1989. Maps showing landslide features and related ground deformation in the Woodlawn area of the Manoa Valley, City and County of Honolulu, Hawaii. U.S. Geological Survey, Open-File Report 89-290, 16 p.

Baum, R.L., Fleming, R.W., and Johnson, A.M., 1988a. Kinematics of the Aspen Grove landslide, Ephraim Canyon, Central Utah. U. S. Geological Survey Bulletin 1842F, 34 pp.

Baum, R.L., Johnson, A.M., and Fleming, R.W., 1988b. Measurement of slope deformation using quadrilaterals. U.S. Geological Survey Bulletin 1842B, 23 pp.

Ben–Zion, Y., 1995. Stress, slip and earthquakes in models of complex single–fault systems incorporating brittle and creep deformations. Submitted to Journal of Geophysical Research.

Ben–Zion, Y., and Rice, J. R., 1993. Earthquake failure sequences along a cellular fault zone in a 3D elastic solid containing asperity and nonasperity regions. Journal Geophysical Research, 98:14109–14131.

Ben–Zion, Y., and Rice, J.R., 1995. Slip patterns and earthquake populations along different classes of faults in elastic solids. Journal Geophysical Research, 100, 12959–12983.

Bilham, R., and King, G., 1989. The morphology of strike-slip faults; examples from the San Andreas fault, California. Journal of Geophysical Research, 94:10204-10216.

Bonilla, M.G., and others, 1971. Surface faulting. In, The San Fernando, California, earthquake, February 9, 1971. U.S. Geological Survey Professional Paper 733, p. 55–76.

Boyer, S.E. and Elliott, D. 1982. Thrust systems. American Association of Petroleum Geologists Bulletin, 66: 1196-1230.

Brown, R.D., Jr., and others. (1967). The Parkfield–Cholame California, earthquakes of June–August 1966—Surface geologic effects, water–resources

aspects, and preliminary seismic data. U.S. Geological Survey Prof. Paper 579, 66 p.

Brown, R.D., Jr., Ward, P.L., and Plafker, G., 1973. Geologic and seismologic aspects of the Managua, Nicaragua, earthquakes of December 3, 1972. U.S. Geological Survey Prof. Paper 838, 34 p.

Clark, M.M., 1972. Surface rupture along the Coyote Creek fault. U.S. Geological Survey Prof. Paper 787, 55–86.

Cottrell, B. and Rice, J.R. 1980. Slightly curved or kinked cracks. International Journal of Fracture 16: 155-169.

Cruikshank, K.M., Zhao, G.Z., and Johnson, A.M., 1991a. Analysis of minor fractures associated with joints and faulted joints. Journal Structural Geology, v. 13, 865–886.

Cruikshank, K.M., Zhao, G.Z., and Johnson, A.M., 1991b. Duplex structures connecting fault segments in Entrada Sandstone. Journal Structural Geology, v. 13, 1185–1196.

D'Onfro, P., and Glagola, P., 1983. Wrench fault, southeast Asia. In, Bally, A.W., ed., Seismic expression of structural styles. Bulletin of the American Association of Petroleum Geologists, 4.2:9-12.

Dibblee, T.W., Jr., 1964. Geologic map of the Rodman Mountains Quadrangle, San Bernardino County, California. Miscellaneous Investigation Map, I 430.

Dibblee, T.W., Jr., 1967a. Geologic map of the Emerson Lake Quadrangle, San Bernardino County, California. Miscellaneous Investigation Map, I 490.

Dibblee, T.W., Jr., 1967b. Geologic map of the Old Woman Springs Quadrangle, San Bernardino County, California. Miscellaneous Investigation Map, I 518.

Dokka, R.K., and Travis, C.T., 1990. Role of the eastern California shear zone in accommodating Pacific–North American plate motion. Geophysical Research Letters, v. 17, p. 1323–1326.

Engineering and Science, 1992. Double fault: The Landers earthquake. California Institute of Technology, 55, 14–19.

Fleming, R.W., 1997. Surface rupture and deformation associated with earthquakes—Final report to the Nuclear Regulatory Commission. U.S. Department of the Interior, U.S. Geological Survey, Administrative Report (Purdue Earth Sciences Library), 17 pp.

Fleming, R.W., Baum, R.L., and Savage, W.Z., 1996. The Slumgullion landslide, Hinsdale County, Colorado. Geological Society of America, Guidebook for Field Trips, 21 p.

Fleming, R.W., Messerich, J.A., and Cruikshank, K.M., 1997. Fractures along a portion of the Emerson fault zone related to the 1992 Landers, CA, earthquake: Evidence for the Galway Lake Road Rotated Block. (in review, Geological Society of America.)

Fleming, R.W., and Johnson, A.M., 1989. Structures associated with strike–slip faults that bound landslide elements. Engineering Geology, 27, 39–114.

Fleming, R. W., and Johnson, A. M., 1997, Growth of a tectonic ridge: Geology, v. 25, p. 323-326.

Fleming, R. W., Johnson, A. M., and Messerich, J. A., 1997, Growth of a tectonic ridge: U. S. Geological Survey Open-file Report 97-153, 94 p, 6 Plates.

Frazer, C.S., and Gruendig, L., 1985. The analysis of photogrammetric deformation measuremetns on Turtle Mountian. Photogrammetric Engineering and Remote Sensing, 51:207-216.

Gabrielov, A., Keilis-Borok, V., and Jackson, D.D., 1996. Geometric incompatibility in a fault system: Proceedings of the National Academy of Science USA, v. 93, p. 3838-3842.

Genik, G.J., 1993. Petroleum geology of Cretaceous-Tertiary rift basins in Niger, Chad, and Central African Republic. Bulletin of the American Association of Petroleum Geologists, 77:1405-1434.

Gilbert, G.K., 1907. The earthquake as a natural phenomenon. In, The San Francisco Earthquake and Fire. U.S. Geological Survey Bulletin 324, 1–13.

Gilbert, G. K., 1928. Studies of Basin–Range structure. U. S. Geological Survey, Professional Paper 153, 92 p.

Harding, T.P., 1983. Divergent wrench fault and negative flower structure, Andaman Sea. In, Bally, A.W., ed., Seismic expression of structural styles. Bulletin of the American Association of Petroleum Geologists, 4.2:1-8.

Harding, T.P., and Lowell, J.D., 1979. Structural styles, their plate-tectonic habitats, and hydrocarbon traps in petroleum provinces. Bulletin of the American Association of Petroleum Geologists, 63:1016-1058.

Harding, T.P., Gregory, R.F., and Stephens, L.H., 1983. Convergent wrench fault and positive flower structure, Ardmore Basin, Oklahoma. In, Bally, A.W., ed., Seismic expression of structural styles. Bulletin of the American Association of Petroleum Geologists, 4.2:13-17.

Hart, E.W., 1992. Fault–rupture hazard zones in California, Calif. Dept. of Conservation, Div. of Mines and Geology, Special Report 42: 1–26.

Hart, E.W., Bryant W.A., and Treiman, J.A., 1993. Surface faulting associated with the June 1992 Landers earthquake, California, California Geology, 46, No. 1, 10–16.

Hobbs, W.H., 1910. The earthquake of 1872 in the Owens Valley, California. Beiträge zur Geophysic, Bd. X, Heft 3:352-385.

Hough, S.E., Ben-Zion, Y., and Leary, P., 1994. Fault-zone waves observed at the southern Josua Tree earthquake rupture zone. Bulletin of the Seismological Society of America, v. 84:p. 661–667.

Hough, S.E., Mori, J., Sembera, E., Glassmoyer, G., Mueller, C., and Lydeen, S., 1993. Southern surface rupture associated with the 1992 M 7.4 Landers earthquake: Did it all happen during the main shock?. Geophysical Research Letters, 20:2615-2618.

Hudnut, K.W., and 16 others, 1994. Co-seismic displacements of the 1992 Landers earthquake sequence. Bulletin of the Seismological Society of America, 84:625-645.

Irvine, P. J. and Hill, R.L., 1993. Surface rupture along a portion of the Emerson fault. Landers Earthquake of June 28, 1992, California Geology, 46, No. 1, 23–26.

Jennings, C.W., 1973. State of California, Preliminary fault and geologic map, south half, scale 1:750000. California Division of Mines and Geology, Preliminary Report 13.

Jennings, C.W., 1994. Fault Activity Map of California and Adjacent Areas. California Division of Mines and Geology, Geologic Data Map No. 65, scale 1:750,000.

Johnson, A.M., 1965. A model for debris flow. Ph.D. dissertation, The Pennsylvania State University,232 p.

Johnson, A.M., 1970. Physical Processes in Geology. Freeman, Cooper and Co., San Francisco.

Johnson, A.M., 1977. Styles of Folding. Elsevier Publishing Co., 406 pp.

Johnson, A.M., 1995. Orientations of faults determined by premonitory shear zones. Tectonophysics, v. 247, p. 161–238.

Johnson, A.M., 1996. A model for grain flow and debris flow. U.S. Geological Survey Open-File Report 96-728, 41 p.

Johnson, A.M. and Berger, P. 1989. Kinematics of fault-bend folding. Engineering Geology, 27: 181-200.

Johnson, A.M., and Fleming, R.W., 1993. Formation of left–lateral fractures within the Summit Ridge shear zone, 1989 Loma Prieta, California, earthquake. Journal of Geophysical Research, 98:21,823–21,837.

Johnson, A.M., Fleming, R.W., and Cruikshank, K.C., 1993. Broad Belts of Shear Zones as the Common Form of Surface Rupture Produced by the 28 June 1992 Landers, California, earthquake. U.S. Geological Survey, Open File Report 93–348, 61 p.

Johnson, A.M., Fleming, R.W., and Cruikshank, K.M., 1994. Broad belts of right–lateral surface rupture along simple segments of fault zones that slipped during the 28 June 1992 Landers, California, earthquake. Bulletin Seismological Society of America, 84:499–510.

Johnson, A.M., Fleming, R.W., Cruikshank, K.M., and Packard, R.F., 1996. Coactive fault of the Northridge earthquake—Granada Hills area, California. U.S. Geological Survey Open–file Report 96–523, 95 p., 3 plates.

Johnson, A.M., and Fletcher, R.C., 1994. Folding of viscous layers: New York, New York, Columbia University Press, 461 p.

Kamb, B., and many others, 1971. Pattern of faulting and nature of fault movement in the San Fernando earthquake. In, The San Fernando, California, earthquake, February 9, 1971. U.S. Geological Survey Professional Paper 733, 41–54.

Kanamori, H., Thio, H.-K. Dreyer, D., Hauksson, E., and Heaton, T. 1992. Initial investigation of the Landers, California, Earthquake of 28 June 1992

using TERRAscope, Geophysical Research Letters, 19, No. 22, 2267–2270.

King, N.E., and Savage, J.C., 1983. Strain-rate profile across the Elsinore, San Jacinto and San Andreas faults near Palm Springs, California, 1973-81. Geophysical Research Letters, 10: 55-57.

Lachenbruch, A.H., 1962. Mechanics of thermal contraction cracks and ice; wedge polygons in permafrost. Geological Society of America, Special Paper, 69 p.

Lajoie, K., 1993. Personal Communication.

Lawn, B.R., and Wilshaw, T.R., 1975. Fracture of brittle solids. Cambridge University Press, N.Y., 204 p.

Lawson, A.C. (editor), 1908. The California earthquake of April 18, 1906. Report of the State Earthquake Investigations Commission: Carnegie Institution of Washington Publication 87, (v. 1) 451 p.

Lazarte, C.A., Bray, J.D., Johnson, A.M., and Lemmer, R.E., 1994. Surface breakage of the 1992 Landers earthquake and its effects on structures. Bulletin Seismological Society of America, 84:547–561.

Li, Y.G., Vidale, J.E., Aki, K., Marone, C.J., and Lee, W.H.K., 1994a. Fine structure of the Landers fault zone: Elementation and the rupture process. Science, 265:367-370.

Li., Y.G., Aki, K., Adams, D., and Hasemi, A., 1994b. Seismic guided waves trapped in the fault zone of the Landers, California, earthquake of 1992. Journal of Geophysical Research, 99:11705-11722.

Martel, S.J., 1990. Formation of compound strike–slip fault zones, Mount Abbot quadrangle, California. Journal of Structural Geology, 12: 869–882.

Martel, S.J., and D.D. Pollard, 1989. Mechanics of slip and fracture along small faults and simple strike–slip fault zones in granitic rock. Journal of Geophysical Research, 94: 9417–9428.

Martel, S.J., Pollard, D.D. and Segall, P. 1988. Development of simple strike-slip fault zones, Mount Abbot Quadrangle, Sierra Nevada, California. Geological Society of America Bulletin 100: 1451-1465.

Martosudarmo, S.Y., A. M. Johnson and R. W. Fleming, 1997. Ground fracturing at southern end of Summit Ridge caused by October 17, 1989 Loma Prieta, California, earthquake sequence. U.S. Geological Survey Open-File Report 97-xxx.

McKinstry, H.E., 1948. Mining geology. Prentice–Hall, Inc., Englewood Cliffs, N.J., 680 p.

Nicholson, R., and Pollard, D.D., 1985. Dilation and linkage of echelon cracks. Journal Structural Geology, 7, 583–590.

Olson, J.E., and Pollard, D.D., 1991. The initiation and growth of *en echelon* veins. Journal Structural Geology, 13, 595–608.

Philip, H., and Meghraoui, M., 1983. Structural analysis and interpretation of the surface deformations of the El Asnam earthquake of October 10, 1980. Tectonics, 2, 17–49.

Plawman, T.L., 1983. Fault with reversal of displacement, central Montana. In, Bally, A.W., ed., Seismic expression of structural styles. Bulletin of the American Association of Petroleum Geologists, 3.3:1-12.

Pollard, D.D., and Aydin, A., 1988. Progress in understanding jointing over the past century. Geological Soc. America Bulletin, 100, 1181–1204.

Pollard, D.D., Segall, P., and Delaney, P.T., 1982. Formation and interpretation of dilatant echelon cracks. Geological Soc. America Bulletin, 93, 1291–1303.

Prescott, W.H., and Lisowski, M., 1983. Strain accumulation along the San Andreas fault sytem east of San Francisco Bay, California. Tectonophysics, 94:41-56.

Reid, H.F., 1910. Report of the State Earthquake Investigation Commission, II: The mechanics of the earthquake. Carnegie Institution of Washington, Washington, D.C., 192 p.

Rice, J.R., 1993. Spatio–temporal complexity of slip on a fault. Journal of Geophysical Research, 98:9885–9907.

Roberts, M.T., 1983. Seismic example of complex faulting from northwest shelf of Palawan, Philippines. In, Bally, A.W., ed., Seismic expression of structural styles. American Association of Petroleum Geologists, 4.2:18-24.

Ron, H., Freund, R., Garfunkel, Z., and Nur, A., 1984. Block rotation by strike–slip faulting: structural and paleomagtnetic evidence. Journal of Geophysical Research, 89, 6256–6270.

Sarna–Wojcicki, A.M., Pampeyan, E.H., and Hall, N.T., 1975. Map showing recently active breaks along the San Andreas fault between the central Santa

Cruz Mountains and the northern Gabilan Range, California: U.S. Geological Survey Map MF–650, Scale 1:24000.

Savage, J.C., and Gu, G., 1985. The 1979 Palmdale, California, strain event in retrospect. Journal of Geophysical Research, 90k:10,301-10309.

Scholz, C. H., 1990. The mechanics of earthquakes and faulting. Cambridge University Press, 439 p.

Segall, P. and Pollard, D.D., 1980. Mechanics of discontinuous faults, Journal of Geophysical Research, 85, 4337–4350.

Segall, P. and Pollard, D.D., 1983. Nucleation and growth of strike–slip faults in granite: Journal of Geophysical Research 88, 555–568.

Sharp, R.V., 1975. Displacement on tectonic ruptures. in San Fernando, California, earthquake of 9 February 1971. Oakeshott, G.B., editor, California Div. Mines and Geology, Bulletin 196, 187–194.

Sibson, R.H., 1980, Transient discontinuities in ductile shear zones. Journal of Structural Geology, vol. 2, p. 165–171.

Sieh, K., and 19 others. 1993. Near–field investigations of the Landers Earthquake Sequence, April to July 1992, Science, 260, 171–176.

Sowers, J.M., Unruh, J.R., Lettis, W.R., and Rubin, T.D., 1994. Relationship of the Kickapoo fault to the Johnson Valley and Homestead Valley faults, San Bernardino County, California. Bulletin of the Seismological Society of America, v. 84, 528–536.

Spotila, J.A., and Sieh, K., 1995. Geologic investigations of a "slip gap" in the surficial ruptures of the 1992 Landers earthquake, southern California. Journal of Geophysical Research, v. 100, p. 543–559.

Stein, R.S., and Thatcher, W., 1981. Seismic and aseismic deformation associated with the 1952 Kern County, California, earthquake and relationship to the Quaternary history of the White Wolf fault. Journal Geophysical Research, 86:4913-4828.

Sylvester, A.G., 1988, Strike–slip faults. Geological Society of America Bulletin, vol. 100, p. 166–1703.

Terres, R. R., and Sylvester, A. G., 1981, Kinematic analysis of rotated fractures and blocks in simple shear: Bulletin of the Seismological Society of America, v. 71, p. 1593-1605.

Thatcher, W., 1975. Strain accumulation in northern California since 1906. Journal of Geophysical Research, 80:4873-4880.

Thatcher, W., 1979. Horizontal crustal deformation from historic geodesic measurements in southern California. Journal of Geophysical Research, 84:2351-2370.

Thatcher, W., 1983. Nonlinear strain buildup and the earthquake cuycle on the San Andreas fault. Journal of Geophysical Research, 88:5893-5902.

Thatcher, W., and Fujita, N., 1984. Deformation of the Mitaka rhombus; strain buildup following the 1923 Kanto earthquake, central Honshu, Japan. Journal of Geophysical Research, 89:3102-3106.

Unrhu, J.R., Lettis, W.R., and Sowers, J.M., 1994, Kinematic interpretation of the 1992 Landers earthquake. Bulletin of the Seismological Society of America, v. 84, 537–546.

Zachariasen, J., and Sieh, K., 1995, The transfer of slip between two en–echelon strike–slip faults: A case study from the 1992 Landers earthquake, southern California. Journal of Geophysical Research, 100:15,281–15,301.

Zhao, G., and Johnson, A.M., 1991. Sequential and incremental formation of conjugate sets of faults. Journal Structural Geology, 13:887–895.

Zhao, G., and Johnson, A.M., 1992. Sequence of deformations recorded in joints and faults, Arches National Park, Utah. Journal Structural Geology, 14, 225–236.

UNITED NATIONS EDUCATIONAL, SCIENTIFIC AND CULTURAL ORGANIZATION
INTERNATIONAL ATOMIC ENERGY AGENCY
INTERNATIONAL CENTRE FOR THEORETICAL PHYSICS
I.C.T.P., P.O. BOX 586, 34100 TRIESTE, ITALY, CABLE: CENTRATOM TRIESTE

H4.SMR/1011 - 5a

Fourth Workshop on Non-Linear Dynamics
and Earthquake Prediction

6 - 24 October 1997

Structures Formed During Landers-Big Bear, California, Earthquake Sequence

Supplement

A.M. JOHNSON

**Purdue University
Depts. of Mathematics and
Earth & Atmospheric Sciences
West Lafayette, Indiana, U.S.A.**

MAIN BUILDING STRADA COSTIERA, 11 TEL. 2240111 TELEFAX 224163 TELEX 460392 ADRIATICO GUEST HOUSE VIA GRIGNANO, 9 TEL. 224241 TELEFAX 224531 TELEX 460449
MICROPROCESSOR LAB. VIA BEIRUT, 31 TEL. 2249911 TELEFAX 224600 TELEX 460392 GALILEO GUEST HOUSE VIA BEIRUT, 7 TEL. 2240311 TELEFAX 2240310 TELEX 460392
ENRICO FERMI BUILDING VIA BEIRUT, 6 (TELEPHONE, FAX AND TELEX THROUGH MAIN BUILDING)

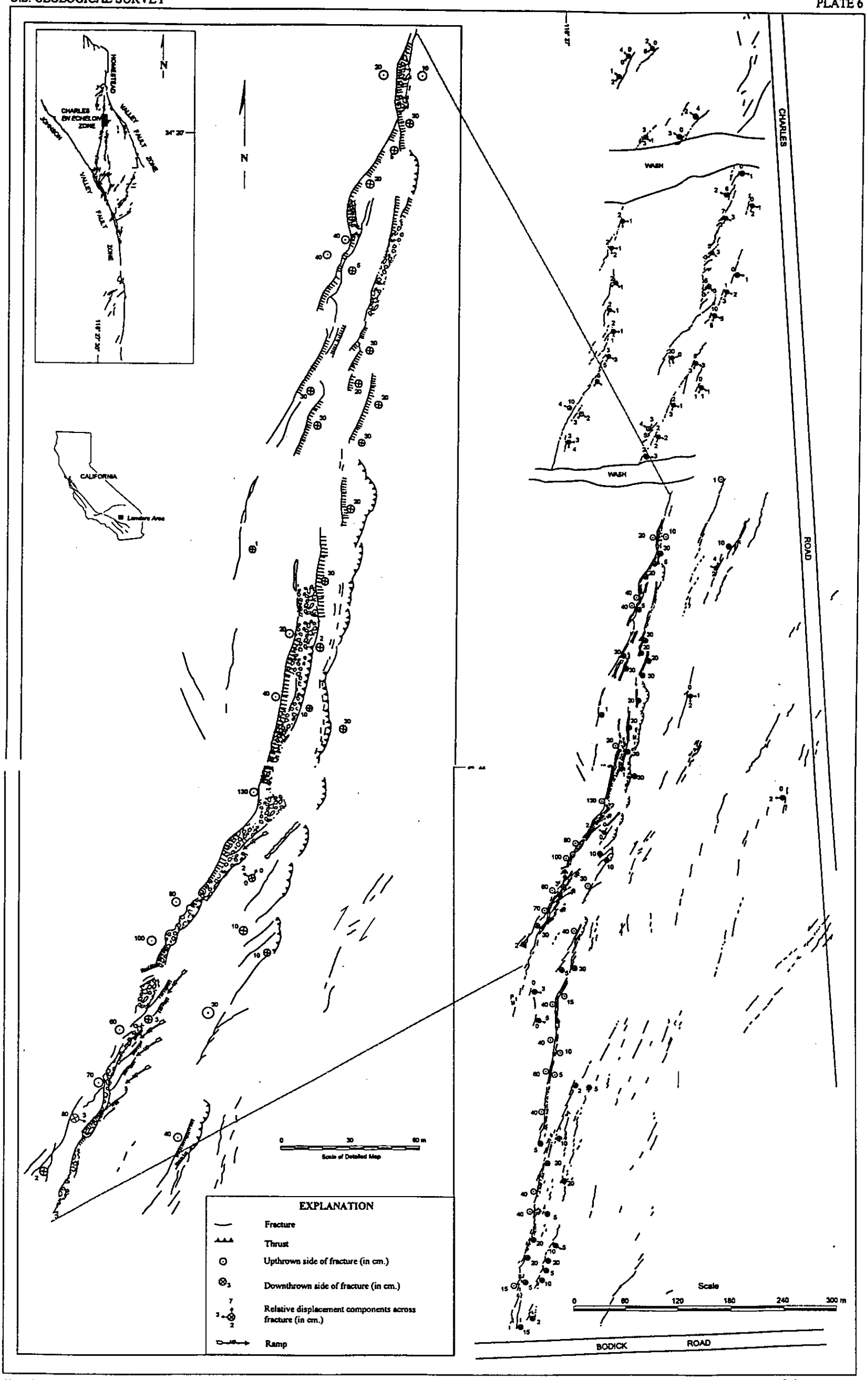

Mapped August 1993 with a total station.
Compiled by Kaj M. Johnson, 1995

This map is preliminary and has not been reviewed for conformity with U.S. Geological Survey editorial standards or with the North American Stratigraphic Code.

FRACTURES IN CHARLES EN ECHELON ZONE FORMED DURING 28 JUNE 1992 LANDERS, CALIFORNIA, EARTHQUAKES

by

Arvid M. Johnson, Sumaryanto Y. Martosudarmo, and Wei Wei

1997

DEPARTMENT OF THE INTERIOR
U.S. GEOLOGICAL SURVEY

OPEN-FILE REPORT 97-94
PLATE 1

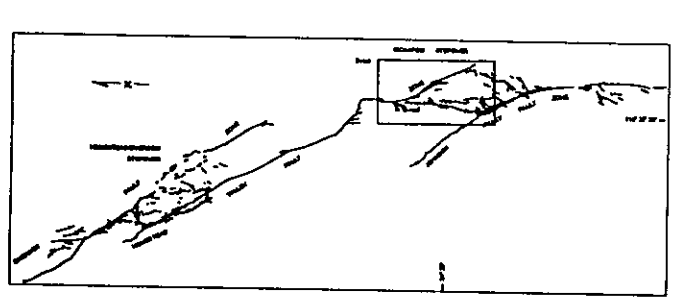

TRACES OF FRACTURES PRODUCED BY THE 28 JUNE 1992 LANDERS EARTHQUAKE, ALONG THE JOHNSON VALLEY AND HOMESTEAD VALLEY FAULT ZONES AND THE KICKAPOO STEPOVER, NEAR LANDERS, CALIFORNIA

by

Robert W. Fleming, Arvid M. Johnson, Kenneth M. Cruikshank, Sumaryanto Y. Martosudarmo, and Wei Wei

1997

U. S. DEPARTMENT OF THE INTERIOR
U. S. GEOLOGICAL SURVEY

OPEN-FILE REPORT 97-133
PLATE 2

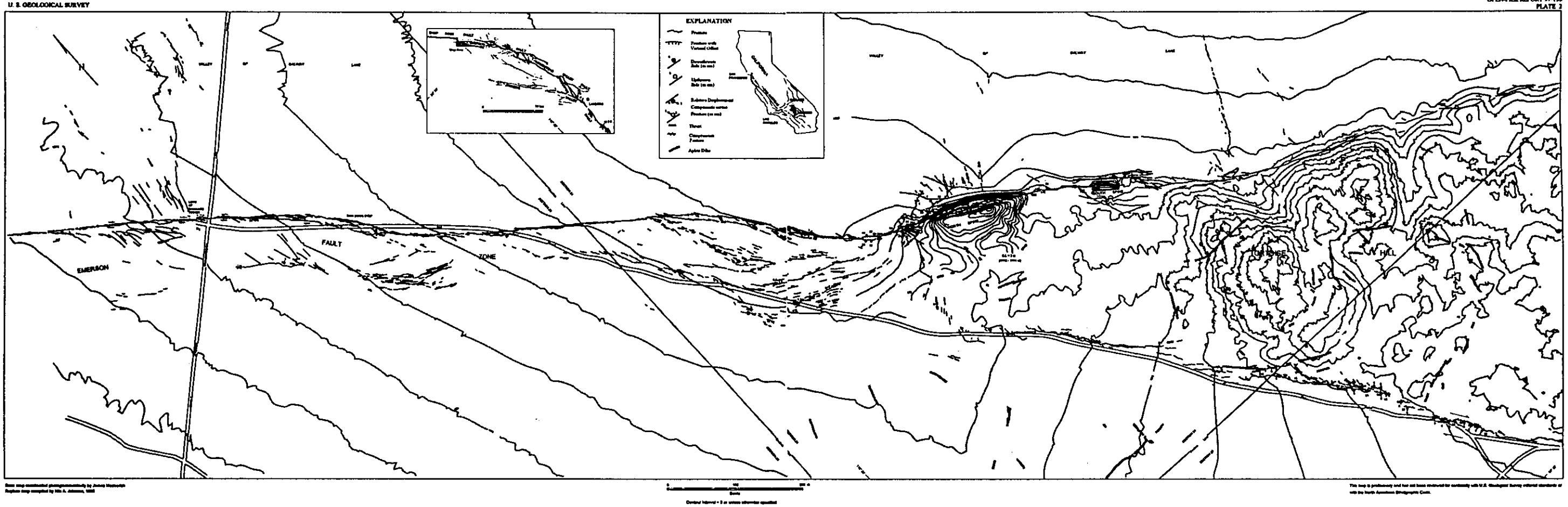

FRACTURES ALONG PART OF THE EMERSON FAULT ZONE PRODUCED BY THE 28 JUNE 1992 LANDERS, CALIFORNIA, EARTHQUAKE

by
Robert W. Fleming, Arvid M. Johnson, Kenneth M. Cruikshank and Sumaryanto Y. Martosudarmo

1997

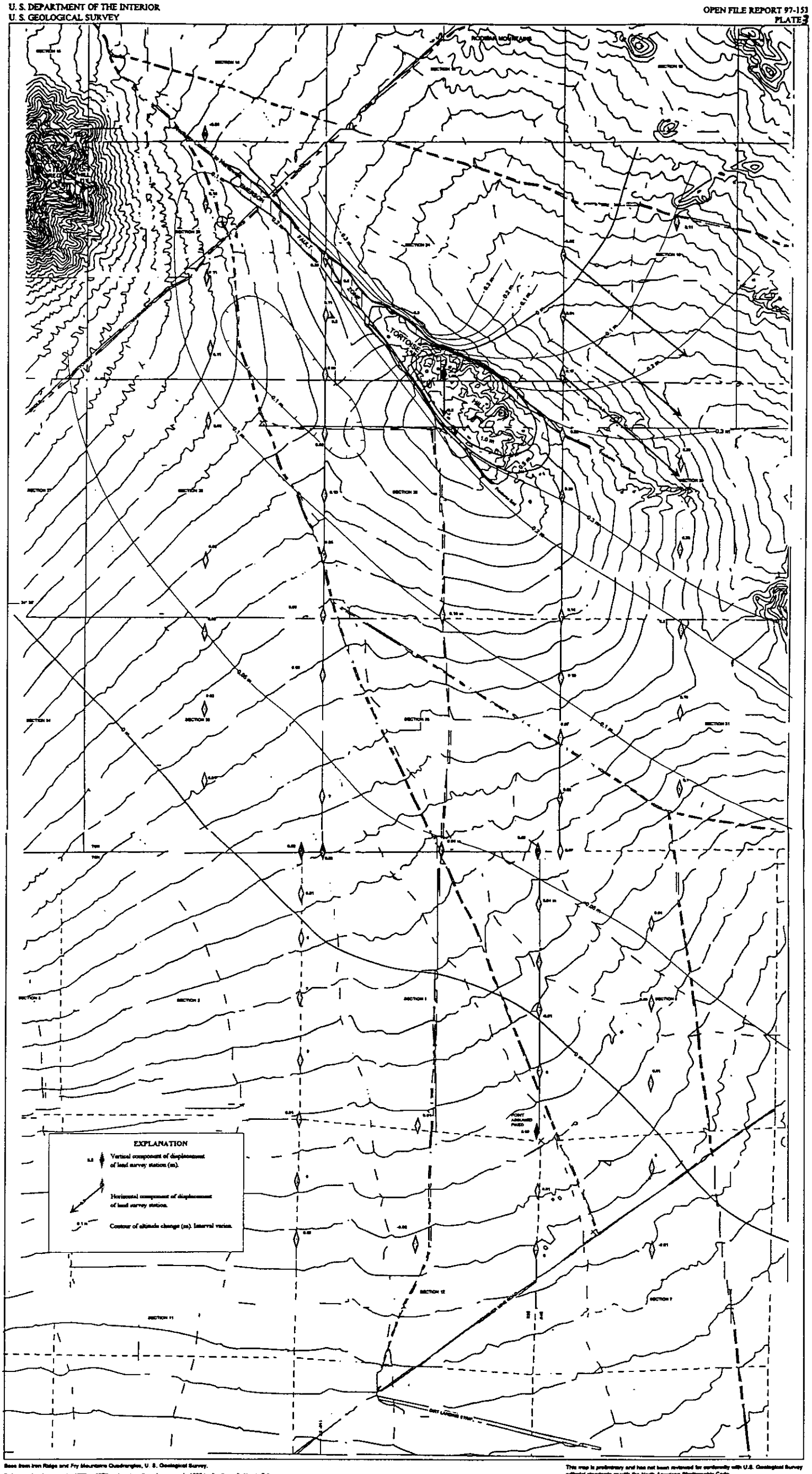

Base from Iron Ridge and Fry Mountains Quadrangles, U. S. Geological Survey.
Reference level surveys in 1973 or 1976 and post-earthquake survey in 1995 by Southern California Edison.
Compiled by Nils A. Johnson, 1995.

This map is preliminary and has not been reviewed for conformity with U.S. Geological Survey editorial standards or with the North American Stratigraphic Code.

Differential Vertical and Horizontal Displacements Along Part of Emerson Fault Zone During 1992 Landers, California, Earthquake (According to Surveys in 1973 and 1995)

by

Robert W. Fleming

1997

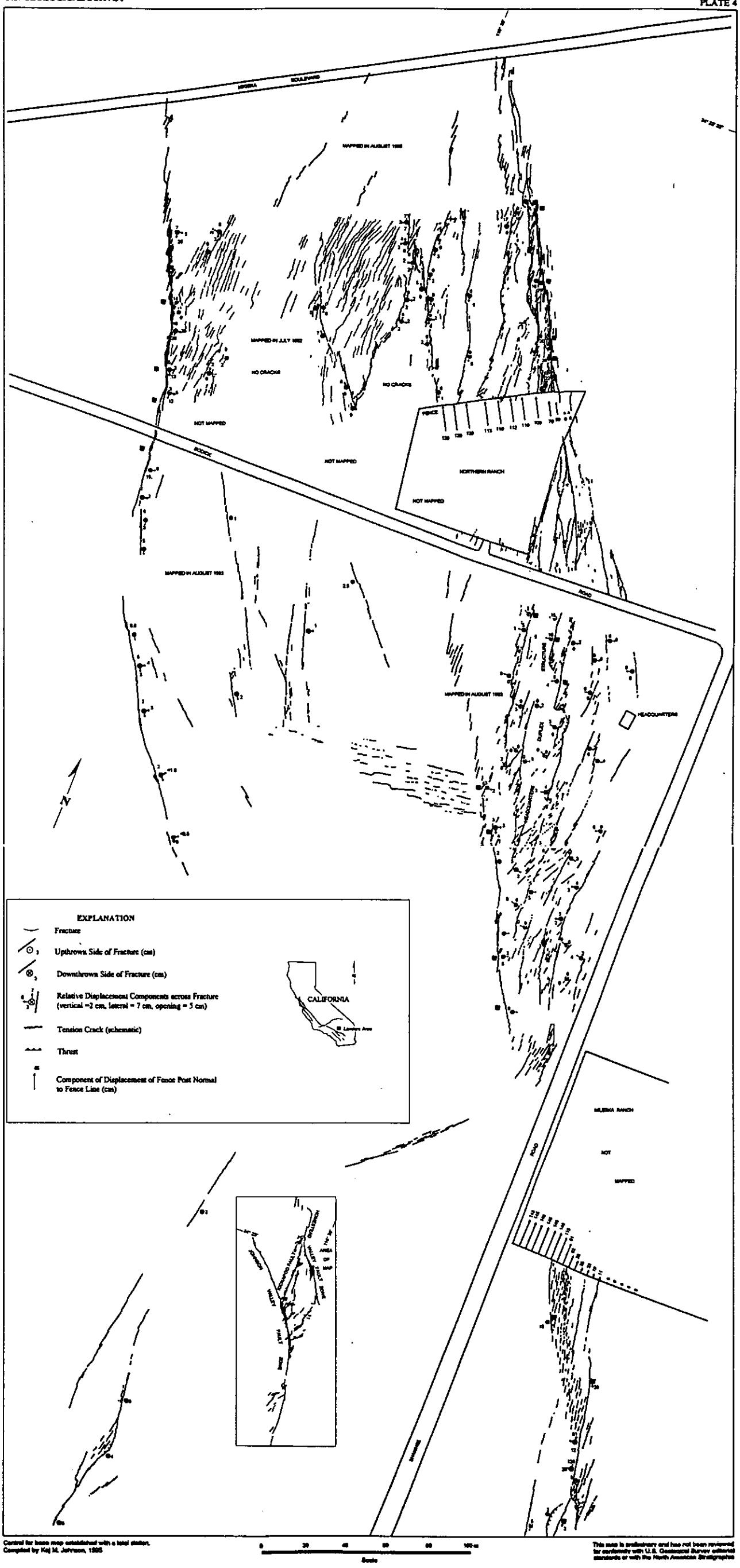

Fractures in Two Ranches Area along Homestead Valley Fault Zone Produced by 28 June 1992 Landers, California, Earthquake

by

Robert W. Fleming, Kenneth M. Cruikshank and Arvid M. Johnson

1997

U. S. DEPARTMENT OF THE INTERIOR
U. S. GEOLOGICAL SURVEY

OPEN-FILE REPORT 97-153
PLATE # 5

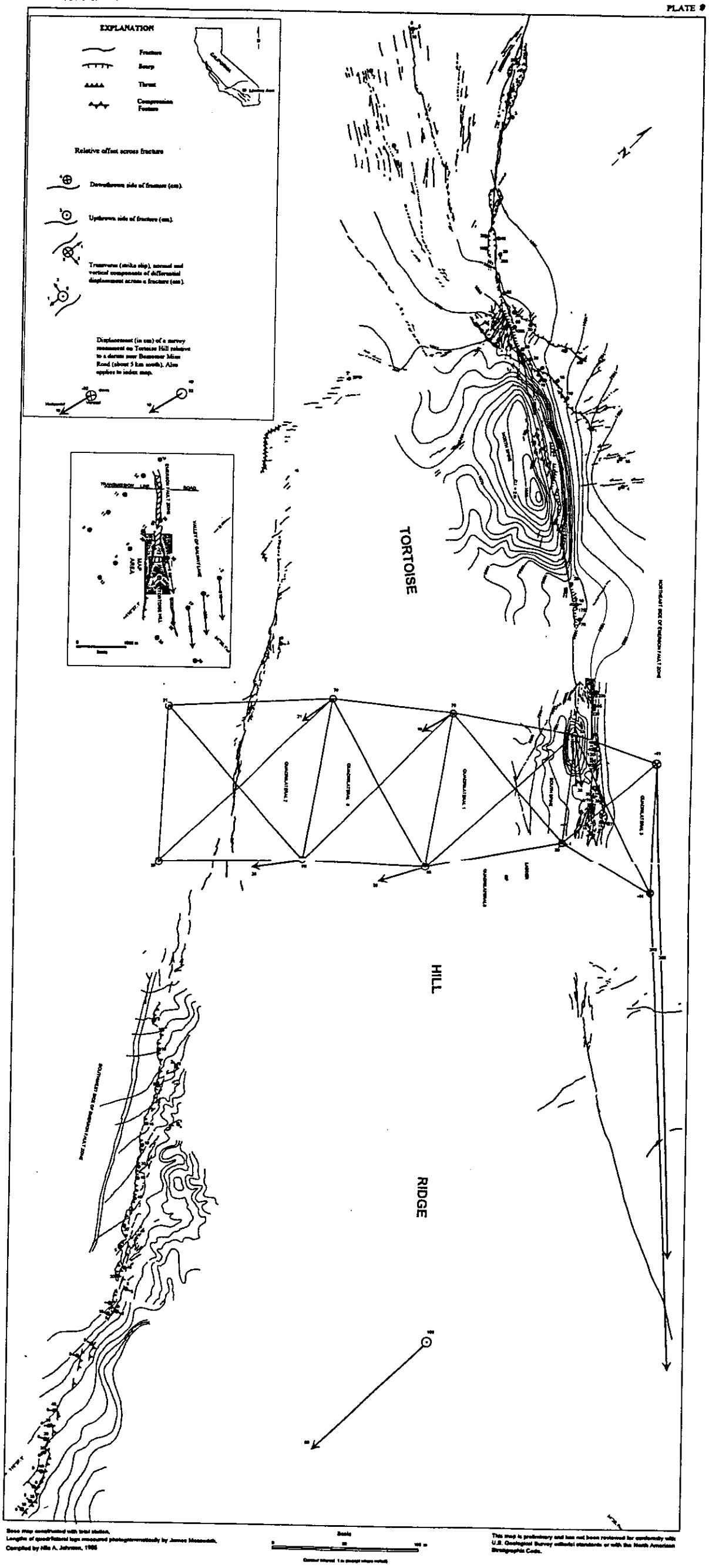

FRACTURES AND RELATIVE DISPLACEMENTS IN EMERSON FAULT ZONE AT TORTOISE HILL RIDGE DURING LANDERS, CALIFORNIA, EARTHQUAKE SEQUENCE 28 JUNE 1992

by

Robert W. Fleming, Kenneth M. Cruikshank, Arvid M. Johnson, Sumaryanto Y. Martosudarmo and Wei Wei

1997